

U.S. DEPARTMENT OF COMMERCE
National Technical Information Service

N79-12163

CARBON FIBRE STUDY NO. 4. FAILURE CRITERIA OF
CFRP COMPOSITES AT CRYOGENIC TEMPERATURES

M. F. RICKETT, ET AL

MAY 1978

DEPARTMENT OF DEFENSE
PLASTICS TECHNICAL EVALUATION CENTER
ATMOSPHERIC CANISTER, R. J. 07801

19960229 112

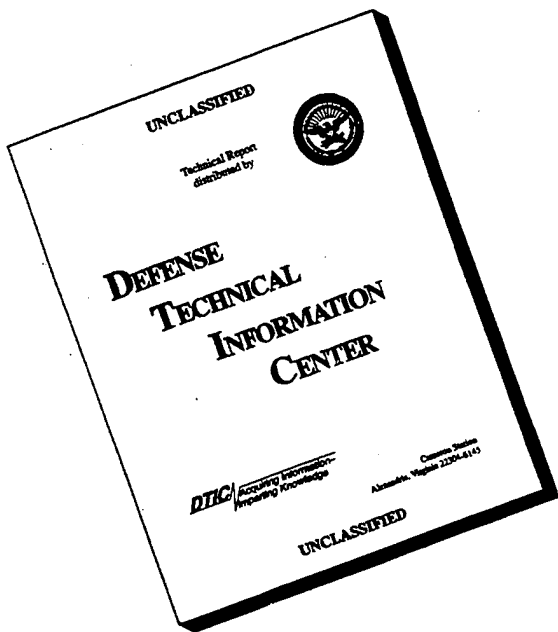
DTIC QUALITY INSPECTED 1

DISTRIBUTION STATEMENT A

Approved for public release;
Distribution Unlimited

PLASTIC
W3226

DISCLAIMER NOTICE



**THIS DOCUMENT IS BEST
QUALITY AVAILABLE. THE
COPY FURNISHED TO DTIC
CONTAINED A SIGNIFICANT
NUMBER OF PAGES WHICH DO
NOT REPRODUCE LEGIBLY.**

~~For Official Use Only~~

**EUROPEAN SPACE AGENCY
CONTRACT REPORT**

The work described in this report was done under ESA contract. Responsibility for the contents resides in the Author or Organisation that prepared it.

TP 7678

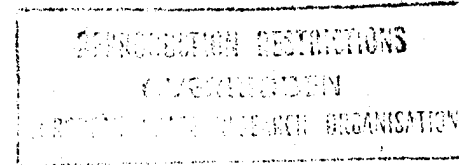
CARBON FIBRE STUDY NO. 4

**FAILURE CRITERIA OF CFRP COMPOSITES
AT CRYOGENIC TEMPERATURES**

**(BAe-TP-7678) CARBON FIBRE STUDY NO. 4:
FAILURE CRITERIA OF CFRP COMPOSITES AT
CRYOGENIC TEMPERATURES (British Aerospace
Dynamics (Space)) 193 p HC A09/MF A01**

N79-12163

**Unclassified
H2/24 91072**



**© ALL RIGHTS RESERVED
BRITISH AEROSPACE DYNAMICS GROUP
PRINTED IN ENGLAND 1978**

**REPRODUCED BY
NATIONAL TECHNICAL
INFORMATION SERVICE
U. S. DEPARTMENT OF COMMERCE
SPRINGFIELD, VA. 22161**

**BRITISH AEROSPACE - DYNAMICS GROUP
HATFIELD/LOSTOCK DIVISION
MANOR ROAD, HATFIELD, HERTFORDSHIRE
Telephone: Hatfield 62300 - Cables: Britair Hatfield
Telex: 22324**

NOTICE

**THIS DOCUMENT HAS BEEN REPRODUCED
FROM THE BEST COPY FURNISHED US BY
THE SPONSORING AGENCY. ALTHOUGH IT
IS RECOGNIZED THAT CERTAIN PORTIONS
ARE ILLEGIBLE, IT IS BEING RELEASED
IN THE INTEREST OF MAKING AVAILABLE
AS MUCH INFORMATION AS POSSIBLE.**

For Official Use Only

**EUROPEAN SPACE AGENCY
CONTRACT REPORT**

The work described in this report was
done under ESA contract. Responsibility
for the contents resides in the
Author or Organisation that prepared it.

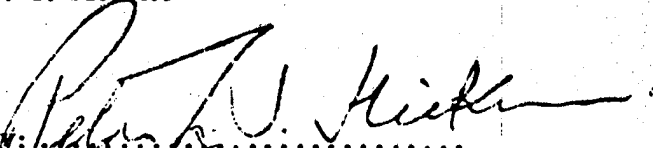
TP 7678

**FAILURE CRITERIA OF CFRP COMPOSITES
AT CRYOGENIC TEMPERATURES**

ESTEC CONTRACT NO. 2931/76/NL/PP(SC)

Compiled by: M.F. Rickett, BAe, N.L. Hancock and D.C.C. Minty, AERE, Harwell

ESA Technical Management: P.M. Molette

Approved by: 
P.L.V. Hickman

Divisional Director (Space)
Dynamics Group.

May 1978

**BRITISH AEROSPACE - DYNAMICS GROUP (SPACE)
SITE B, STEVENAGE, HERTFORDSHIRE**

Abstract

Test performed during the Spacelab Support Research and Technology Programme involving a Carbon Fibre Reinforced Plastic faced honeycomb panel have been rerun using an improved experimental technique. The original theoretical analysis has been revised using CFRP material parameters derived from a separate coupon test programme. Results from this programme have shown only small changes in material properties with decreasing temperatures. Discrepancies that were found between theoretical and practical panel performance have been put down to anomalous expansion coefficients and detail model problems.

Acknowledgement

This report has been prepared by the Mechanical Design Department of the Space Division, British Aerospace Dynamics Group, Stevenage, with the Atomic Energy Research Establishment, Harwell as major subcontractor.

The Advanced Engineering Materials Group at AERE Harwell embraces a number of departments and is led by Dr. D. H. Bowen.

CONTENTS

	Page No.
1. INTRODUCTION	1
2. STUDY STRUCTURE	3
3. COUPON TESTING	23
4. FULL PANEL TEST	64
5. DISCUSSION	95
6. CONCLUSIONS	111
7. REFERENCES	112

APPENDICES

A. Theoretical Prediction of Honeycomb CTE	114
B. List of Specimens	121
C. Complete Panel Test Procedure	132
D. Straincal Computer Program	140
E. Strain Gauge Outputs	167
F. Mathematical Model Description	181
G. Calculation of Stress from the Measured Orthogonal Strains	183

LIST OF FIGURES

1. Thermal Test Frame and CFRP Panel Study Structure
2. Study Structure
3. Finite Element Model
4. Incorporation of Variable Material Properties (1)
5. Incorporation of Variable Material Properties (2)
6. Anisotropy Plots
7. Stress vs Strain for Hypothetical $0^\circ/90^\circ$ laminate
8. Orthogonal Fibre Proportions for $0^\circ/60^\circ/120^\circ$ laminate
9. Apparent Strain Characteristics for Strain Gauges fitted to (a) Aluminium (b) A CFRP laminate
10. Original and Improved Test Arrangement for Complete Panel Thermal Test.
11. Dial Test Indicator Measuring Arrangement.
12. 120mm x 75mm Lay-up Tool
13. 260mm x 260mm Lay-up Tool
14. Test Machine Used to Carry Out Specimen Tests
15. Photograph Showing Cooling Arrangement for Specimen Cooling
16. Longitudinal and Transverse Tensile Modulus for Unidirectional CFRP Material
17. Longitudinal and Transverse Tensile Strength for Unidirectional CFRP Material
18. Longitudinal and Transverse Compressive Strength for Unidirectional CFRP Material
- 19A. Shear Modulus for Unidirectional CFRP Material
- 19B. Predicted Angle Ply Shear Modulus vs Temperature
20. Shear Strength for Unidirectional CFRP Material
21. Angular Deflection at Failure for Unidirectional CFRP Material
22. Micrograph Showing Cracking and Fibre Distribution in Shear Specimen
23. Micrograph Showing Cracking and Fibre Distribution in Shear Specimen
24. Micrograph Showing Cracking and Fibre Distribution in Shear Specimen

LIST OF FIGURES (Continued)

25. Longitudinal and Transverse Tensile Modulus for Angle Ply CFRP Material
26. Longitudinal and Transverse Tensile Strengths for Angle-Ply Material
27. Longitudinal and Transverse Compressive Strength for Angle-Ply CFRP Material
28. Longitudinal and Transverse Poisson's Ratio's for Angle-Ply CFRP Material
29. Longitudinal and Transverse Compressive Strengths for Angle-Ply Faced Aluminium Honeycomb
30. Effect of 100 Hours Exposure at 75% of Ultimate Load on Flexural Modulus and Strength
31. Change in Length as a Function of Temperature for Unidirectional CFRP Material
32. Change in Length as a Function of Temperature for Angle Ply CFRP Material
33. Coefficient of Thermal Expansion for Unidirectional CFRP Material
34. Coefficient of Thermal Expansion for Angle Ply CFRP Material
35. Change in Length of Angle Ply Faced Aluminium Honeycomb Sandwich as a Function of Temperature
36. CFRP Panel
37. Edge Member Moulding Tool
38. Acoustic Bond Tester
39. Acoustic Bond Tester Scans
40. Location of Panel and Test Frame Instrumentation
41. Panel Free (Test 2)
42. SG Curves for Panel Free Condition
43. DTI Measured Strain Effects on Free Panel
44. Strain Distribution Measured in X-Direction
45. Strain Distribution Measured in Y-Direction
46. Strain Distribution Measured in X-Direction
47. Strain Distribution Measured in Y-Direction
48. Strain Distribution Measured in X-Direction
49. Strain Distribution Measured in Y-Direction

LIST OF FIGURES (Continued)

- 50. Strain Distribution Measured in Y-Direction
- 51. Strain Distribution Measured in X-Direction
- 52. Strain Distribution Measured in Y-Direction
- 53. Strain Distribution Measured in X-Direction
- 54. Strain Distribution Measured in Y-Direction
- 55. Strain Distribution Measured in X-Direction
- 56. Theoretical Deflections of Carbon Fibre Panel When Panel is Attached to the Aluminium Frame 50°C Rise in Temp.
- 57. Plot of Theoretical and Actual Deflections of Carbon Fibre Panel When Attached to Aluminium Frame
- 58. Plot of Dial Test Indicator Reading (9) V Temperature Drop
- 59. Plot of Theoretical and Actual Strains For Top and Bottom Surfaces of Carbon Fibre Panel
- 60. Plot of Theoretical and Actual Strains for Top and Bottom Surfaces of Carbon Fibre Panel
- 61. Plot of Theoretical and Actual Strains for Top and Bottom Surfaces of Carbon Fibre Panel
- 62. Plot of Theoretical and Actual Strains for Top and Bottom Surfaces of Carbon Fibre Panel

1.

INTRODUCTION

In 1974 BAe (then HSD), Space Division, Stevenage, proposed the use of Carbon Fibre Reinforced Plastic (CFRP) face honeycomb panels for the Spacelab Pallet.

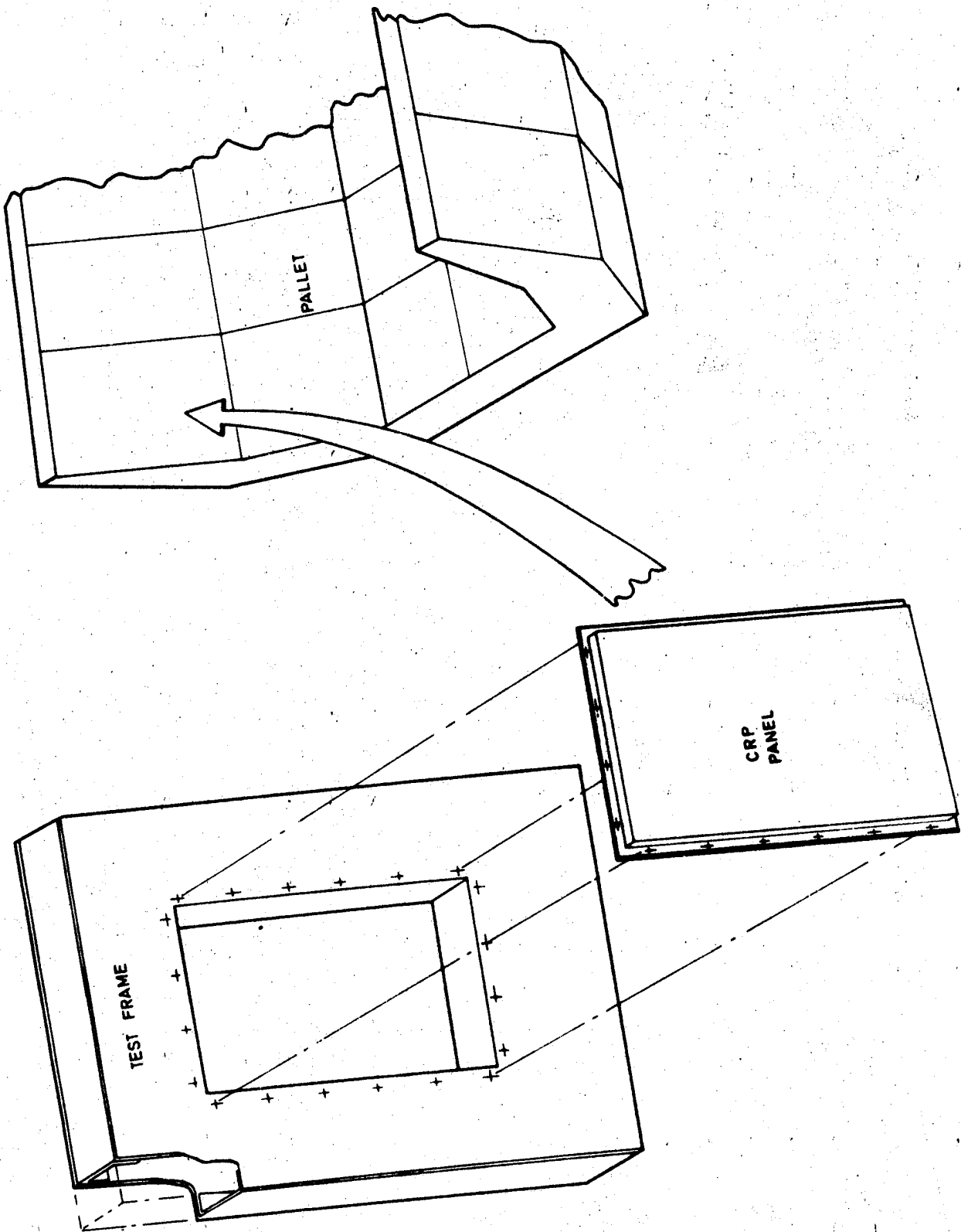
Due to the high technology that was involved, it was decided to proceed with a development programme before adopting carbon fibre as a baseline material. The Support, Research and Technology (SR and T) Programme which followed was completed in October 1975 with the issue of the final report HSD TP 7553.

One of the major problem areas was the accurate prediction of low temperature failures which could occur as the result of the build up of internal material stresses and/or the differential contraction between the carbon fibre panels and the aluminium frames to which they were to be attached. Unfortunately, programme timescales allowed neither detailed theoretical analysis nor exacting experimental procedure with the result that the theoretical predictions were not achieved in practice.

Figure 1 shows the test arrangement that was used to simulate the proposed configuration. It consisted of a representative carbon fibre faced honeycomb panel bolted to a rigid, aluminium box frame. This arrangement was cycled in a fixed and free condition to the maximum limits of + 100°C to -180°C and strains induced in the panel were recorded using a series of strain gauge rosettes.

The theoretical analysis, developed at that time, predicted a buckling failure of the panel at -70°C whereas in practice there was no failure down to the lowest temperature achieved of -180°C. The Pallet design temperature range was then -150°C to 110°C and so with no design confidence in failure prediction it was decided to terminate further research and adopt aluminium faced panels.

The aim of this Study was to win back this confidence by achieving a better understanding of the complex behaviour of CFRP at cryogenic temperatures.



ORIGINAL PAGE IS
OF POOR QUALITY

THERMAL TEST FRAME AND CRP PANEL

FIG. 1

2. STUDY STRUCTURE

The structure of the Study is summarised in block form in Figure 2. The top and bottom blocks represent the starting points; the theoretical analysis and the practical tests of the SR and T programme.

The objectives were to improve systematically both the theoretical analysis and the experimental technique so as to narrow the gulf between prediction and actual behaviour.

The major proposals for modifications to the theoretical analysis were as follows:

- Improvement of mathematical model
- Accommodation of material property variations.
- Modification of failure criteria.
- Incorporation of possible creep effects.

These proposals were to be investigated by means of a comprehensive programme of coupon testing designed to identify their respective sensitivities.

The major proposals for modifications to the experimental technique were as follows:

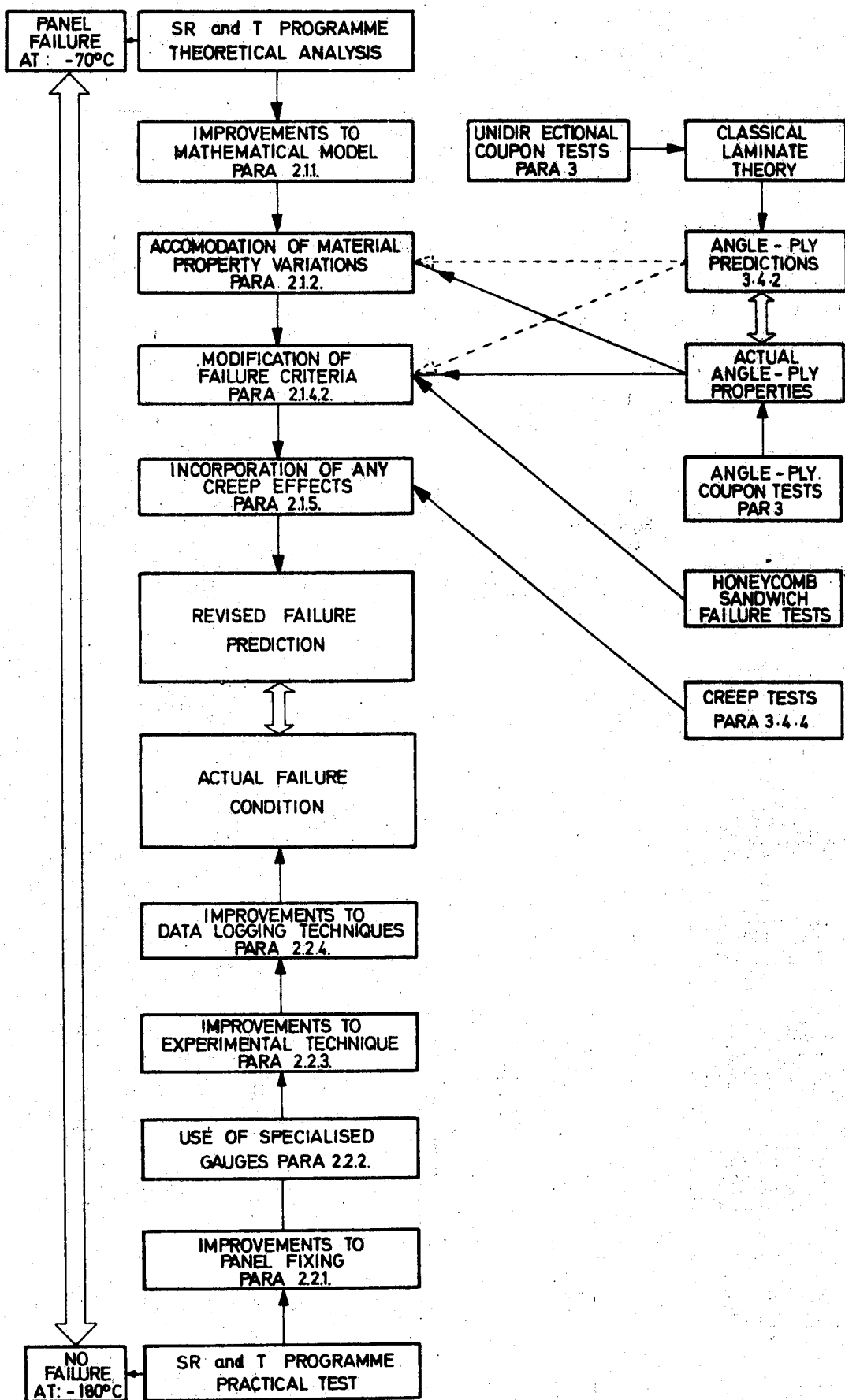
- Improvements to panel fixing
- Use of specialised strain gauges
- Improvements to test arrangement
- Adoption of automated data logging.

2.1 Theoretical Analysis

2.1.1 Improvements to Mathematical Model (See Appendix F)

There were two major changes to the SR and T model as follows:

- Addition of bending stiffness to plate elements which were previously modelled with only membrane stiffness
- CFRP panel was remodelled using triangular instead of quadrilateral sandwich elements.



STUDY STRUCTURE

FIG. 2

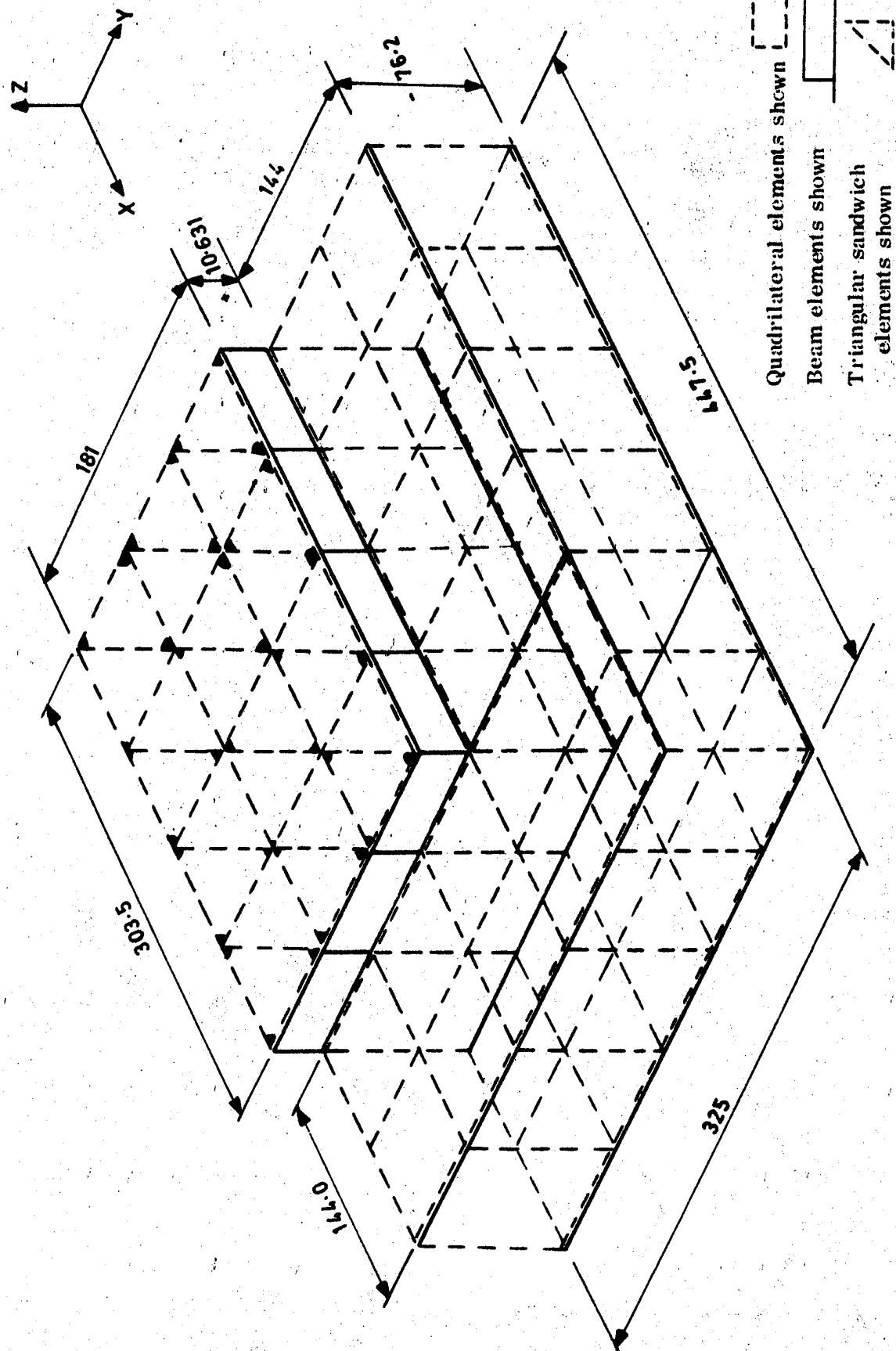
The final model, as depicted in Figure 3, comprised the following elements:

- Aluminium framework ($\frac{1}{4}$)
 - 54 plate elements representing top and bottom plates and channel webs.
 - 40 beam elements representing channel flanges.
- CFRP Panel ($\frac{1}{4}$)
 - 24 triangular sandwich elements representing the main body.
 - 7 beam elements representing the panel edge stiffening.
- Connection
 - Panel and framework were connected using rigid beam elements representing the panel offset.

2.1.2

Material Property Variations

Previous studies on the low temperature performance of carbon fibre composite materials have been made by References (1) and (2). It was found that the moduli tended to increase with decreasing temperature, while flexural and shear strengths were a maximum at room temperature and decreased with rising or falling temperature. For strength measurements considerable scatter was noted. The coefficient of thermal expansion (CTE) in the fibre direction was small, possibly negative depending on the fibre resin system used, and substantially constant with changes in temperature, but in the transverse direction it was much larger and increased steadily with rising temperature as might be expected for a property controlled by the resin matrix. Work on glass, carbon, and aramid fibre composites has been reviewed by (3) who noted that, generally, the tensile or flexural moduli in the fibre direction increase as the temperature falls to 77°K, but that the ultimate tensile strength decreases. Below 77°K results for either property become erratic, possibly because the mechanical behaviour of the resin becomes very sensitive to liquid or gas in contact with it. In a later publication, (4), the modulus and strength properties of a limited number of composite materials were measured at temperatures as low as 4°K. In most cases the properties increased with decreasing temperature.



FINITE ELEMENT MODEL

Table 1 shows changes in certain material properties that were identified for unidirectional laminates of CIBA Fibredux 914 in the range 20°C to -190°C.

Property	Units	at 20°C	at -190°C	% Change
Longitudinal Flexural Modulus	GN/m ²	214	243	+14
Longitudinal Flexural Strength	MN/m ²	900	510	-43
Interlaminar Shear Strength	MN/m ²	79	54	-32

Table 1

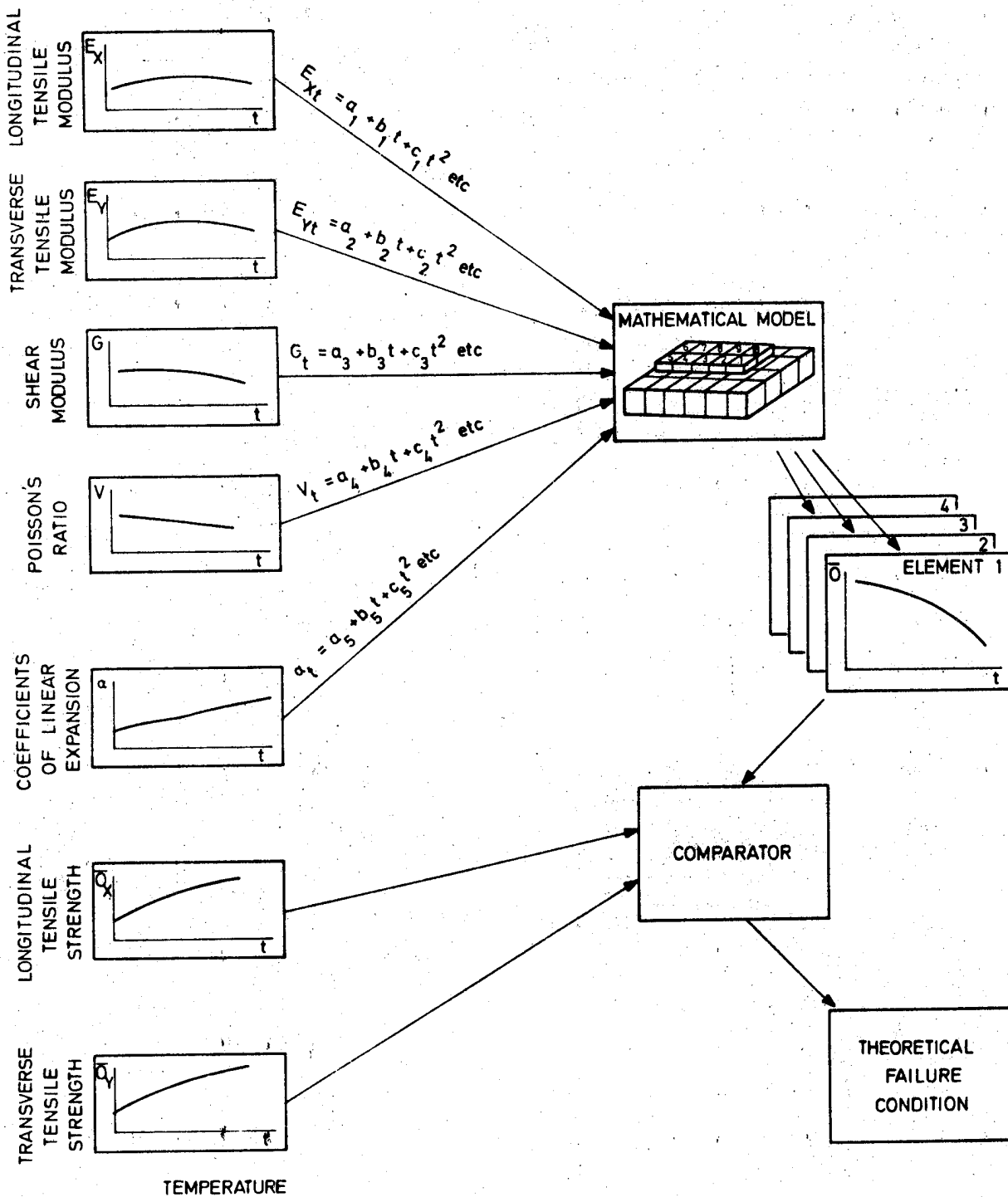
The original analysis of the panel/frame combination assumed the CFRP material properties to be invariant over the above temperature range and this was thought to have been a significant source of error. It was therefore decided that methods for incorporating such deviations into the theoretical analysis would be devised.

One approach is depicted in Figure 4. Angle ply coupon tests are used to construct a series of graphs showing the relationship between material properties and decreasing temperature. A polynomial approximation is then made to each of these curves and the polynomials are fed in as input data for the mathematical model. Plots of stress versus temperature produced by the model can then be compared with strength data obtained from coupon tests and used to establish failure conditions. Despite its apparent simplicity this method was rejected on the following grounds:

1. Few finite element packages have the facility for incorporating polynomial expressions as material input data.

For example, the 'STARODYNE' package commonly used by BAe has not got this facility.

2. Packages that can accept polynomial material inputs often have other limitations. For example 'ANSIS' cannot handle anisotropic sandwich elements.
3. The major problem is one of cost since iterative techniques are used to incorporate material variables. The combination of small temperature decrements and a relatively large number of elements was considered to be cost prohibitive.



INCORPORATION OF VARIABLE MATERIAL PROPERTIES (1)

A simplified approach based on this former method was subsequently proposed by BAe and accepted by ESTEC. The approach is shown diagrammatically in Figure 5. The same set of coupon-derived property versus temperature curves are used to provide sets of material data for each of a series of temperature decrements. The mathematical model is then run for each set of properties, deflections at the end of each decrement being used as the starting conditions for the next run. At the end of each decrement, the derived stresses are compared with ultimate coupon-determined values to identify failure conditions.

Since the choice of decrement(s) is a function of the degree of property variation, it was decided that the precise technique to be employed would be left until coupon results had been obtained.

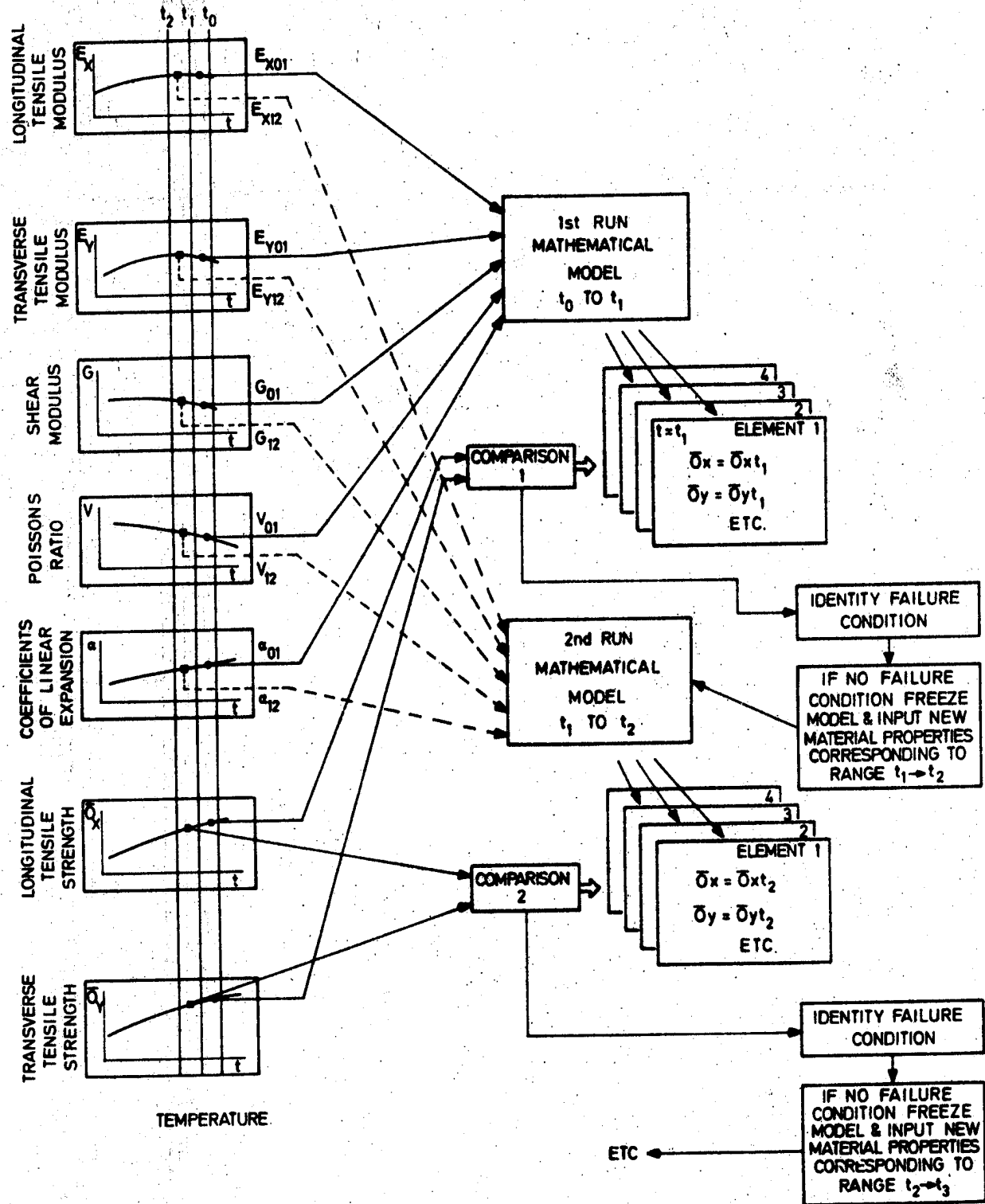
A further limitation imposed by certain finite element packages is that they are not capable of dealing with anisotropic material properties. In particular the 'STARDYNE' package proposed for use in this Study does not have this capability. The $0, 60, 120^{\circ}$ lay-up under consideration was however considered to be orthotropic and so a check was run using an anisotropy routine recently developed by BAe. The result is shown in Figure 6 and confirms the orthotropy of the considered lay-up. A $0, 90, 0^{\circ}$ plot is shown for interest.

2.1.3 Modification to Failure Criteria

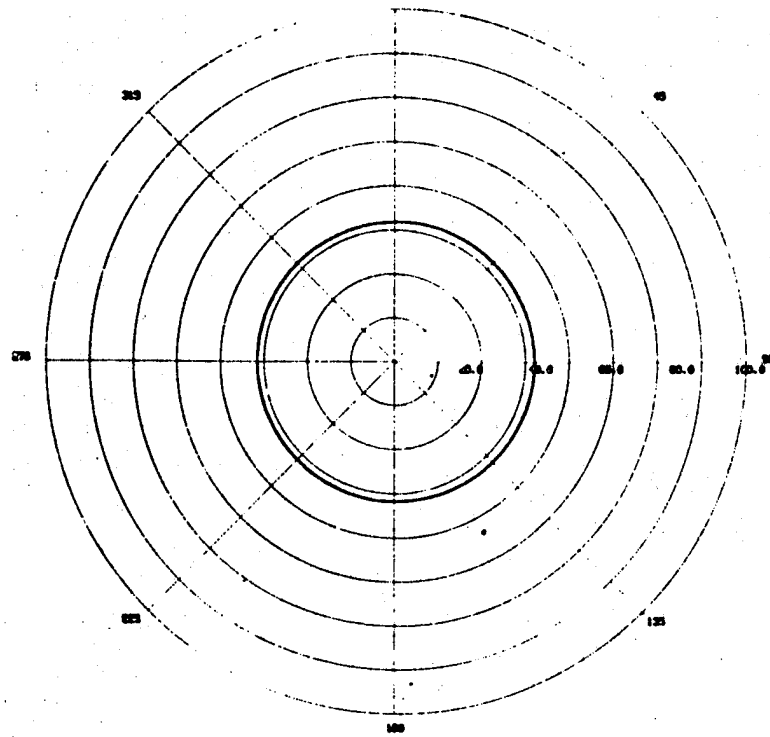
Figure 7 shows a typical stress/strain curve that might be obtained from the loading to failure of a $0^{\circ}/90^{\circ}$ cross ply laminate. The change in slope corresponds to a failure in the 90° ply and is analogous to the yield point of conventional metallic materials. Load is transferred to the 0° ply at this point which carries on taking load until the ultimate failure stress is achieved.

In many cases the sudden load transfer, and violent crack propagation typical of composite material failures may cause ultimate failure to occur at the yield point. The exhibition of this yield characteristic is dependent on many factors, but in particular the rate of loading, the number of plies and their orientations.

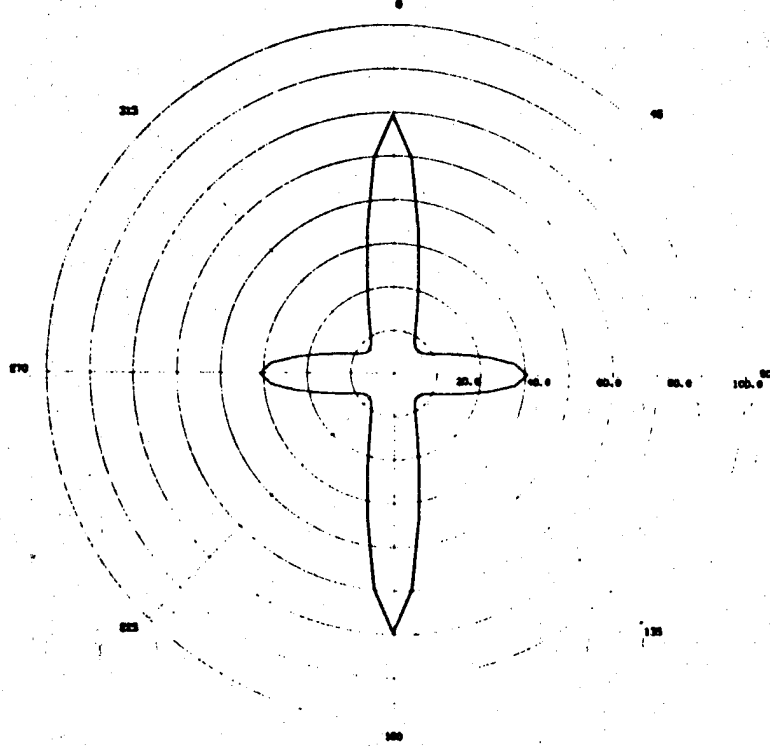
Fahmy et al (5) conclude that transverse crack propagation is inhibited by large angular variations between adjacent plies. Thus a $0/90^{\circ}$ lay-up would be more likely to exhibit a yield characteristic than a $0^{\circ}/45^{\circ}$ lay-up. Torsion testing of $0^{\circ}, 0^{\circ}, \pm 45^{\circ}$ tube sections conducted during the Phase 2 Study (6) showed distinct changes of slope corresponding to what was considered to be failure of the 0° plies. The onset of yield was often accompanied by a sharp crack sound, again characteristic of composite failures.



INCORPORATION OF VARIABLE MATERIAL PROPERTIES (2)

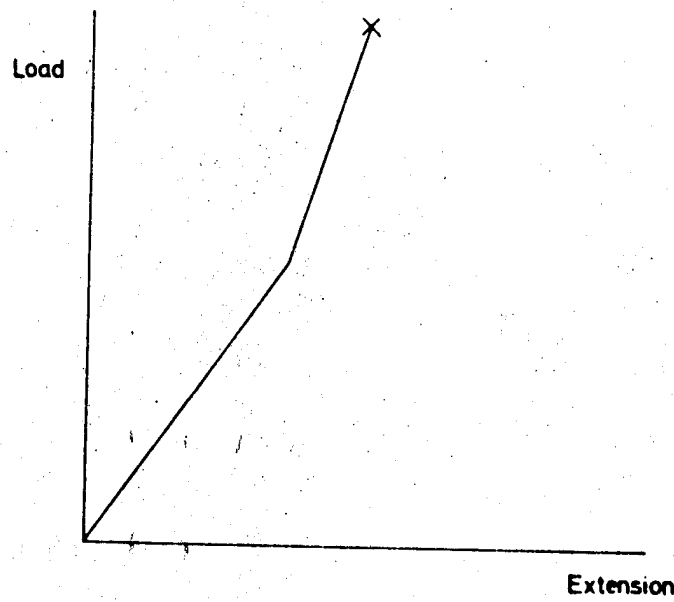
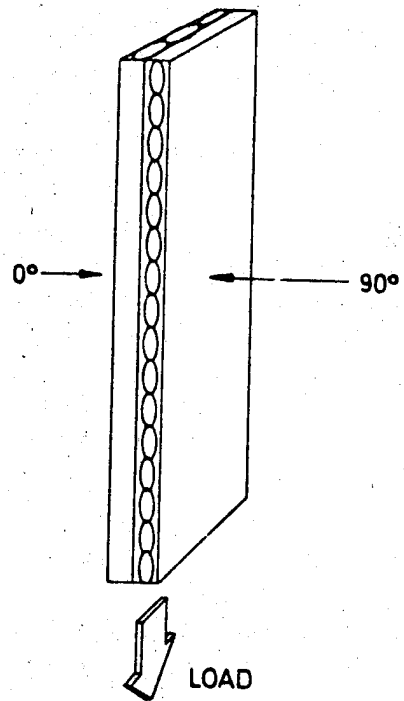


0 60 120 ANISOTROPY PLOT



0 90 0 ANISOTROPY PLOT

COMPUTER GENERATED ANISOTROPY PLOTS



Stress vs Strain for Hypothetical 0/90° Laminate

Fig. 7

Tests conducted during the latter stages of the SR and T programme showed similar curves and Table 2 gives stresses corresponding to the yield point and the ultimate failure.

Data Source	Yield σ_{11}	Yield σ_{22}	Ultimate σ_{11}
Derived from unidirectional properties	302	236	481 *
Angle Ply Test	350	296	478
MN/m ²			

* See text below.

Table 2

The theoretical values for yield strengths are the ultimate values determined from classical analysis which assumes failure in any one ply to be indicative of failure of the complete laminate. If it is assumed that redistribution of load occurs at yield then the classical yield criteria will require modification. For a multiply laminate it is not sufficient to assume that a failed ply makes no further contribution to the laminate strength since some load transfer will still occur in practice. By means of an iterative procedure an ultimate theoretical stress corresponding closely with the practical value was determined during the SR and T programme. This value, shown in the table, was derived by assuming the transverse stiffness and shear modulus for the unidirectional material to be reduced to 1% of their original values.

Due to the random nature of crack formation it would be difficult to justify theoretically such an assumption. It was hoped however, that by carrying out further angle ply tests that a parametric relationship might be established, albeit one peculiar to this lay-up.

2.1.4

Honeycomb Sandwich Effects

Coefficient of Thermal Expansion (CTE)

Tests performed during the SR and T programme showed that contrary to what had been expected, the aluminium core of a CFRP faced honeycomb sandwich can contribute significantly to the overall CTE of the sandwich. Theoretical analyses, (See Appendix A), have confirmed the effect but have failed to predict the apparent values shown in practice. Table 3 summarises the theoretical and practical results that were determined.

Item	Source	Coefficient of thermal expansion in	
		X-direction	Y-direction
Facesheet	Predicted	1.4	1.4
	Actual	1.0	1.0
Honeycomb Sandwich	Predicted	5.2	5.2
	Actual (DTI)	7.3	4.6
	Actual (Strain Gauge)	10.6	6.6
$\times 10^{-6}/^{\circ}\text{C}$ at 20°C			

Table 3

The large differences between theoretical and practical values, and indeed between two sets of practical values, are indicative of the problems of both analysis and measurement of this property.

Since the theoretical predictions were based on practically determined unidirectional values it was proposed that a part of the Study be devoted to accurate expansion measurements. AERE Harwell proposed the use of a laser interferometric technique and this would be applied to the three basic material configurations:

- Unidirectional Material
- Angle Ply (0° , 60° , 120°)
- Angle Ply faced honeycomb.

Failure Mode

The predicted mode of failure for the panel/ frame arrangement was through buckling at the centre of the panel. It was therefore proposed that edgewise compression tests be performed on honeycomb sandwich specimens to determine load levels to induce failure and the mode of failure produced.

2.1.5

Creep Effects

Many researchers have identified the existence of creep in reinforced plastic materials. In most cases these movements have been extremely small, resulting in the need for non-contacting micromechanical measurements.

Room temperature microyield and microcreep experiments performed on CFRP laminates and sandwich structures having a 0°, 60°, 120° fibre orientation have been reported by Goggin (7). Although the experiments were concerned with absolute deflections at low stress levels, it can be deduced from the specimen geometry that 1.5×10^{-6} permanent strain was induced in the 90° direction after 2½ hours and in the 0° direction after 40 hours with a constant stress level of 2% of ultimate. The reduced resistance of the 90° direction is concluded to be due to the lower resolved fibre effect, see Figure 8.

Work by Wang et al (8) on the transverse creep properties of unidirectional laminates tends to confirm the effect being resin dominated with considerably higher creep strains of the order 100×10^{-6} being produced after 2½ hours at a constant stress of 30% of ultimate at room temperature.

It was suggested following the SR and T programme thermal test that such movements could have off loaded the panel as the stresses built up and thereby helped it to survive a much lower temperature excursion.

Since no information was available on the creep properties of laminates at cryogenic temperatures it was decided to include some preliminary investigations as part of this programme.

2. Experimental Procedure

2.2.1 Improvement to Panel Fixing

For the SR and T programme, the panel and frame fixing holes were drilled 5.3mm in accordance with the standard defined for the Pallet. Test results showed that this clearance allowed for considerable bolt slippage during thermal cycling which prevented effective loading of the panel in the range $\pm 50^{\circ}\text{C}$.

Since the mathematical model assumed perfect fixing between the panel and frame at all temperatures it was proposed to tighten the tolerance on the fixing holes and if necessary fit each bolt individually.

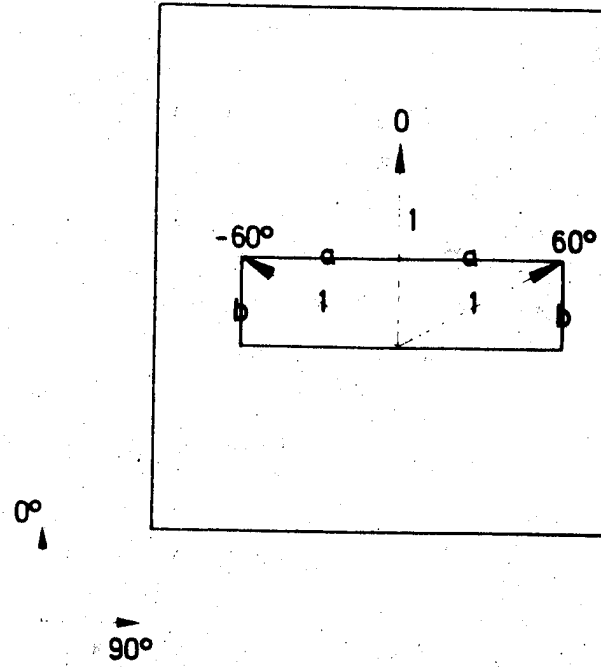
The same frame as that used for the SR and T programme was to be used for this Study and so in order to achieve close tolerance fixing it was necessary to bore out the existing 5.3 mm holes to 6mm. The specified tolerance was:

$$6\text{mm} + 0.018\text{mm}$$

This allowed the use of standard bi-hex, titanium pallet bolts to drawing no. HSD F3 92048 having a shank tolerance

$$5.990\text{mm} -0.012\text{mm}$$

There was therefore a maximum of 0.04mm free movement in each fixing as compared with 0.328mm in the SR and T thermal test.



$$\begin{aligned}\text{Resolved component in } 0^\circ \text{ direction} &= 1 + 2b = 1 + 2 \sin 30^\circ \\ &= 2\end{aligned}$$

$$\begin{aligned}\text{Resolved component in } 90^\circ \text{ direction} &= 2a = 2 \cos 30^\circ \\ &= 1.73\end{aligned}$$

Orthogonal Fibre Proportions for 0, 60, 120, Laminate Fig. 8.

2.2.2

Use of Improved Strain Gauges

Due to timescale limitations there was no scope during the SR and T programme for detailed investigation and subsequent procurement of specialised strain gauges. General purpose HSD manufactured gauges were therefore used in hand laid 0° , 60° , 120° rosettes. Several problems associated with these gauges were thought to have contributed errors to the strain readings:

- Instability at temperatures approaching -190°C
- Slight characteristic variations between gauges
- Large apparent strains at sub-zero temperatures
- Inaccuracy of hand laid rosettes.

It was proposed that high precision rosettes be used for this Study having certified apparent strain characteristics.

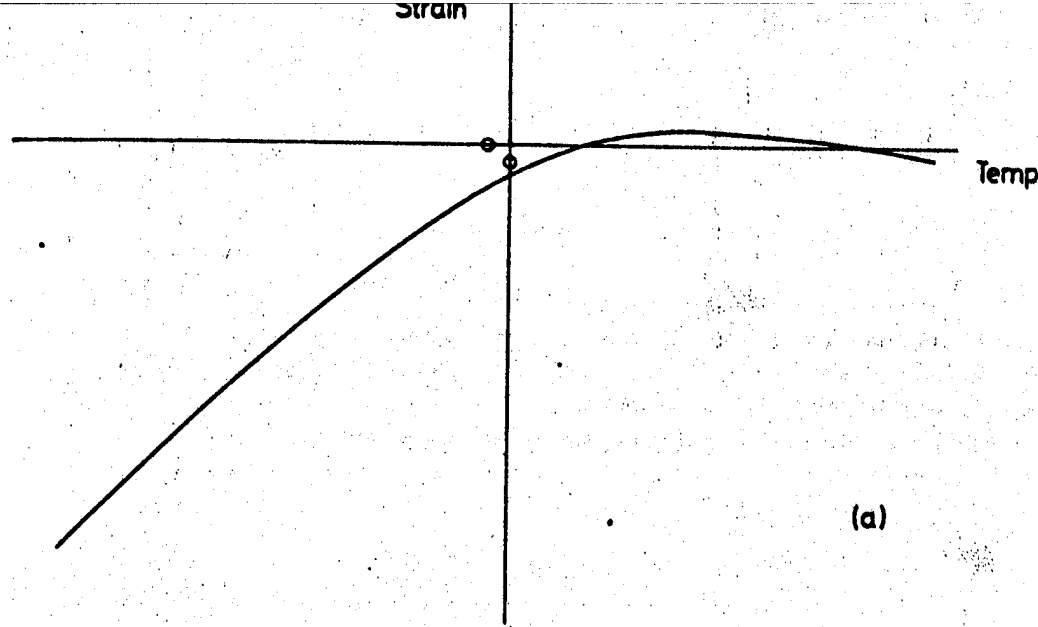
Precision gauges made by the Micro-Measurements Division of Vishay Intertechnology Inc. were identified as having the necessary attributes. A series of gauges is available for each type which allows for matching to specific materials via their expansion coefficient. By such matching the apparent strains and thus strain corrections can be minimised.

Members of the series are identified by an 'STC' number in the range 00 to 15 corresponding to expansion coefficients 0.03 to $26.1 \times 10^{-6}/^\circ\text{C}$. Gauges with STC number 03 corresponding to an expansion coefficient of 5.4×10^{-6} would have been ideal had there not been a prohibitive lead time.

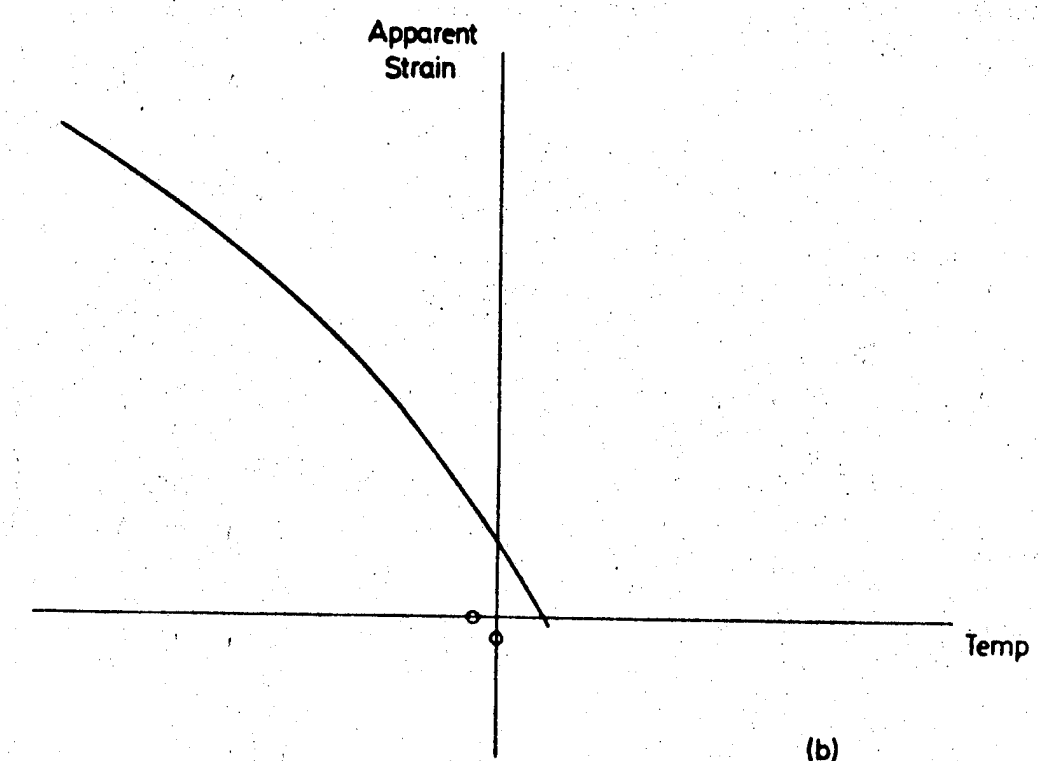
With the need for a quick delivery it was decided to select an aluminium matched gauge, STC 13, having a characteristic as shown in Figure 9(a) and then by using expansion coefficients determined by coupon testing of CFRP samples, derive a carbon fibre correction curve similar to that shown in Figure 9(b). See Reference (9). This derived curve would then be checked against readings from similar gauges fixed to an unrestrained CFRP faced honeycomb sample cycled to liquid nitrogen temperatures.

The exact designations for the chosen gauges and adhesives were as follows:

45° Rosettes:	WK-13-125RA-350
Linear:	WK-13-125AD-350
Adhesive:	M-Bond Type AE10/15
Outer coating:	M-Coat 'A' Polyurethane coating



(a)



(b)

Apparent Strain Characteristics for Strain Gauges

fitted to (a) Aluminium (b) A CFRP laminate

Fig. 9.

All these items were supplied by:

Welwyn Strain Measurement Ltd.
Armstrong Road,
Basingstoke RG 24 OQA
England.

The linear gauges were proposed for checking the stress distribution in the edge members. This was not investigated during the SR and T programme but was later thought to be important to the understanding of the overall distributions.

2.2.3

Improvements to Experimental Technique

The major problem encountered during the SR and T programme thermal test was that of control over the temperature stabilisations. Due to the relatively large thermal capacity of the aluminium frame there was a tendency towards the panel dropping rapidly in temperature well in advance of the frame. The problem was amplified by coarse cooling control provided by a valve on the Liquid Nitrogen (LN) supply line.

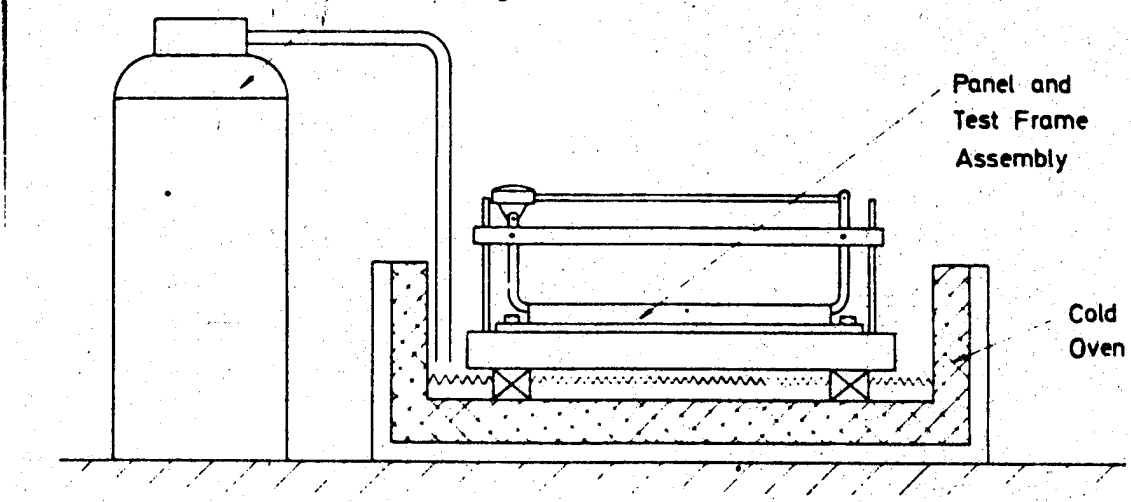
The original and improved schemes are shown in Figure 10. The improved version featured a completely enclosed oven in which it was considered a more uniform temperature environment could be achieved. LN was supplied to the oven reservoir by a manually controlled electric pump. Controlled amounts of Gaseous Nitrogen (GN) were then supplied to the test arrangement by means of heating coils evenly distributed inside the reservoir. By careful control of the rate of supply of LN to the reservoir and amount of energy supplied to the coils, it was predicted that more uniform temperature environments could be established.

Similarly it was thought that provision of a controlled heat electrical blower would allow more uniform warm up conditions.

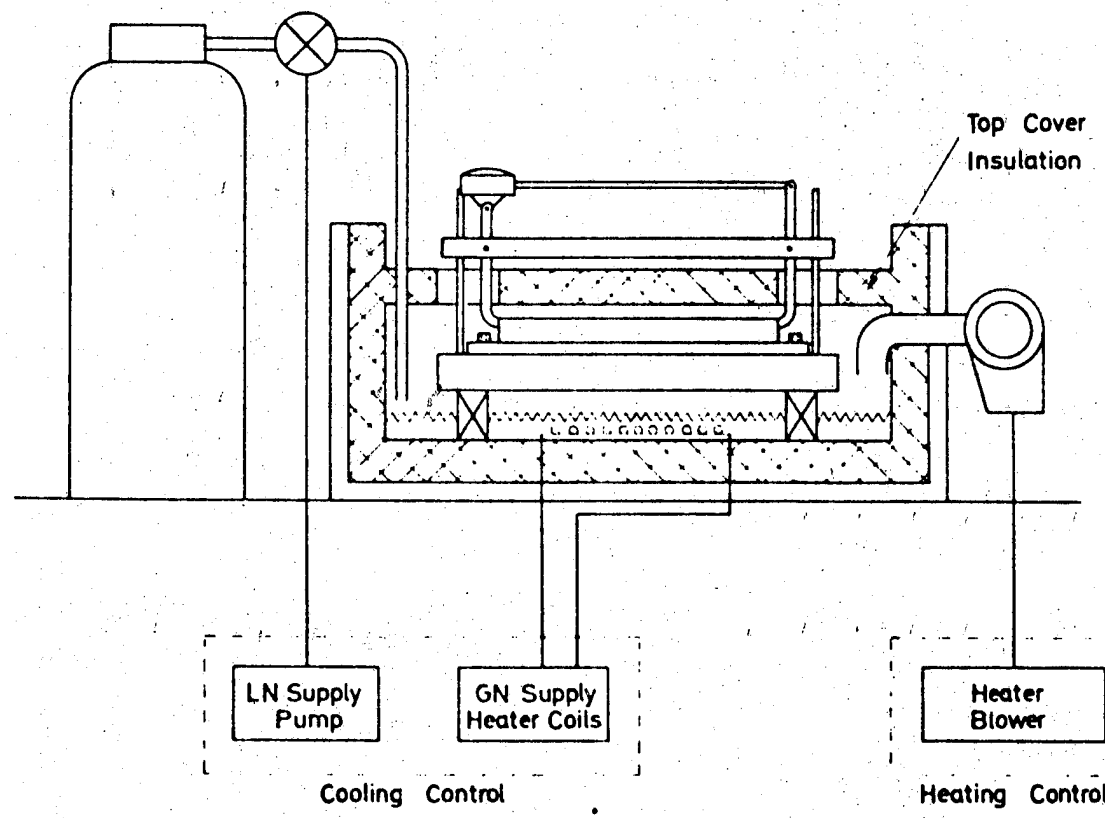
The Dial Test Indicator (DTI) distortion measuring arrangements (See Figure 11) were thought to be subject to errors from icing and thermal gradients between the measuring plane and the instrument plane. Icing was to be minimised in the new arrangement by means of the surface closure of the oven.

A method of overcoming the thermal gradient effect was proposed by the use of a low expansion support frame. Such a frame could have been made from rods of Invar or poltruded carbon fibre stock. Time and cost factors did not however allow this proposal to be pursued and so it was decided that an aluminium framework similar to that used previously would be used and corrections due to thermal gradients would be applied. Correction accuracy would be improved through better knowledge of frame temperature by means of an increased number of thermocouples.

Liquid Nitrogen Dewar



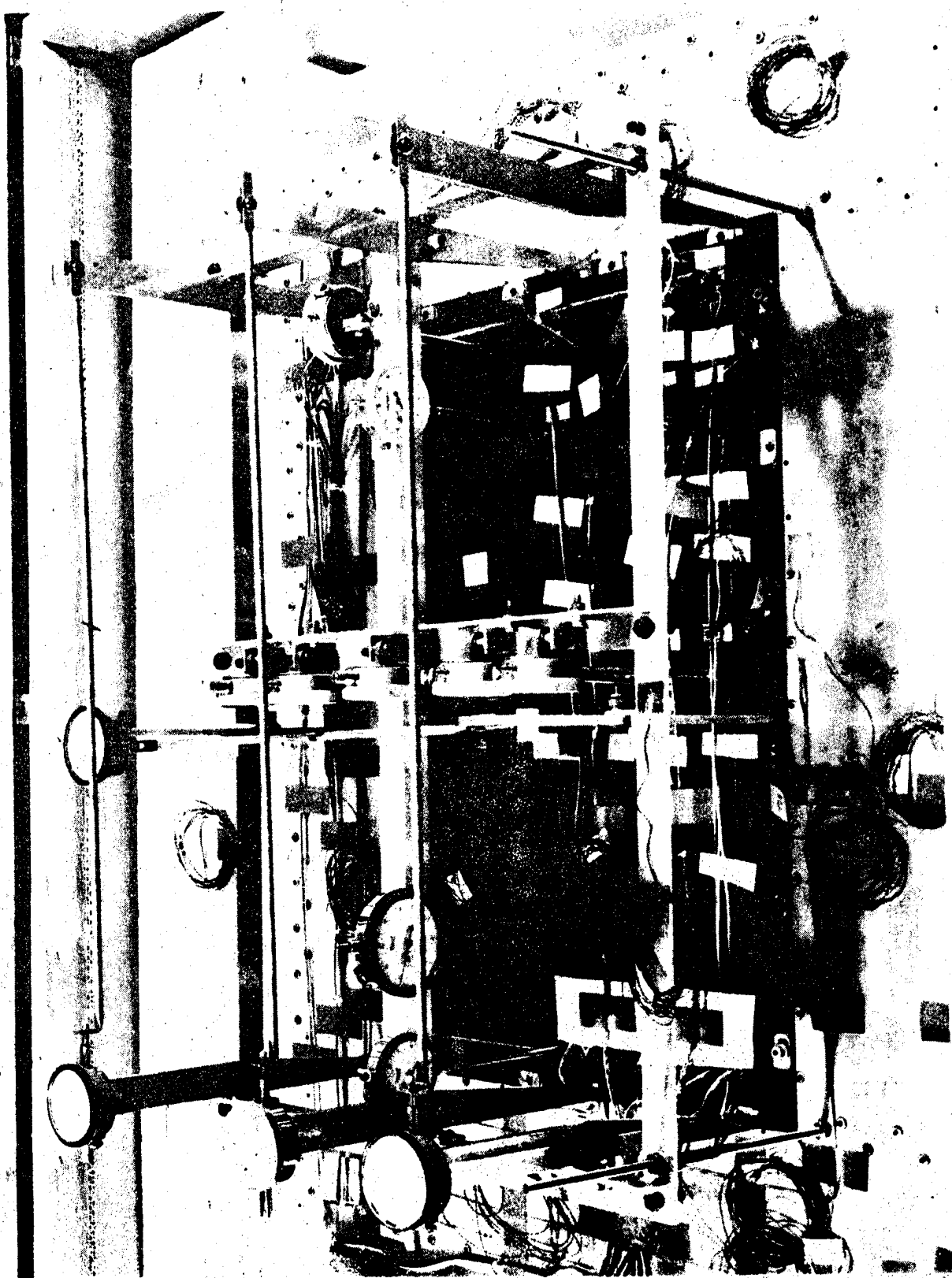
SR and T Programme Thermal Test
Arrangement



Improved Thermal Test Arrangement

20

Fig. 10.



DIAL TEST INDICATOR MEASURING ARRANGEMENT

FIG. 11

More thermocouples were also to be attached to the panel and frame to increase confidence in temperature uniformity.

2.2.4

Improvement to Data Logging

Data logging for the original test was a long and laborious task. It involved the use of a manually operated commutator for the selection of each channel and once selected the channel output had to be manually zeroed on a bridge to produce the required reading. Considerable temperature changes resulting in comparable errors could and probably did occur between the first and last readings.

To improve the scan time an automatic data logger was used for the revised test. This device scanned all channels and output the results on a line printer in a matter of seconds.

3. COUPON TESTING

3.1 Introduction

In order to provide the property/temperature relationships and failure modes required for the theory modifications analysed in Section 2, HSD TP 7600 proposed the following series of coupon tests:

- Unidirectional Specimens
 - longitudinal and transverse moduli and strengths
 - longitudinal and transverse compressive strengths
 - torsional or shear modulus and strength
 - principal Poisson's ratio
 - longitudinal and transverse coefficients of thermal expansion
 - flexural creep over 100 hours.

2 specimens were to be tested for each property at each of 5 temperatures (three temperatures only for flexural creep) in the range ambient to -196°C. The precise temperatures that were subsequently selected by AERE Harwell were as follows:

+20°, -60°, -100°, -170° and -196°C.

- Angle Ply (0/60/120 balanced lay-up)

- longitudinal and transverse tensile moduli and strength
 - longitudinal and transverse compressive strength
 - longitudinal and transverse coefficients of thermal expansion.

2 specimens were to be tested for each property at each of 3 temperatures in the range ambient to -196°C. The precise temperatures subsequently selected were as follows:

+20°C, -100 and -196°C.

(longitudinal and transverse directions were defined as being respectively parallel and at right angles to the 0° direction of the angle ply).

- Angle Ply faced Honeycomb Sandwich

- longitudinal and transverse coefficients of thermal expansion
- longitudinal and transverse compressive strengths.

2 specimens were to be tested for each property. The expansion measurements were to be in the range ambient to -70°C and the compressive strength at 3 temperatures in the range ambient to -196°C. The actual temperatures selected were as for the angle-ply specimens.

A full list of the specimen types and numbers is given in Appendix B.

3.2 Specimen Manufacture

3.2.1 Materials

Carbon Fibre

Unidirectional, angle ply and honeycomb faceskin laminates were manufactured from unidirectional carbon fibre prepreg sheet supplied to British Ministry specification NM547.

The exact requirements were as follows:

Fibre type	:	Courtaulds A-S
Resin type	:	Fothergill and Harvey Code 69
Nominal thickness	:	0.127mm at 60% volume fraction
Resin content	:	41 ± 3%
Flexural strength at 20°C*	:	≥ 1.5 GN/m ²
Flexural modulus at 10°C*	:	≥ 110 GN/m ²
Interlaminar shear strength at 20°C*	:	≥ 90 GN/m ²
Interlaminar shear strength at 120°C*	:	≥ 45 GN/m ²
Volatile content	:	≤ 1.5%

* Properties to be achieved from unidirectional laminates manufactured using a platten press according to the following cure cycle:

Gel at 160°C under contact pressure, cure for 1 hour at 160°C under 100 psi, post cure for 3 hours at 170°C.

Material was supplied by:

Fothergill and Harvey Ltd.,
Composite Materials Division,
Summit Littleborough,
Lancashire OL15 9QP,
England.

Honeycomb

The honeycomb type used for the sandwich specimens was as follows:

CIBA-Aeroweb Aluminium Honeycomb E142MPS* x 14 mm thickness.

This material was procured during the SR and T programme from:

CIBA-GEIGY (UK) Limited,
Bonded Structures Division,
Duxford,
Cambridge CB2 4QD,
England.

* Note this material designation is now defunct, the nearest equivalent specification is 3.4 - $\frac{1}{4}$ - 15.

Film Adhesive

The adhesive used for bonding the faceskins to the core for the sandwich specimens was as follows:

CIBA - Redux BSL 312UL

This material was procured from CIBA - Geigy (UK) Limited

3.2.2 Dimensions and Form

3.2.2.1 Longitudinal Tensile Modulus, Unidirectional Material

Specimens were 150mm x 10mm x 2mm with 50mm long aluminium end tabs bonded to either end. The inside edges of these tabs were chamfered to give an angle of 45°.

3.2.2.2 Longitudinal Tensile Strength, Unidirectional Material

As above except that the centre portion was reduced in thickness to 1mm, with a radius of 125mm.

3.2.2.3 Transverse Tensile Modulus, Unidirectional Material

Specimens were 50mm x 10mm x 2mm with 15mm long aluminium end tabs bonded to either end. The chamfer angle of the inside edges of the tabs was 45°.

3.2.2.4 Transverse Tensile Strength, Unidirectional Material

As in 3.2.2.3 except that the centre portion was reduced in thickness to 1.25mm, with a radius of 125mm.

3.2.2.5 Longitudinal Compressive Strength, Unidirectional Material

Specimens were 48mm x 10mm x 2mm, with the centre portion reduced in thickness to 1.35mm, with a radius of 125mm.

3.2.2.6 Transverse Compressive Strength, Unidirectional Material

As in 3.2.2.5 except that the centre portion was reduced in thickness to 1.6mm, with a radius of 125mm.

3.2.2.7 Shear Strength and Modulus, Unidirectional Material

Specimens were 150mm x 6.5mm with the centre 100mm turned down to a diameter of 6mm, with a 5mm radius at the shoulders.

3.2.2.8 Longitudinal and Transverse Thermal Expansion Coefficients, Unidirectional Material

Specimens were 20mm x 7.5mm x 1mm.

3.2.2.9 Longitudinal and Transverse Tensile Modulus and Strength, Angle-Ply Material

Specimens were 150mm x 35mm x 1.5mm with aluminium end tabs 35mm x 40mm bonded to either end. The inside end chamfer angle was 45°. The specimen width was reduced to 25mm, the shoulder radius being 75mm.

3.2.2.10 Longitudinal and Transverse Compressive Strength, Angle-Ply Material

Specimens were 48mm x 10mm x 2.25mm, with the centre portion reduced in thickness to 1.6mm, with a radius of 125mm.

3.2.2.11 Longitudinal and Transverse Coefficient of Thermal Expansion, Angle-Ply Material

Specimens were 20mm x 7.5mm x 2.25mm.

3.2.2.12 Longitudinal and Transverse Compressive Strength, Sandwich Material

Specimens were 70mm x 20mm x 14.76mm. The skins were each normally 0.38mm thick, and the aluminium honeycomb 14mm deep.

3.2.2.13 Coefficient of Thermal Expansion, Sandwich Material

Specimens were 10mm x 100mm x 14.76mm. Other details as in 3.2.2.12.

3.2.2.14 Flexural Creep Test Specimens, Unidirectional Material

Specimens were 155mm x 10mm x 2mm.

3.2.2.15 All dimensions quoted are nominal and in calculating the results of a given test the actual dimensions of the specimens were used. The geometry of the test samples used in Sections 3.2.2.4, 3.2.2.5 and 3.2.2.6 was as specified by (10). The longitudinal tensile strength test pieces employed were shorter and with a smaller waisting radius of curvature than recommended by (10), because of the machining facilities available. The shear modulus and strength test piece has been successfully used before by (11). The design of the angle-ply and skinned honeycomb samples were based on the experience of BAe, Stevenage and AERE, Harwell, in testing these materials.

3.2.3 Method of Manufacture

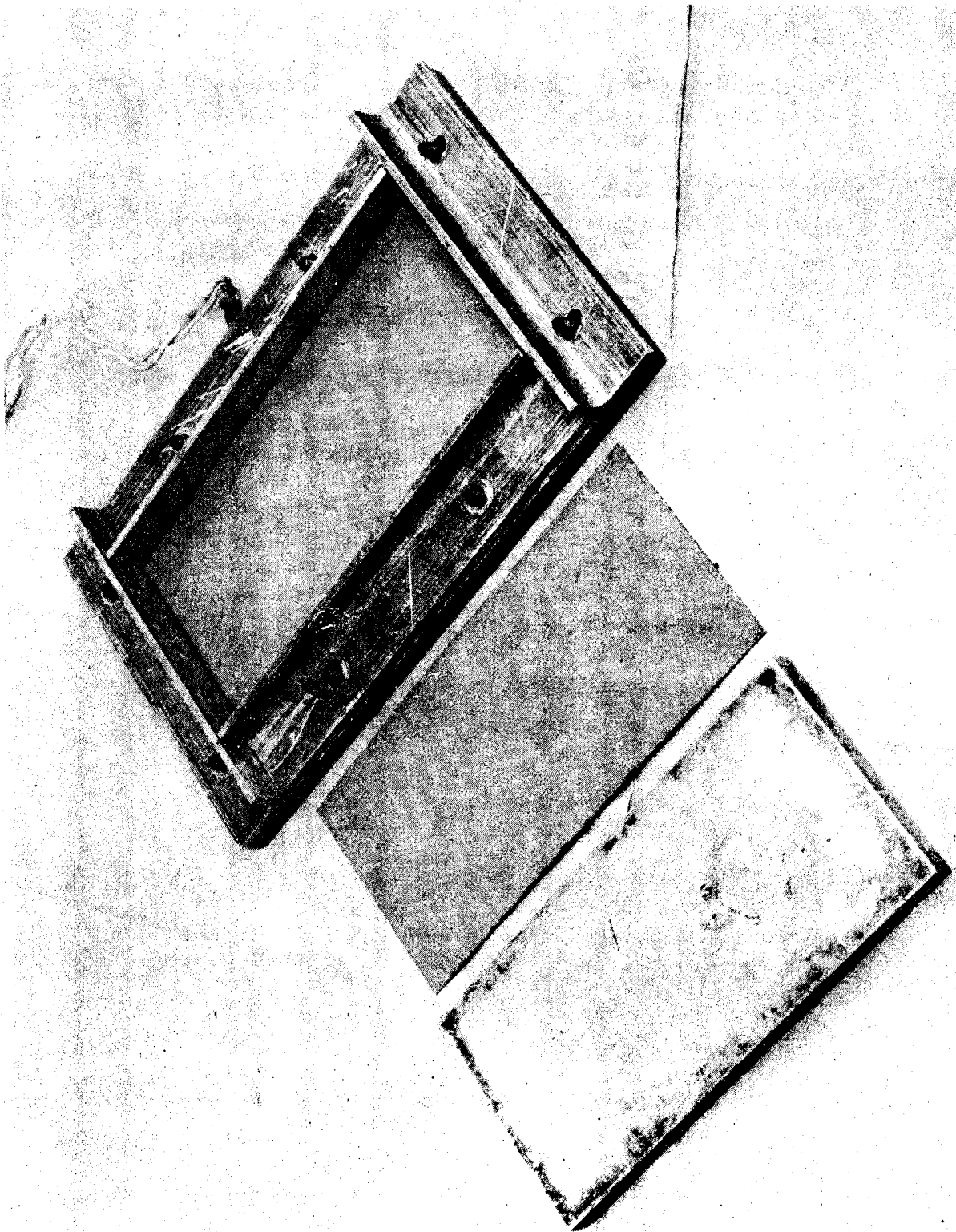
Unidirectional and Angle Ply Laminates

Specimens were cut using a Dessouter oscillating circular saw from larger press moulded plates. These plates were layed up and moulded using material as specified in para. 3.2.1 in accordance with BAe specification PSS/GP/50039. Special tools were used as shown in Figures 12 and 13.

Where applicable, aluminium doubler plates were bonded on following cutting to size, using CIBA Redux BSL 312 in accordance with the manufacturer's instruction sheet No. RTA 312a. A special jig was devised to ensure correct alignment during cure.

Honeycomb Specimens

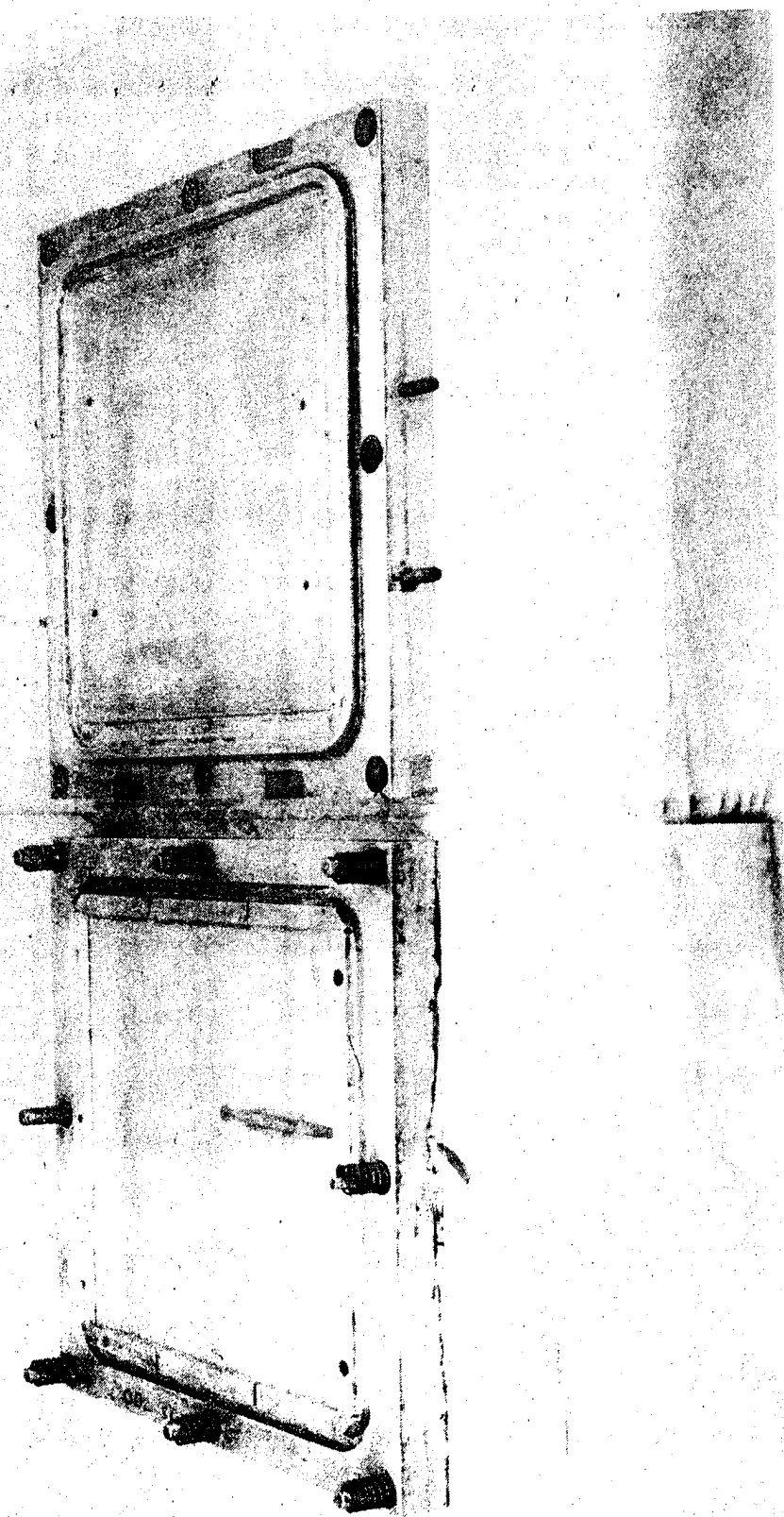
Specimens were cut from 260mm x 260mm panels using a Dessouter oscillating circular saw. The panels were manufactured in accordance with BAe specification PSS/GP/50074 using CFRP plates manufactured as above, adhesive in accordance with para. 3.2.1 and aluminium honeycomb in accordance with para. 3.2.1. The 'Vacuum Bag' technique was used.



23

120 mm x 75 mm LAY-UP TOOL

FIG. 12



260 mm x 260 mm LAY-UP TOOL

FIG. 13

3.3 Test Methods

3.3.1 Longitudinal and Transverse Moduli and Strengths

Tensile measurements were made by direct pulling of the specimens between the test machine jaws. A tensometer was used to determine moduli. Flexural measurements were made by using a 3 point loading rig using span to depth ratios of 25 : 1 and 16 : 1 for modulus and strength respectively. Exact methods were as specified in (12).

Tests were carried out using a 10,000kg floor model Instron testing machine as shown in Figure 14.

Low temperatures were obtained by surrounding the specimen with a coil of copper tubing through which cooled nitrogen gas or liquid nitrogen was circulated. See Figure 15. For measurements at 77°K the gas was blown directly over the specimen. Temperatures were monitored with thermocouples attached to the specimens, the time for the bulk of the specimen to achieve the temperature having been determined previously by inserting a thermocouple into the centre of the carbon fibre composite. Low temperature strain gauges were employed for modulus measurements. The temperature response of these when unloaded was determined in a separate set of experiments.

3.3.2 Longitudinal and Transverse Compressive Strengths

Steel end caps were used to measure specimen compressive strengths. These were 35mm long, 15mm deep and 1.0mm wide, with a central slot 20mm deep and parallel to the long axis, into which the specimen was bonded. The ends of the caps and specimens were machined square so that off-axis stressing was minimised.

Test machine and temperature control were as per para. 3.3.1.

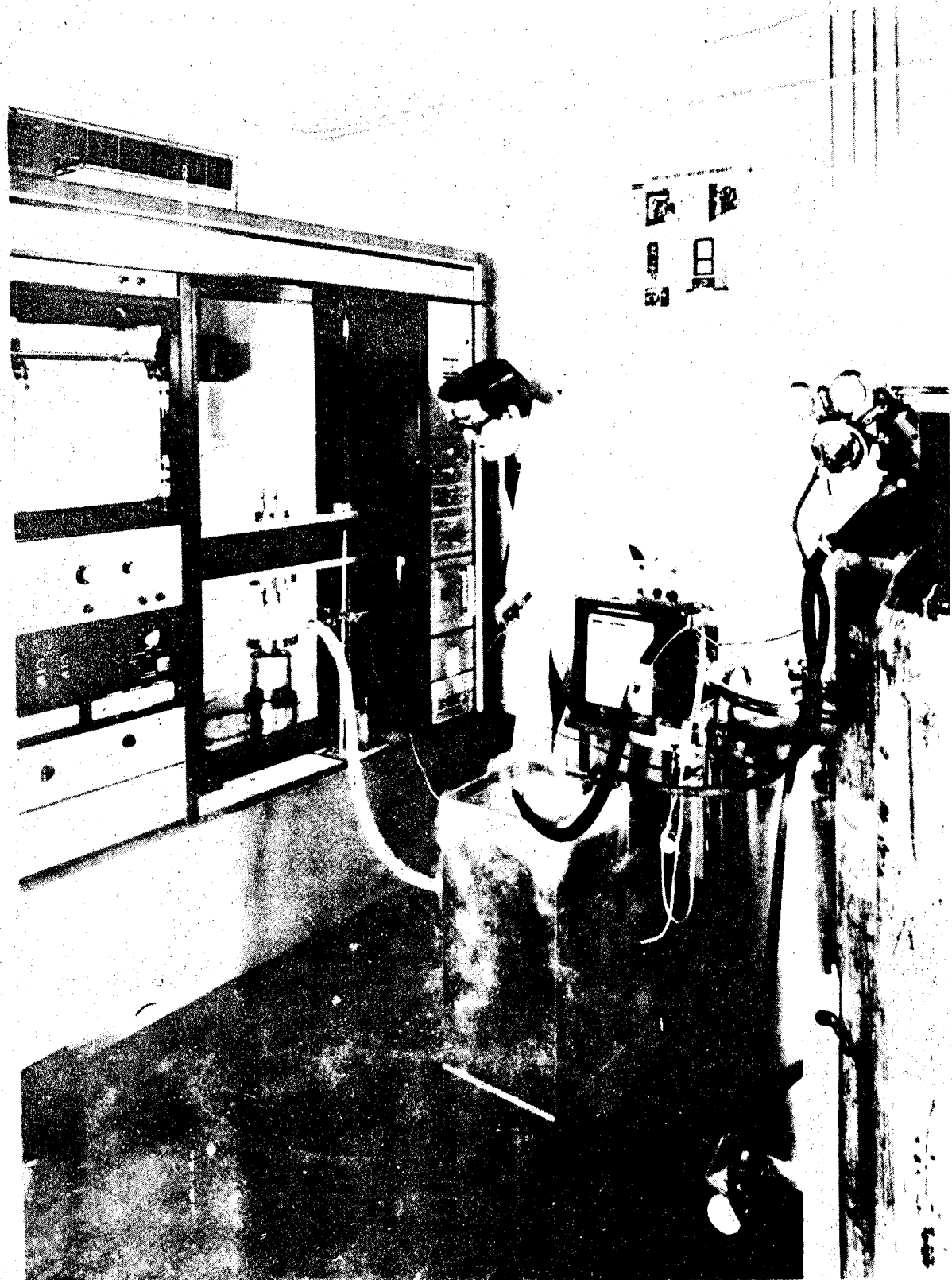
3.3.3 Torsional Test

Shear properties were determined in torsion using a rig and technique as described by (13).

Temperature control was as per para. 3.3.1.

3.3.4 Coefficient of Thermal Expansion

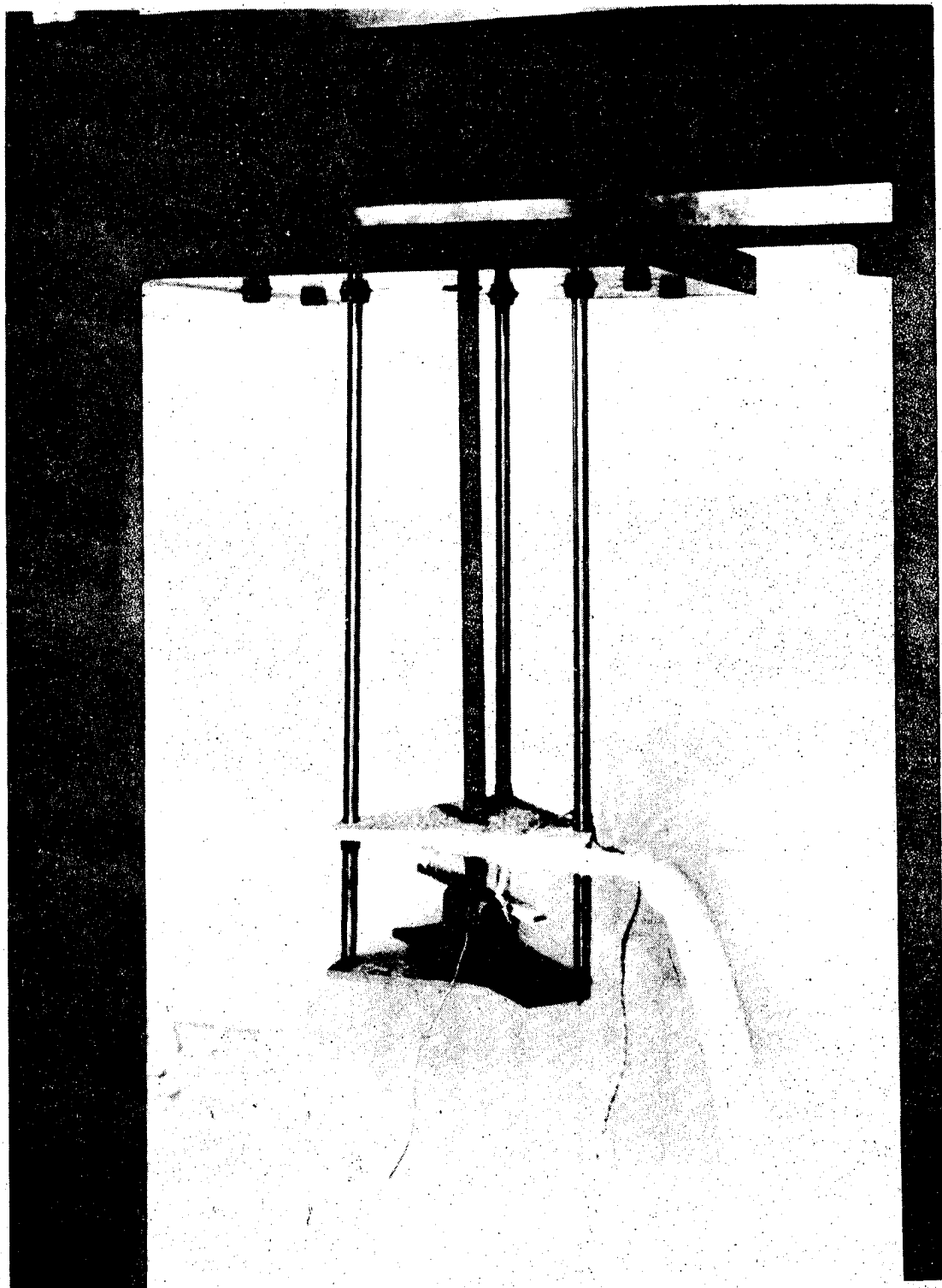
Measurements of the coefficient of thermal expansion of unidirectional and angle-ply materials were made using a Perkins Elmer dilatometer. Each specimen was cooled to liquid nitrogen temperature and allowed to stabilise. The temperature was then raised at a rate of 1.25°K/minute and the resulting change in length recorded. The silica correction was applied and the apparatus standardised using copper.



31

TEST MACHINE USED TO CARRY OUT SPECIMEN TESTS

FIG. 14



32

PHOTOGRAPH SHOWING SPECIMEN COOLING ARRANGEMENT
(Note that specimen was only a dummy)

FIG. 15

To determine the expansion characteristics of the honeycomb core sandwich panels, the method used by (14) was employed.

3.3.5 Flexural Creep

See Para. 3.4.4.

3.4 Results and Discussion

The results of the mechanical tests are shown in Figures 16 to 30. Thermal expansion data for the unidirectional and angle-ply material is given in Figures 31 to 34 and for the honeycomb samples in Figure 35. Results are the mean of two readings and the error bars represent the standard error of the mean.

3.4.1 Mechanical Properties of Unidirectional Material

The longitudinal and transverse tensile moduli and strengths for unidirectional material are shown, as a function of temperature, in Figures 16 and 17. The longitudinal modulus increases initially and then remains steady below 173°K. The transverse modulus, being primarily determined by the fibre/resin bond and nature of the matrix is much smaller and decreases below 173°K. The transverse strength is constant over the entire temperature range, but the longitudinal strength after rising initially shows considerable variation. For both types of test failure occurred in the gauge length, but the longitudinal samples showed extensive delamination through the thickness of the specimen, often extending back into the material under the end tabs. This could account for some of the spread in the results noted in Figure 17.

Longitudinal and transverse compressive strengths are shown in Figure 18. These properties were difficult to measure at sub-zero temperatures because the recommended test jig, (14), proved to be too massive to be cooled satisfactorily, and an alternative had to be employed. The transverse compressive strength is low but remains reasonably constant with falling temperature. Longitudinal compressive strengths are less than the corresponding tensile values, there is a large spread, and also a considerable drop at lower temperatures. Failure usually occurred in the gauge length, often, for longitudinal samples, with localised delamination between plies. Some of the specimens were found to have a void content approaching 2.5% by volume and it has been noted, (14), that this leads to reduced compressive properties.

The shear modulus, strength and angular deflection at failure are shown in Figures 19 to 21. The modulus increases with decreasing temperature indicating an increase in the resin modulus since the fibre properties are not affected by low temperatures, (15).

The increase in resin modulus required to cause this change can be calculated using the appropriate Halpin-Tsai equation, (16). Assuming that the shear modulus of A-S carbon fibre is 24 GPa, (17), and that the fibre volume loading is 60%, the resin shear modulus must increase from 1.2 to 1.7 GPa to cause the observed change in composite shear modulus.

It is reasonable to expect that as the resin gets stiffer its shear strength will increase and strain at failure decrease, trends shown in Figures 20 and 21. As the torque deflection characteristic is not linear to failure it is not possible to relate shear strength and shear failure strain directly. All the torsional specimens showed longitudinal surface cracking after failure, and sectioning and polishing revealed severe cracking in specimens tested at 293, 123 and 77°K. Photographs of the cracks are shown in Figures 22 to 24. In each case the crack starts at the surface and runs for several millimetres into the specimen often linking up with voids that tended to accumulate between layers of prepreg. The photographs also provide a good indication of the fibre distribution in the specimens.

3.4.2

Mechanical Properties of Angle-ply Material

The influence of temperature on the longitudinal and transverse tensile moduli and strengths, the compressive strengths and Poisson's ratios of 0, 60, 120° balanced, angle-ply laminates are shown in Figures 25 to 28. Allowing for the errors involved, tensile properties and Poisson's ratio are similar in either direction, and show no significant change with temperatures. Compressive properties show more scatter and a possibly significant difference at 77°K. In the tensile tests most specimens failed in the gauge length, approximately equal numbers breaking straight across and at an angle of 60° to the long axis. It was not possible to correlate the mode of failure with either temperature or strength. In compression several specimens failed at the shoulder but most suffered severe delamination of the outer plies, within the gauge length. These compressive specimens were waisted in depth. If this operation was not carried out so as to leave an equal distribution of material about the centre plane in every case, variation is to be expected among the results.

It is possible to calculate the elastic constants of the balanced angle-ply material in terms of those of the unidirectional material, assuming that all the plies making up the laminate are strained equally, (12). Values for the longitudinal and transverse tensile moduli and shear modulus of the unidirectional material at temperatures of 293, 173 and 77°K have been taken from the previous experimental results in Figures 16 to 19. It is assumed that the principal Poisson's ratio, ν_{12} , of the unidirectional composite, is 0.3 and that it remains constant over the temperature range considered. From the relation:

$$\nu_{21} E_{11} = \nu_{12} E_{22} \quad \dots (1)$$

where E_{11} and E_{22} are the longitudinal and transverse tensile moduli, ν_{21} is found to be 0.026 at 293, 0.025 at 173, and 0.0156 at 77°K. The reduced stiffnesses (Q_{11} , Q_{22} , Q_{12} , Q_{66}) can now be calculated and hence the elastic constants (A_{11} , A_{22} , A_{12}), moduli and Poisson's ratios (E_{11} , E_{22} , ν_{12} , ν_{21}) of the 0, 60, 120° balanced angle-ply laminate derived. For full details reference 16, should be consulted. The results of these calculations are listed in Table 4. The moduli and Poisson's ratios in the two directions are equal. The agreement between calculated and experimental tensile moduli is good at 173°K. Above and below this temperature calculated values are rather less than observed ones. Agreement between calculated and observed Poisson's ratios is good at 293 and 173°K, but the calculated value is low at 77°K. Errors in the data obtained on the unidirectional material will carry over and affect calculated values for the angle-ply laminates, and this together with the assumption concerning the major Poisson's ratio of the unidirectional composite and its constancy with changing temperature would contribute to the discrepancies mentioned.

The calculation of the failure strength of an angle-ply laminate is more difficult, (16). However a simple estimation can be made by assuming that each ply contributes proportionately to the overall strength. Take the room temperature strength and strain properties of unidirectional material to be 1450, 55 and 80 MPa, and 0.014, 0.006 and 0.024, for the longitudinal, transverse and shear strengths and strains respectively. Using the stress transformation equations developed in (18) and assuming each ply contributes fully to the overall strength, the longitudinal and transverse strengths of the angle-ply laminate are both equal to 752 MPa, compared with a measured value of 400 MPa. Compressive properties can be calculated in a similar manner. A more rigorous approach based on the work of (19) and incorporated in an in-house developed BAe Computer Programme gave values of 300 MPa and 240 MPa in the 0° and 90° directions respectively which agree more closely with the measured value.

A calculation of the strains in the 60 and 120° laminates shows that these should fail before the 0° ply. The effect of a ply failure at an intermediate stress and the resultant stress redistribution might cause stress transients and overloading effects that could help account for the differences between calculated and measured values.

3.4.3

Mechanical Properties of Sandwich Material

The longitudinal and transverse compressive strengths of the aluminium honeycomb/carbon fibre composite skin, sandwich panels is shown in Figure 29. In both cases the skins and core were loaded in parallel, the difference being that in the longitudinal case the distance between the loading faces was 60mm while for the other case it was 10mm. The results for the two types of specimen are similar and virtually independent of temperature. Numerical results have, in either instance, been calculated on the overall dimensions of the samples. The stress at failure in the carbon fibre skins was of the order of 100 to 150 MPa. Failed longitudinal specimens exhibited skin buckling and sometimes shear failure at one end and delamination between skin and core. Transverse ones showed core and skin buckling and sometimes shear damage in the skins.

3.4.4

Flexural Creep

To investigate flexural creep specimens were loaded to 500N (75% of the failure load) in an Instron testing machine and allowed to remain thus for 100 hours. The tensile strain on the lower surface was monitored with a strain gauge. After the first few minutes, very little change in strain or applied load was noted and virtually no creep occurred. At the end of the 100 hour period the flexural strength and modulus of the specimens were measured at room temperature. The results, with readings on unstressed specimens, are shown in Figure 30. The flexural strength is substantially constant and independent of prestressing, but the modulus shows a marked fall off when stressed at 173 or 77°K. Since only two specimens were tested at any one temperature this difference could be associated with, for instance, a higher fibre volume loading, rather than creep damage. No specimens showed any visual evidence of damage after stressing in the creep rig.

3.4.5

Thermal Expansion Properties

Typical curves relating the fractional change in length of a specimen with the change in temperature are shown in Figures 31 and 32. The former is for unidirectional material in the longitudinal direction and the latter for an angle-ply specimen in the transverse direction. In most cases the curves were as shown in Figure 31, but in two cases for angle-ply material tested in the transverse direction, a marked decrease in slope occurs, as shown in Figure 32, this result was repeatable. It appears as if the specimens started to bend at about 200°K rather than simply change in length, and it was suggested that this might be due to an excess of fibre on one side. Sectioning and polishing did not support this conjecture; the carbon fibre and ply distribution was even and very few voids were present. The effect is presumably due to coupling between layers, because of differences in bonding, which did not show up in the optical examination.

TABLE 4
Calculated Elastic Constants for a 0, 60, 120° Angle-Ply Laminate

		293°K	173°K	77°K
Unidirectional Material	Q_{11} (GPa)	105.8	120.9	116.5
	Q_{22} (GPa)	9.01	10.07	6.03
	Q_{12} (GPa)	2.72	3.02	1.81
	Q_{66} (GPa)	3.6	4.6	5.6
	$Q_{16} = Q_{26}$ (GPa)	0	0	0
Angle-Ply Material	A_{11} (GPa)	45.6	52.27	50.26
	A_{22} (GPa)	45.6	52.27	50.26
	A_{12} (GPa)	15.69	16.33	13.87
Elastic Moduli of Angle-Ply Material	E_{11} (GPa)	40.2	47.2	46.4
	E_{22} (GPa)	40.2	47.2	46.4
	ν_{12}	0.34	0.31	0.28
	ν_{21}	0.34	0.31	0.28

The coefficients of the thermal expansion (CTE) derived from the fractional length change curves are shown as a function of temperature in Figures 33 and 34. For unidirectional specimens along the fibre direction the CTE is small and virtually constant with decreasing temperature, but in the transverse direction where the resin is dominant, the CTE is much larger and increases rapidly with rising temperature. Results for the angle-ply material are similar in both the principal directions and of the same magnitude as the longitudinal results for the unidirectional material. The individual curves for nominally similar specimens give an indication of the variation in CTE to be expected. Calculated CTEs, (16), are listed in Table 5. They are the same for both longitudinal and transverse directions. The values, though of the same order of magnitude as those measured, are rather higher, with a maximum at 173°K. They were obtained using reduced stiffness data from Table 4 and experimentally determined CTEs for the unidirectional material. The discrepancies between calculated and measured results no doubt reflect errors in the experimental data for the unidirectional specimens.

TABLE 5
Calculated Thermal Expansion Coefficients of
0, 60, 120° Angle-Ply Laminate

	293°K	173°K	77°K
CTE °K^{-1}	2.93×10^{-6}	3.82×10^{-6}	3.1×10^{-6}

The change in length of sandwich panels, at right angles to the long glue line in the honeycomb, is shown in Figure 35. Similar results were noted along the glue line and for another sandwich sample. Each point is the average of three readings. For either direction, and sample, the CTE was constant over the temperature range 200 to 300°K. Individual values are listed in Table 6. Previously, with this type of specimen, it was noted, (13), that the CTE along the long glue line is greater than at right angles to it by a factor of about 2, because of the preferential expansion of the aluminium. In this work there is no clear distinction between the two cases. It appears that the skins completely suppress the effects of its expansion on those of the overall sandwich panel. In some ways this is surprising as a careful examination revealed that the fibre layer immediately adjacent to the honeycomb was at right angles to the long glue line, that is in the worst direction to resist expansion of the core.

TABLE 6

Measured Thermal Expansion Coefficients
For Sandwich Specimens

	Temp range °K	Along long glue line	Transverse to long glue line
CTE $^{\circ}\text{K}^{-1} \times 10^{-6}$	203-303 (Specimen 1)	3.82 $^{+0.13}_{-0.21}$	3.30 $^{+0.16}_{-0.11}$
	203-303 (Specimen 2)	2.89 $^{+0.23}_{-0.12}$	3.82 $^{+0.13}_{-0.11}$

3.5 Conclusions From Specimen Testing

A variety of thermal and mechanical properties of unidirectional, balanced 0, 60, 120° angle-ply laminate, and sandwich specimens have been determined over the temperature range 77 to 293°K. Moduli tended to increase with falling temperature, but the behaviour of strength, particularly compression strength, was more erratic. The thermal expansion of unidirectional material parallel to the long axis was constant, while perpendicular to this direction the CTE increased with increasing temperature. For angle-ply specimens there was a small increase in CTE with decreasing temperature. The CTEs for sandwich specimens were similar in directions along and at right angles to the long glue line in the honeycomb.

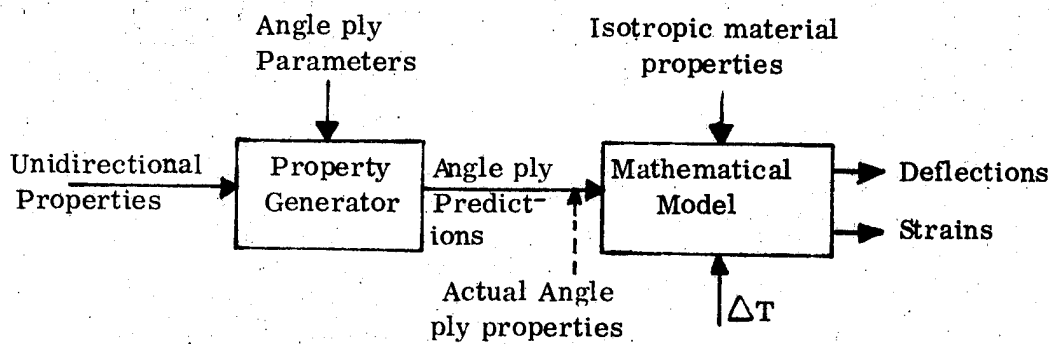
Calculated modulus, strength and CTE values for the angle-ply material tended to be higher than the measured values, particularly for strength. This would be expected since the theoretical values assume a perfect transformation of the unidirectional properties which can never be fully realised in practice.

It has been BAe's experience with modulus values that providing good unidirectional data is used (for example, not information presented in Manufacturers' Data Sheets) then classical theory gives an accurate prediction of angle-ply performance. Furthermore, the magnitude of the discrepancies provides a good indication of the quality of the laminate.

Larger discrepancies that have been found for the strength values are explained as in para. 2.1.3 and can be traced to the failure criteria assumed by the theory.

Selection of Material Inputs for Model

The main aim of the specimen test programme was to provide accurate material data for the mathematical model. The analysis as finally envisaged would use only unidirectional properties, generating angle-ply predictions for the model as shown below.



This would allow complete flexibility of the chosen lay-up. As has been demonstrated, however, by the test programme there are errors associated with angle-ply predictions and so the first consideration was the direct input of actual angle-ply data obtained from the testing.

The mathematical model requires the following material properties for the carbon fibre panel elements.

E_X	=	longitudinal tensile modulus
E_Y	=	transverse tensile modulus
G	=	shear modulus
α_{XC}	=	longitudinal CTE for carbon fibre alone
α_{YC}	=	transverse CTE for carbon fibre alone
ν_{XY}	=	Poisson's Ratio $X \rightarrow Y$
ν_{YX}	=	Poisson's Ratio $Y \rightarrow X$
α_{XH}	=	longitudinal CTE for CFRP faced honeycomb
α_{YH}	=	transverse CTE for CFRP faced honeycomb

For the particular finite element package used for this Study the properties were required to be orthotropic and it has been proved by theory and test that for the 0° , 60° , 120° lay up this is the case.

$$\text{Hence } E_X = E_Y = E$$

$$\alpha_{XC} = \alpha_{YC} = \alpha_C \quad \alpha_{XH} = \alpha_{YH} = \alpha_H$$

$$\nu_{XY} = \nu_{YZ} = \nu$$

As was discussed in para. 2.1.2 it was decided to run the model through a series of temperature decrements using average material properties obtained from the test programme for corresponding decrements.

The chosen decrement was 50°C and from Figures 25, 28, 34 and 35 the following average properties can be derived:

TABLE 7

Temperature Range $^\circ\text{C}$	E^* GN/m^2	α_C^* $\times 10^{-6}/^\circ\text{C}$	α_H^{**} $\times 10^{-6}/^\circ\text{C}$	ν^*	G^{***} GN/m^2
$20 \rightarrow -30$	49	1.5	3.5	0.34	16.0
$-30 \rightarrow -80$	48	1.8	3.5	0.33	16.8
$-80 \rightarrow -130$	49	1.9	3.5	0.32	17.6
$-130 \rightarrow -180$	53	2.4	3.5	0.32	17.7
Average	50	1.9	3.5	0.33	17.0

* For a property M, from the relevant graph

$$M = \frac{M_{Xt2} + M_{Xt1} + M_{Yt2} + M_{Yt1}}{4}$$

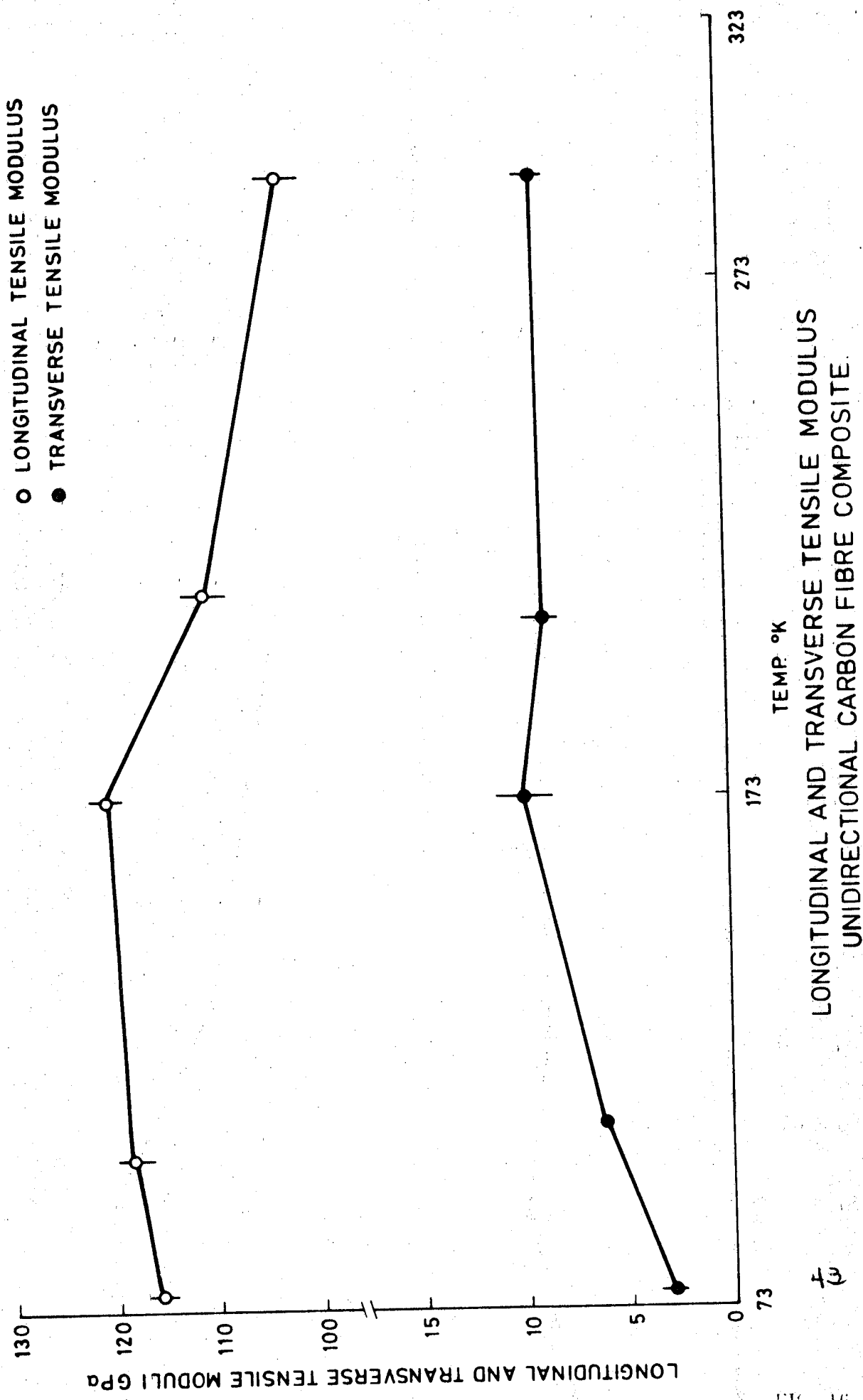
where X = longitudinal direction
 Y = transverse direction
 t₁ = lower temperature bound
 t₂ = upper temperature bound

** Honeycomb expansion coefficient was found to constant. These values are average of those given in Table 6.

*** Shear moduli from Figure 9 were used in conjunction with values of E and ν to give by computer analysis, these predicted values. See Figure 19B.

It can be seen from the table that the changes in property with temperature are very small and would not account for the large discrepancies observed during the SR and T programme. It was therefore decided, in view of the high costs involved with multiple computer runs, to use the average values given at the foot of Table 7.

Section 6 of this report details the findings of the parallel practical tests and Section 7 compares the results obtained from the model, using the above input parameters, with these test results.



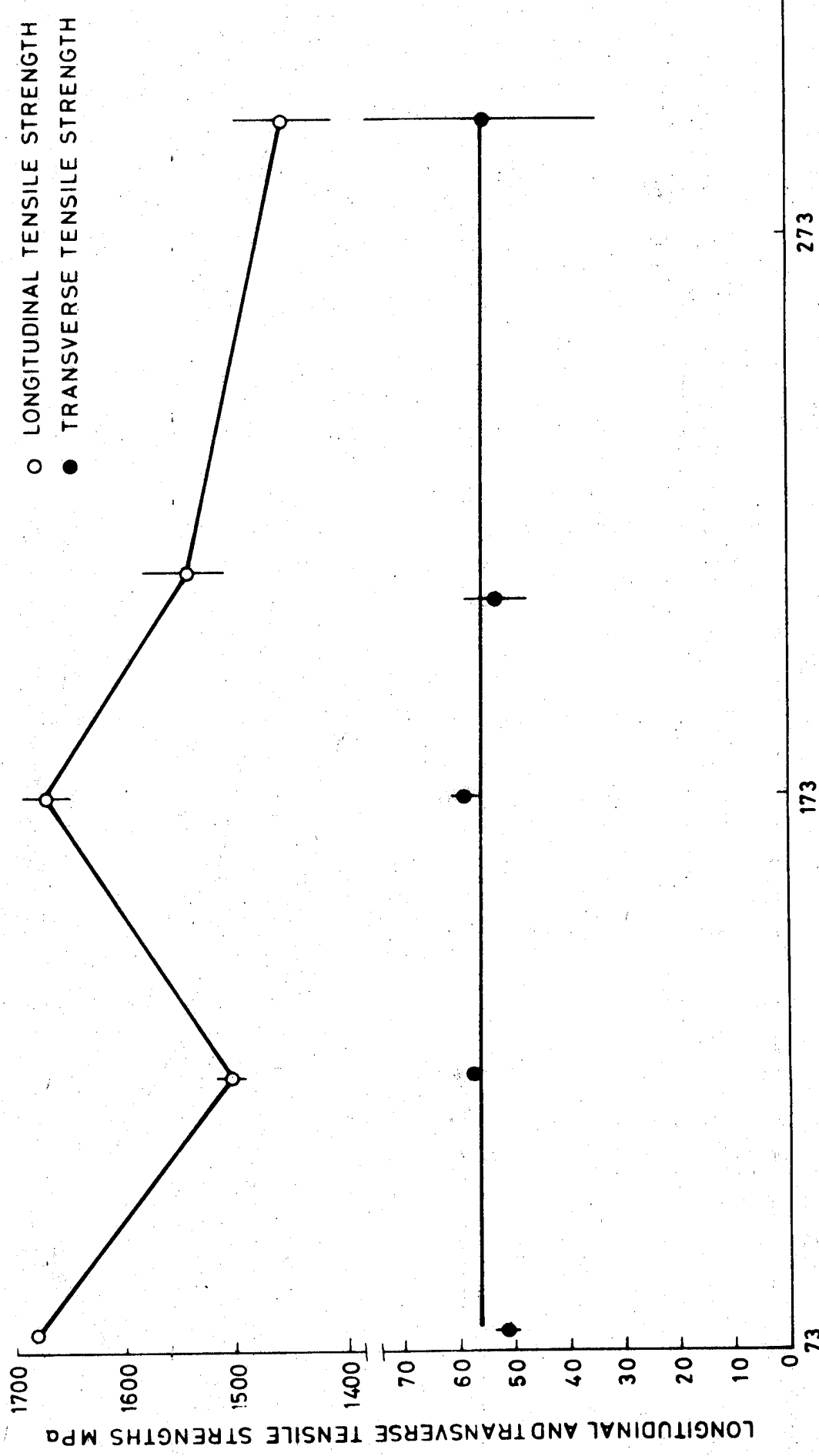


FIG. 17

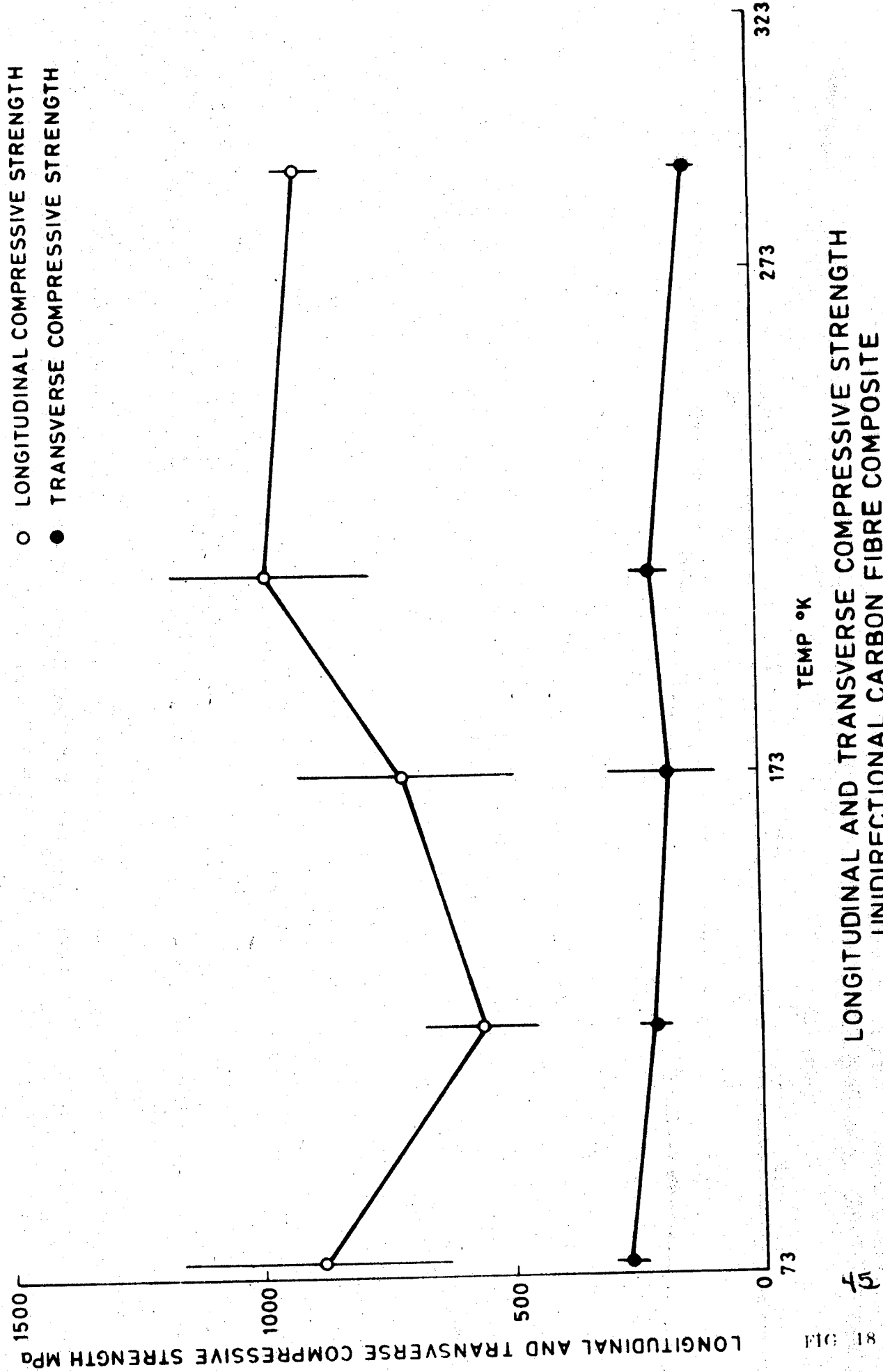


FIG. 18

UNIDIRECTIONAL CARBON FIBRE COMPOSITE.

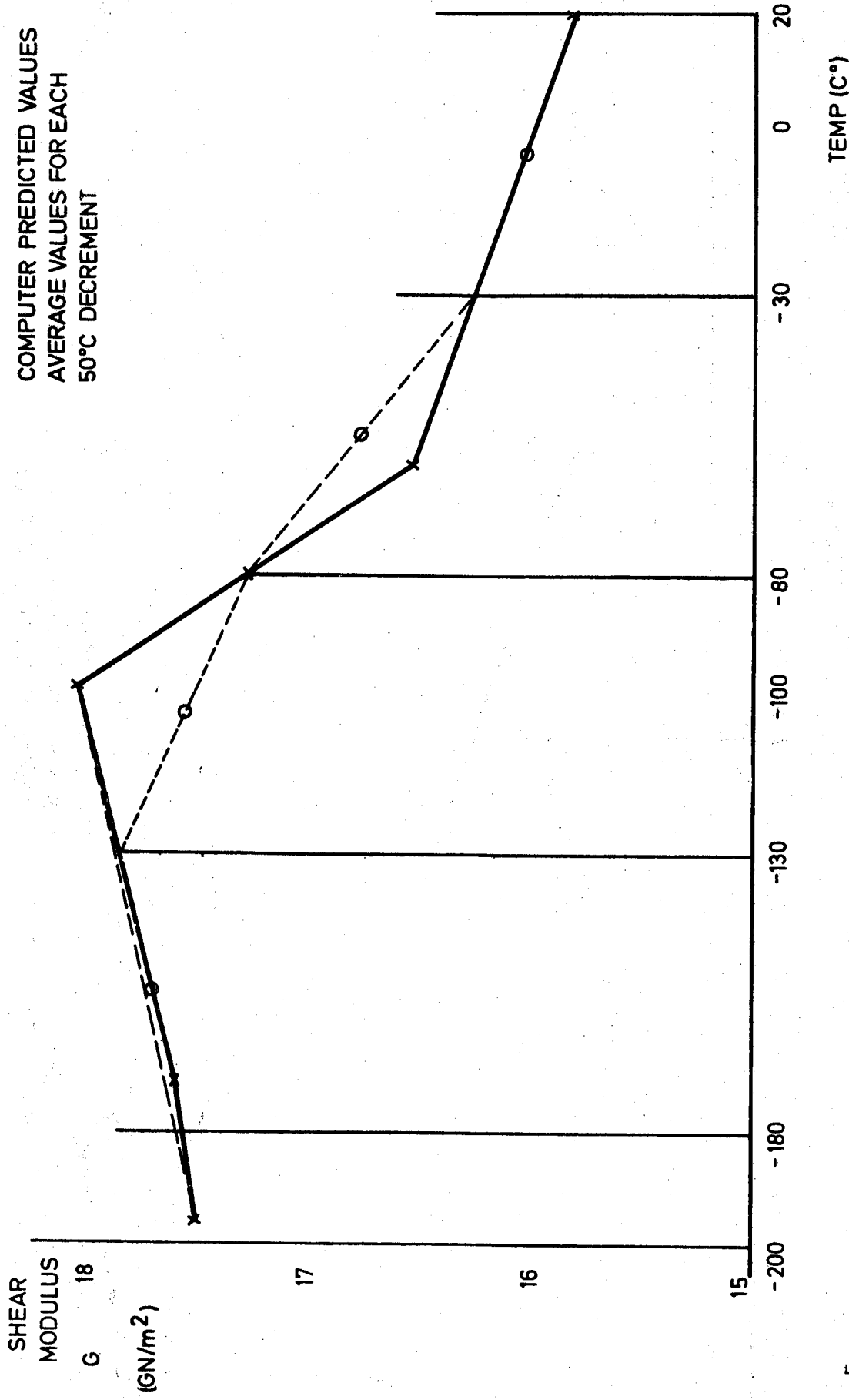
SHEAR MODULUS

TEMP. °K



FIG. 19A

COMPUTER PREDICTED VALUES
AVERAGE VALUES FOR EACH
50°C DECREMENT



GRAPH OF PREDICTED ANGLE PLY SHEAR MODULUS AGAINST TEMPERATURE FIG. 19 B

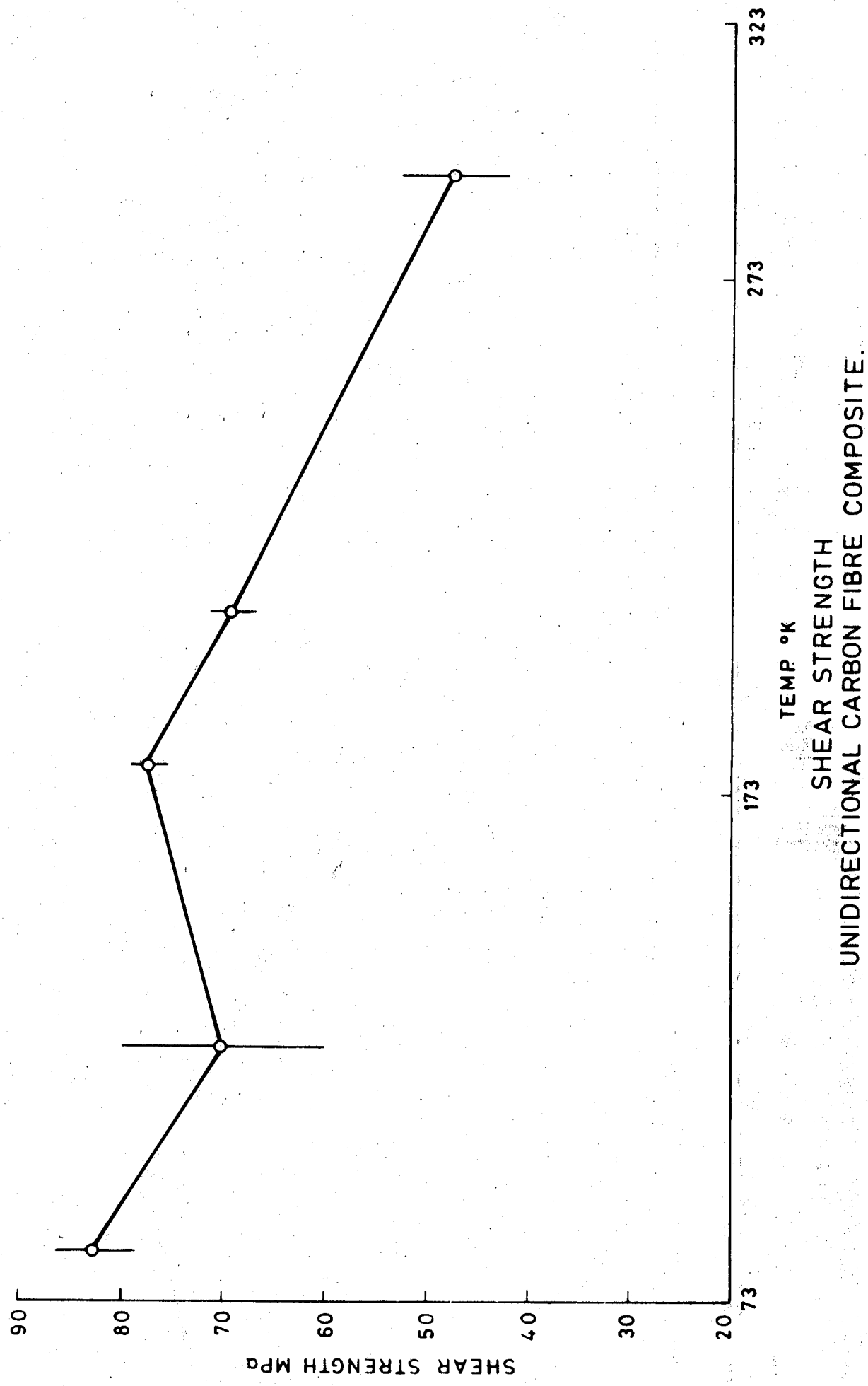
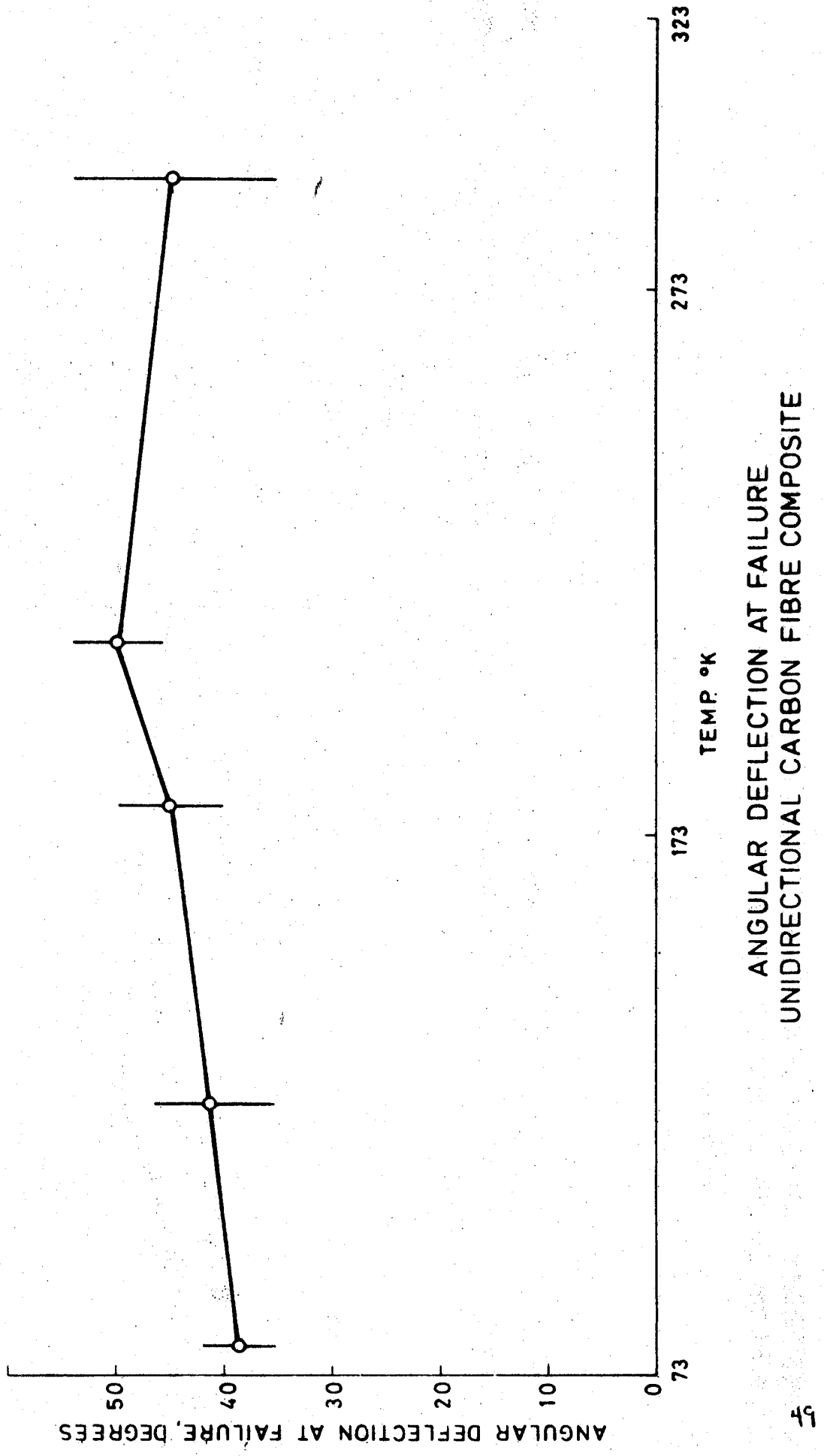


FIG. 20



ANGULAR DEFLECTION AT FAILURE
UNIDIRECTIONAL CARBON FIBRE COMPOSITE

FIG. 21

50

MICROGRAPH SHOWING CRACKING AND FIBRE DISTRIBUTION
IN SHEAR SPECIMEN

FIG. 22



MICROGRAPH SHOWING CRACKING AND FIBRE DISTRIBUTION
IN SHEAR SPECIMEN

FIG. 23

51



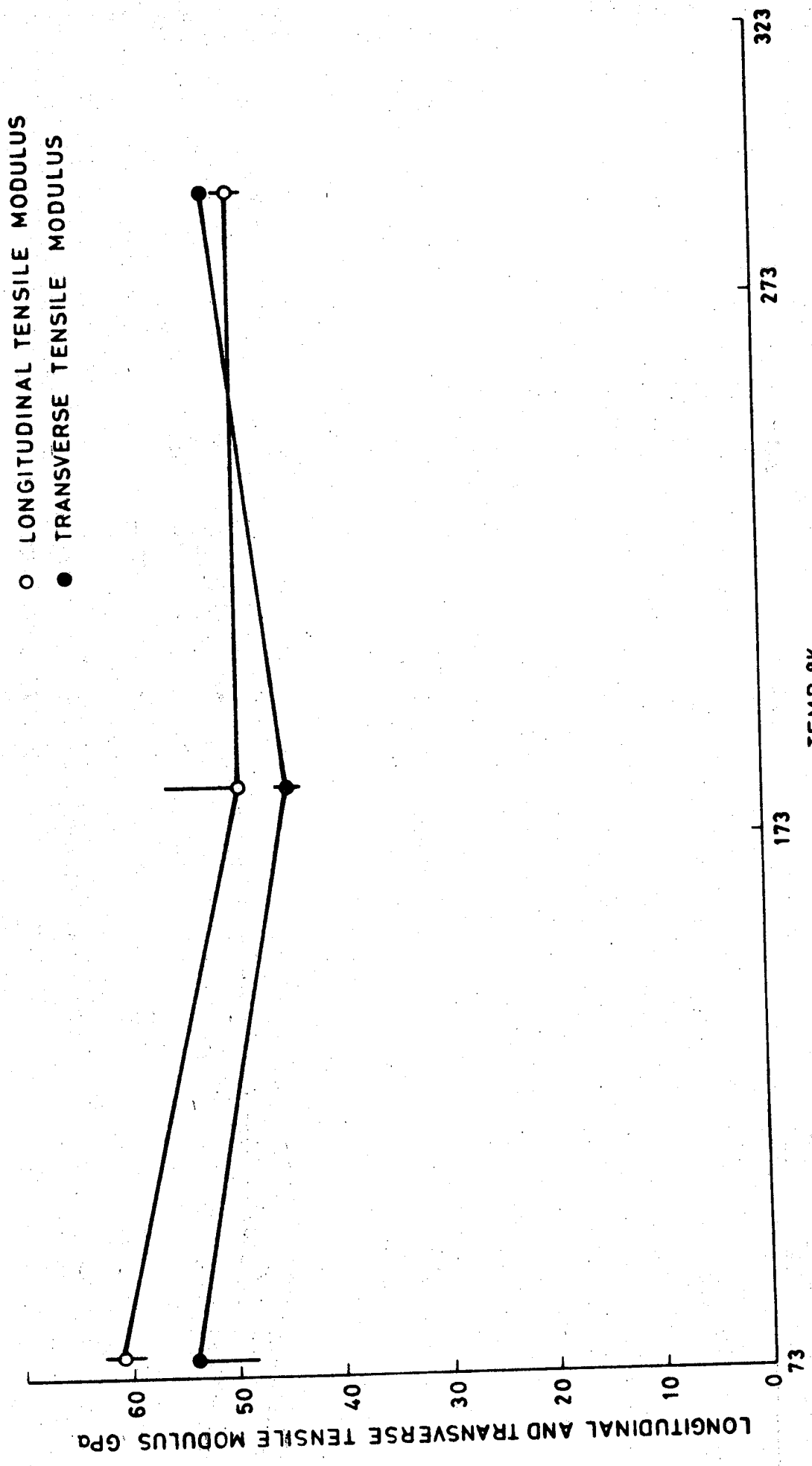
52

MICROGRAPH SHOWING CRACKING AND FIBRE DISTRIBUTION
IN SHEAR SPECIMEN

FIG. 24

LONGITUDINAL AND TRANSVERSE TENSILE MODULUS
ANGLE PLY CARBON FIBRE COMPOSITE.

FIG. 25



53

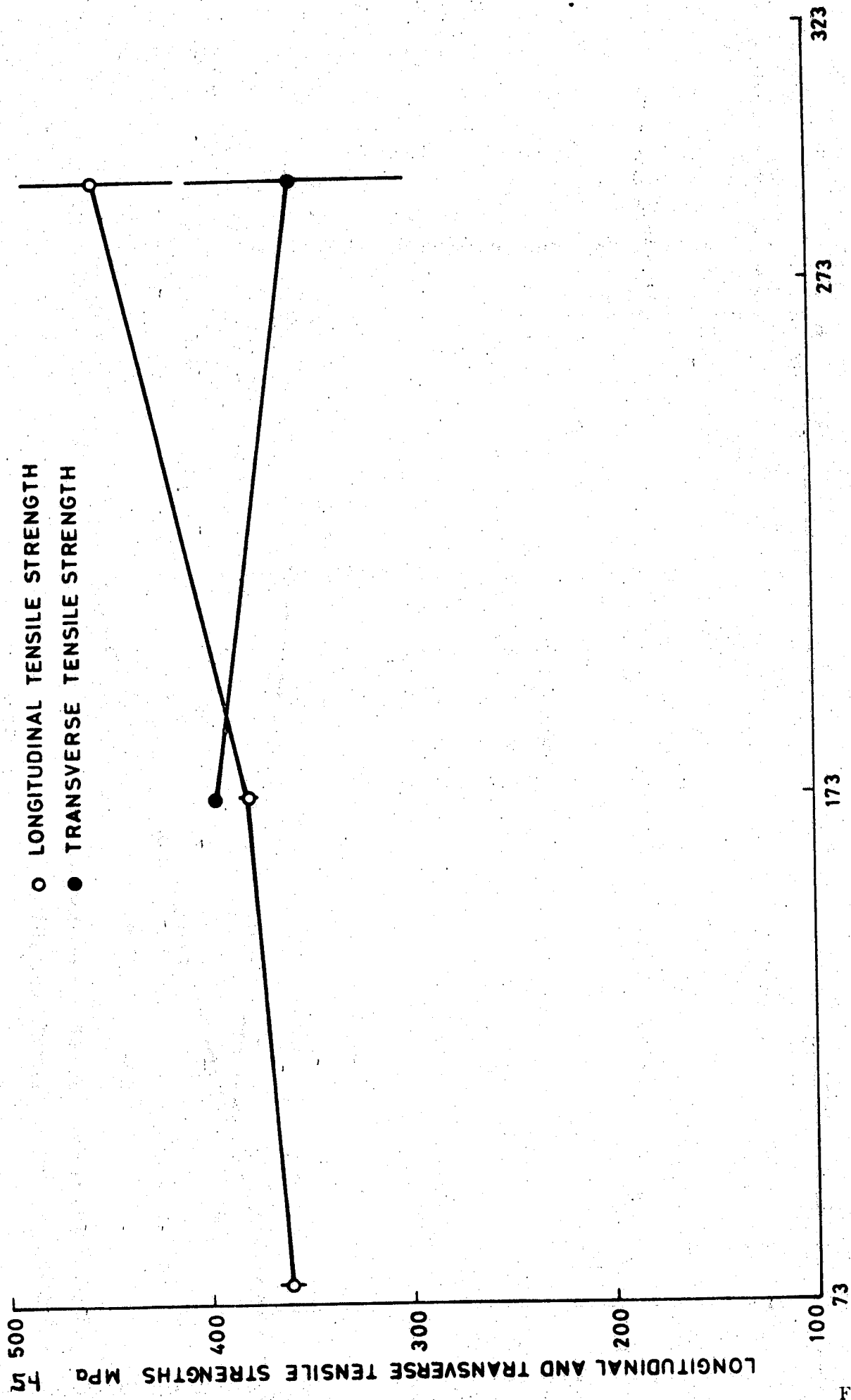
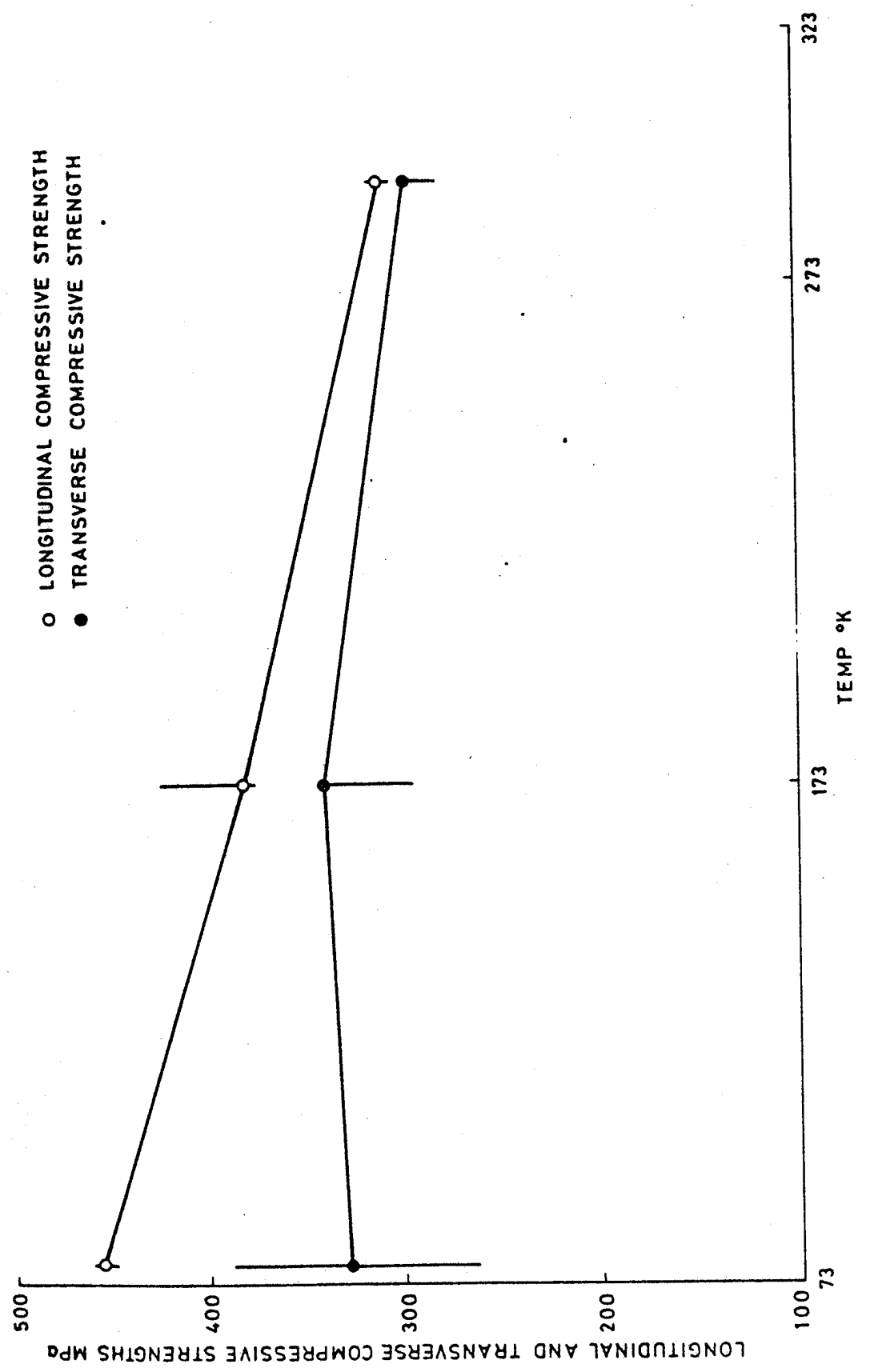


FIG. 26
 LONGITUDINAL AND TRANSVERSE TENSILE STRENGTH
 ANGLE PLY CARBON FIBRE COMPOSITE.



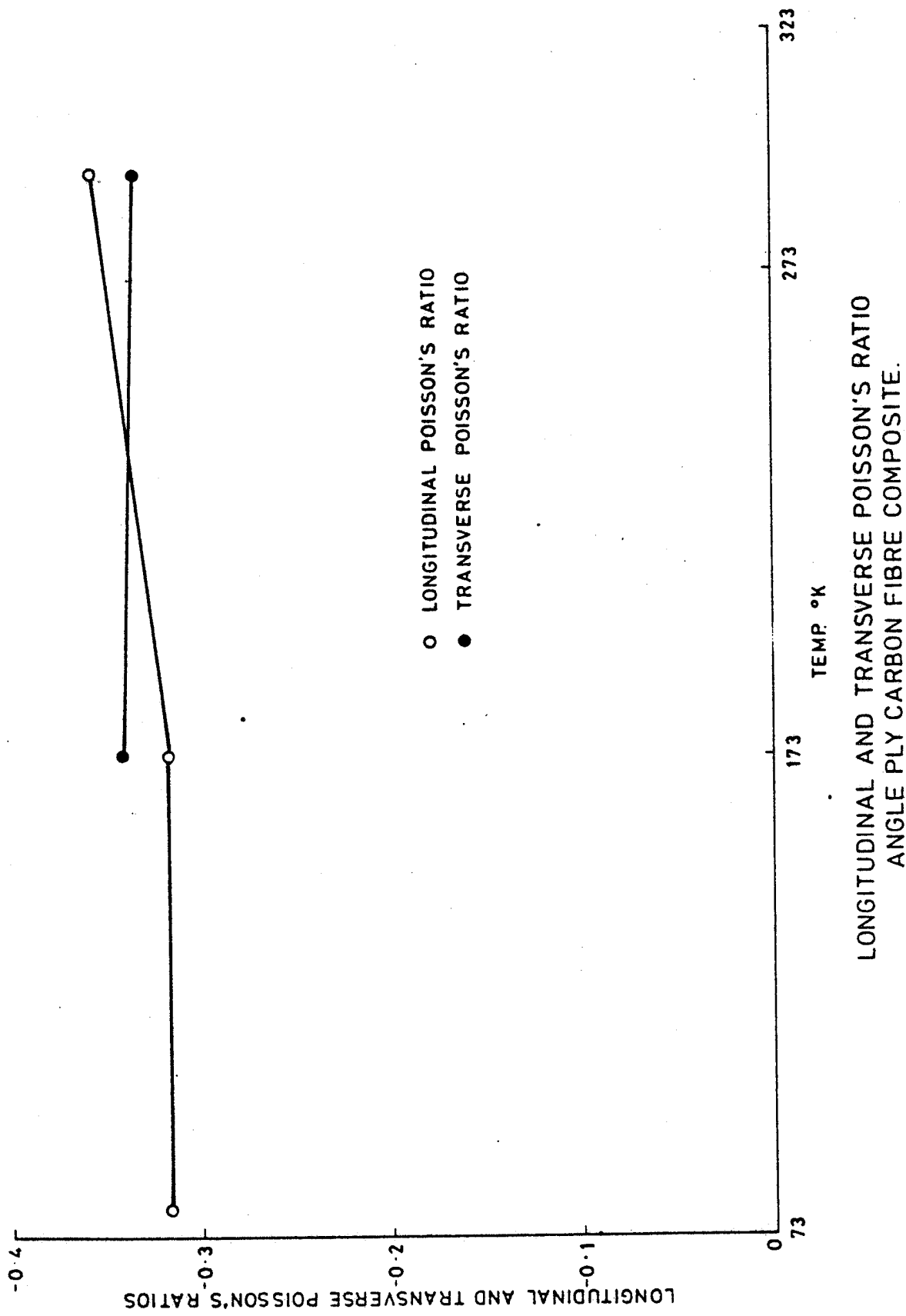
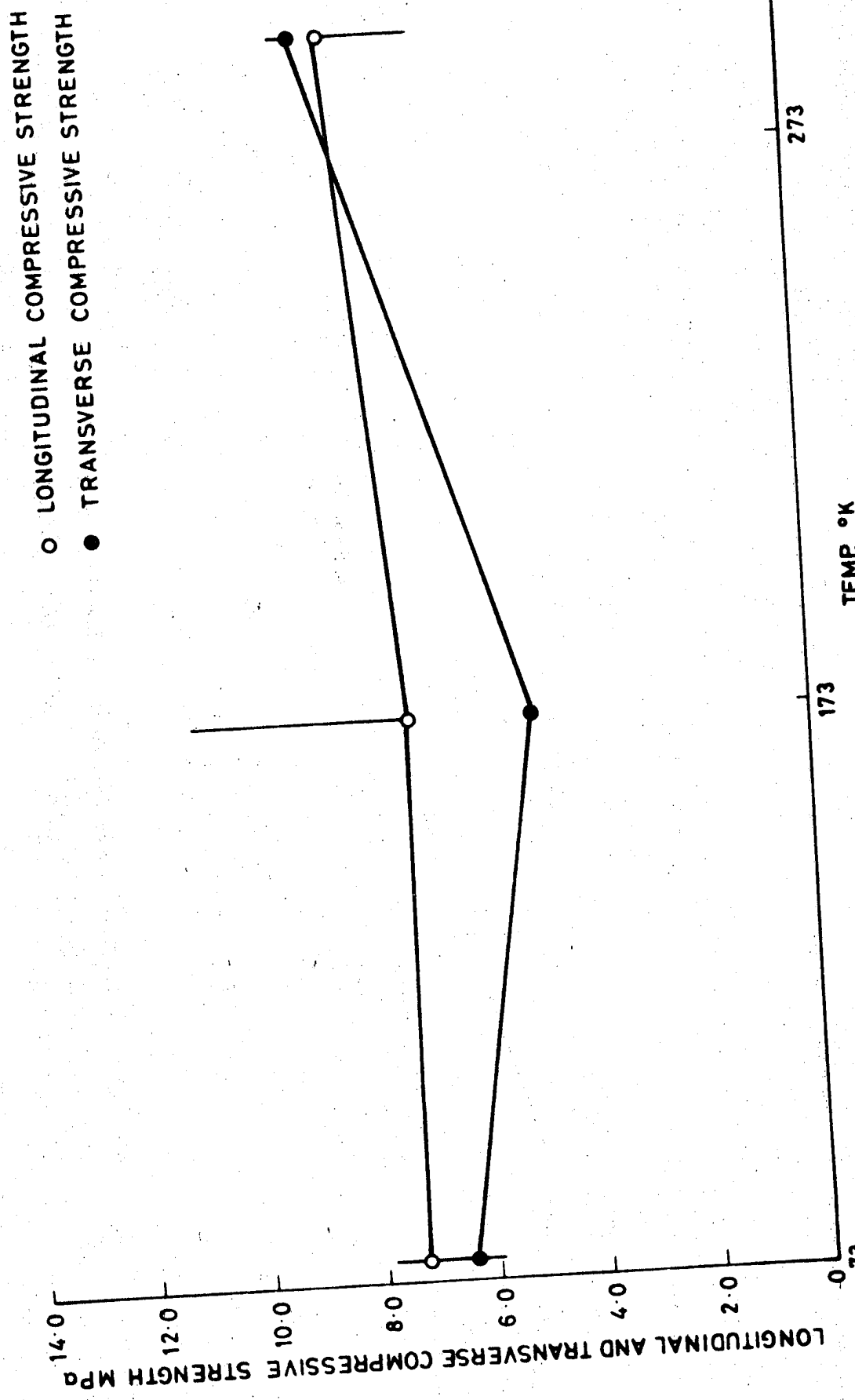


FIG. 28



LONGITUDINAL AND TRANSVERSE COMPRESSIVE STRENGTH
LONGITUDINAL HONEYCOMB CORE WITH PLIED CARBON FIBRE COMPOSITE SKINS
ALUMINIUM

85

- FLEXURAL MODULUS AFTER 100 HOURS AT 75% OF ULT. FLEX. STRENGTH.
- FLEXURAL STRENGTH AFTER 100 HOURS AT 75% OF ULT. FLEX. STRENGTH.
- ▲ EITHER PROPERTY, NO PRESTRESSING.

FLEXURAL MODULUS GPa

80

75

70

65

60

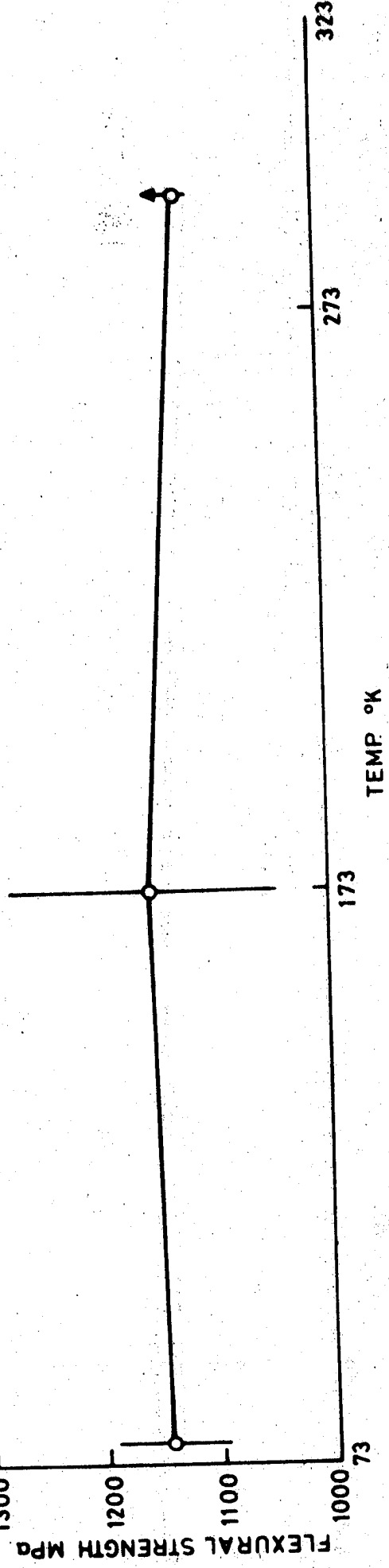
55

50

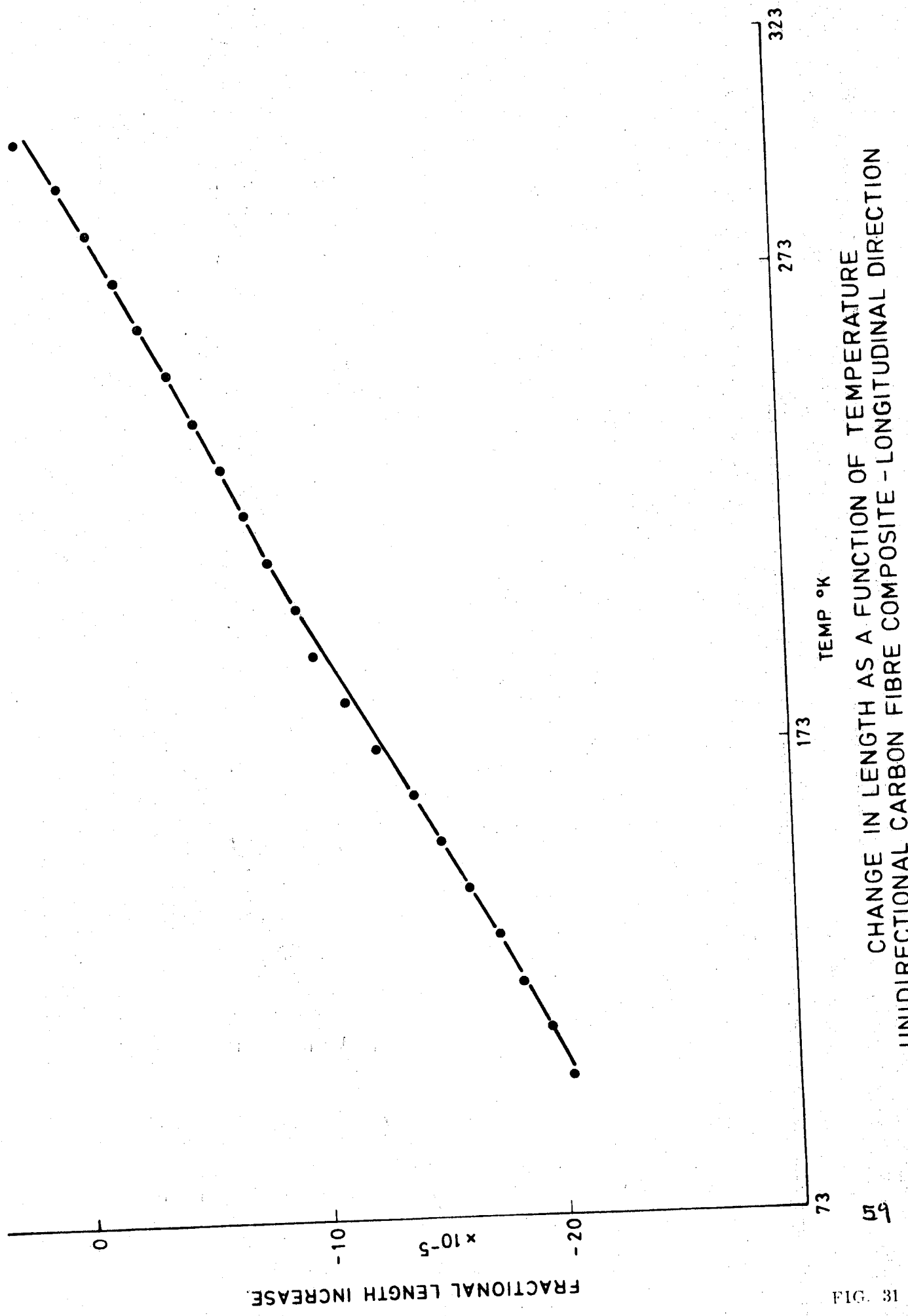
45

40

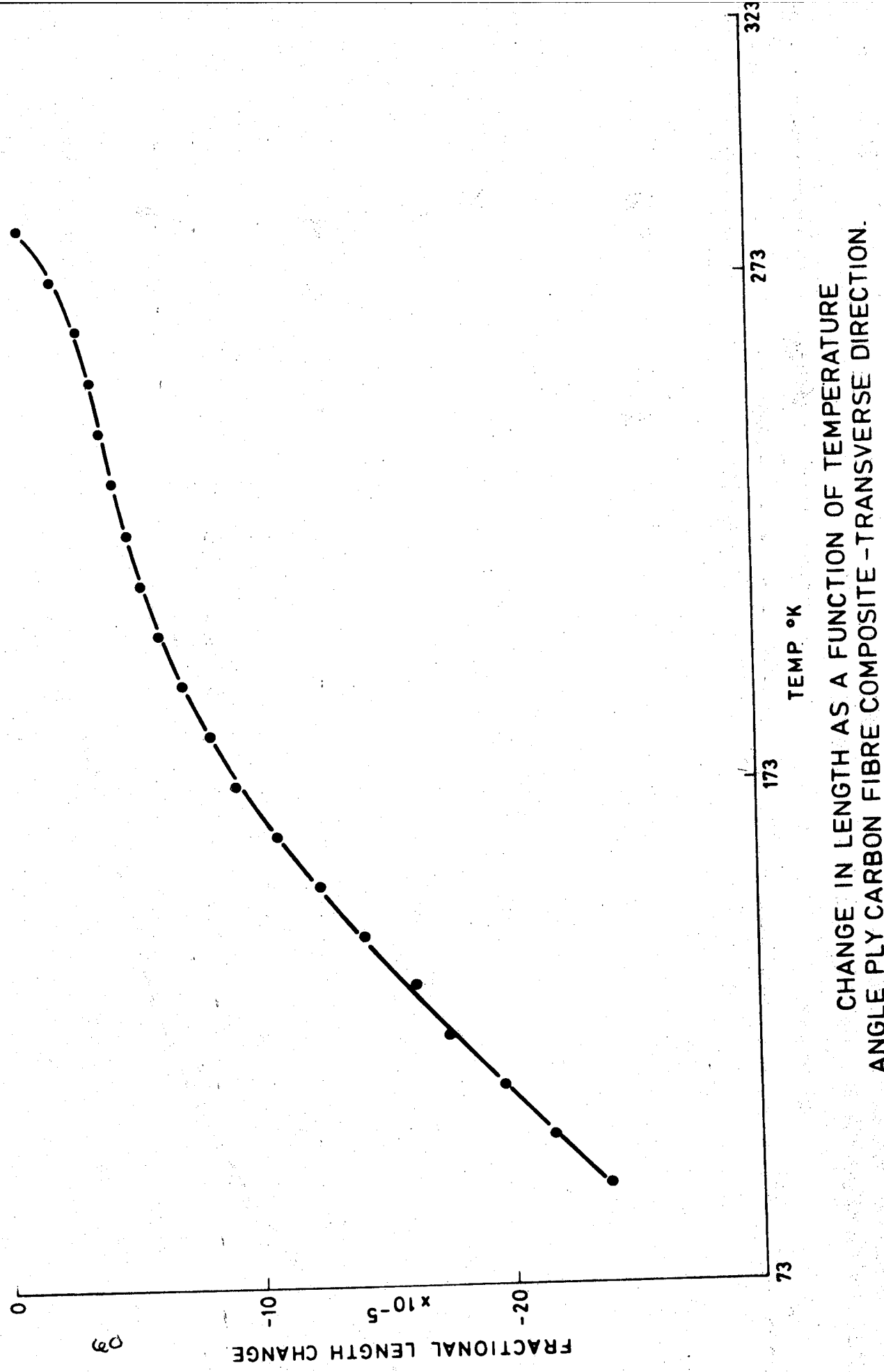
TEMPERATURES SHOWN ON THE GRAPHS ARE
CONDITIONING TEMPERATURES ONLY;
PROPERTY DETERMINATIONS WERE ALL MADE
AT ROOM TEMPERATURE.



EFFECT OF 100 HOURS EXPOSURE AT 75% OF ULTIMATE FLEXURAL STRENGTH
AND TEMPERATURE SPECIFIED, ON FLEXURAL MODULUS AND STRENGTH.

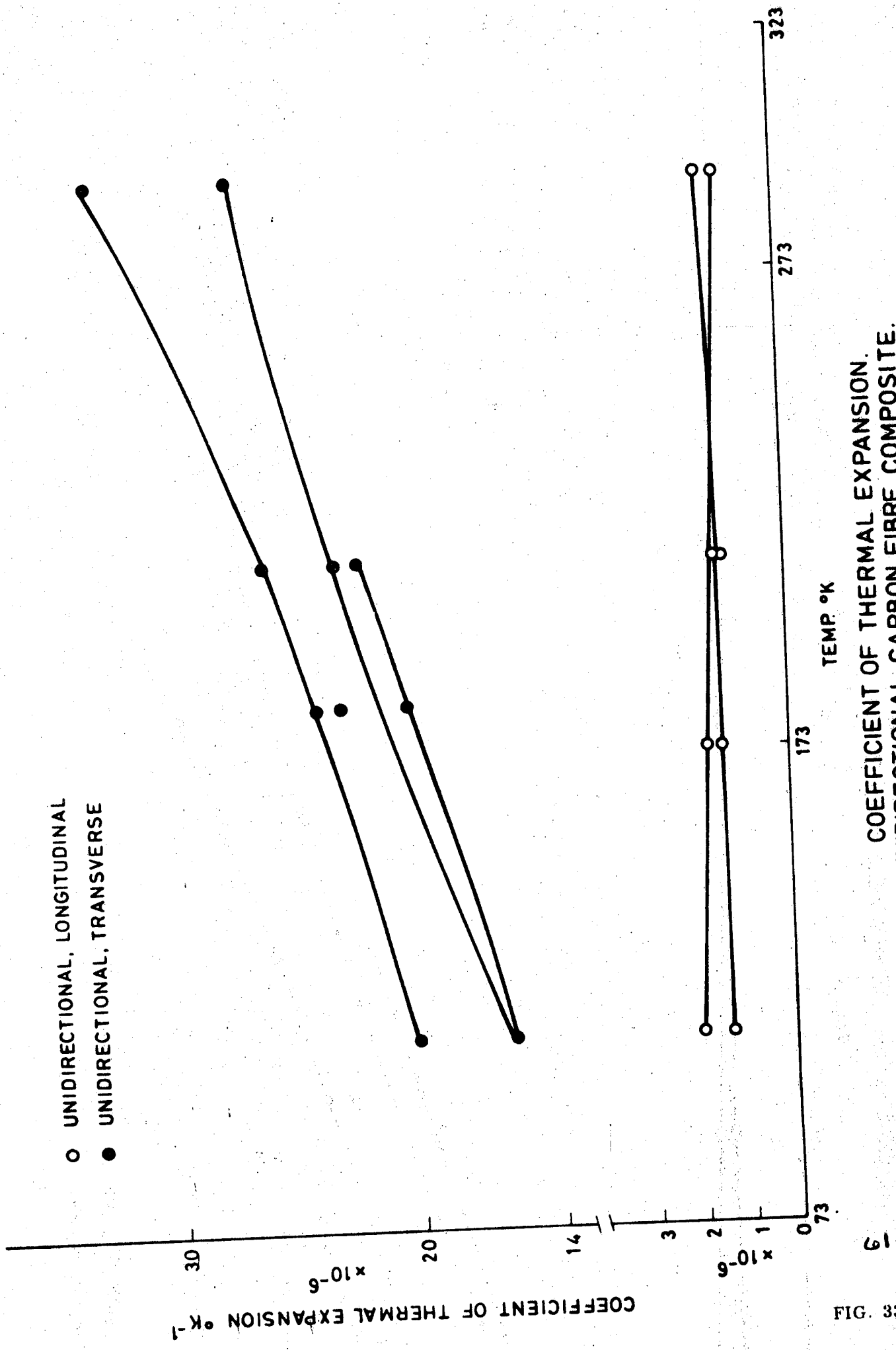


CHANGE IN LENGTH AS A FUNCTION OF TEMPERATURE
UNIDIRECTIONAL CARBON FIBRE COMPOSITE - LONGITUDINAL DIRECTION



CHANGE IN LENGTH AS A FUNCTION OF TEMPERATURE
ANGLE PLY CARBON FIBRE COMPOSITE - TRANSVERSE DIRECTION.

FIG. 32



COEFFICIENT OF THERMAL EXPANSION.
 UNIDIRECTIONAL CARBON FIBRE COMPOSITE.

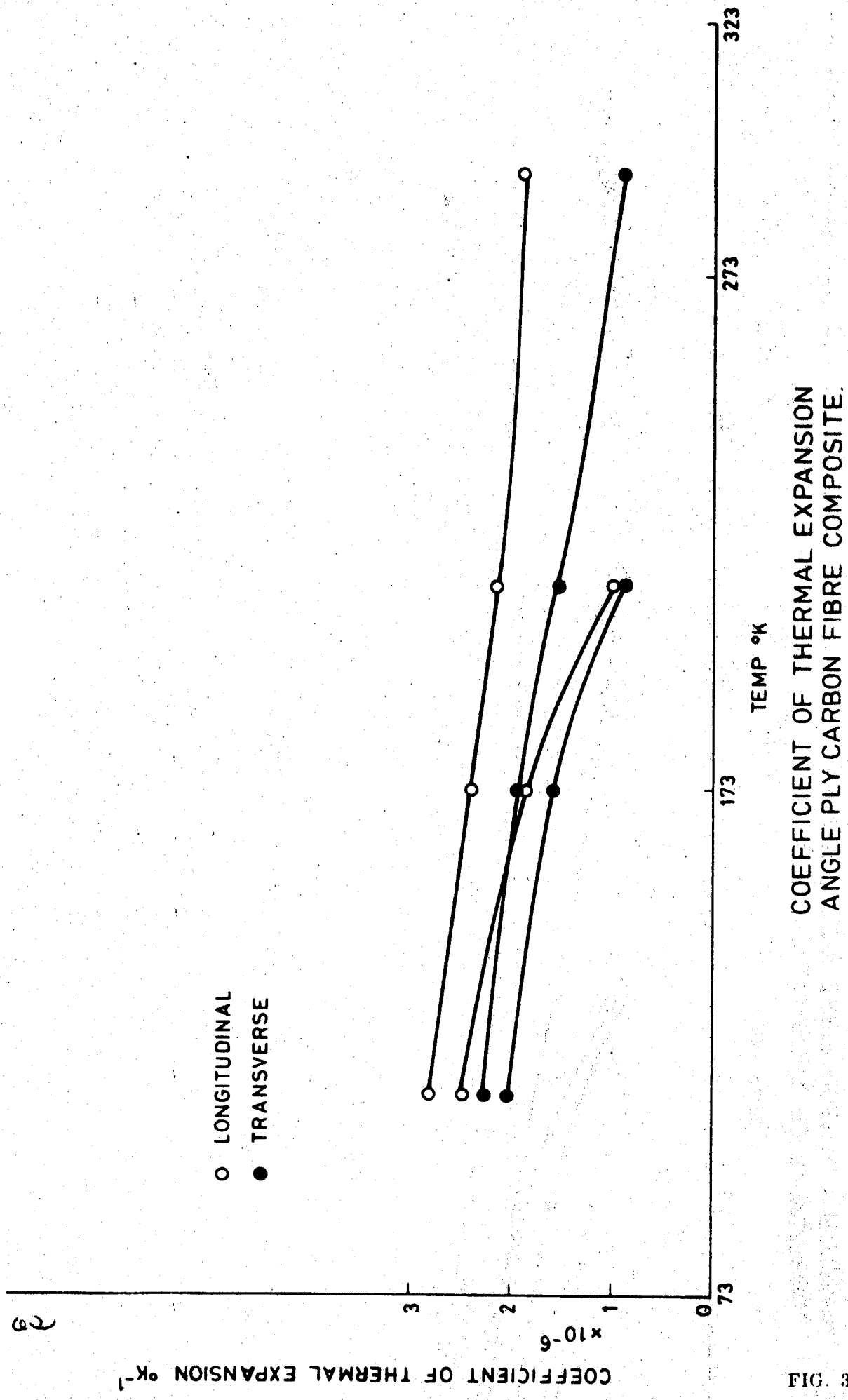


FIG. 34

CHANGE IN LENGTH OF CARBON FIBRE SKIN ALUMINIUM HONEYCOMB CORE SANDWICH PANELS.
DIRECTION: AT RIGHT ANGLES TO LONG GLUE LINE.

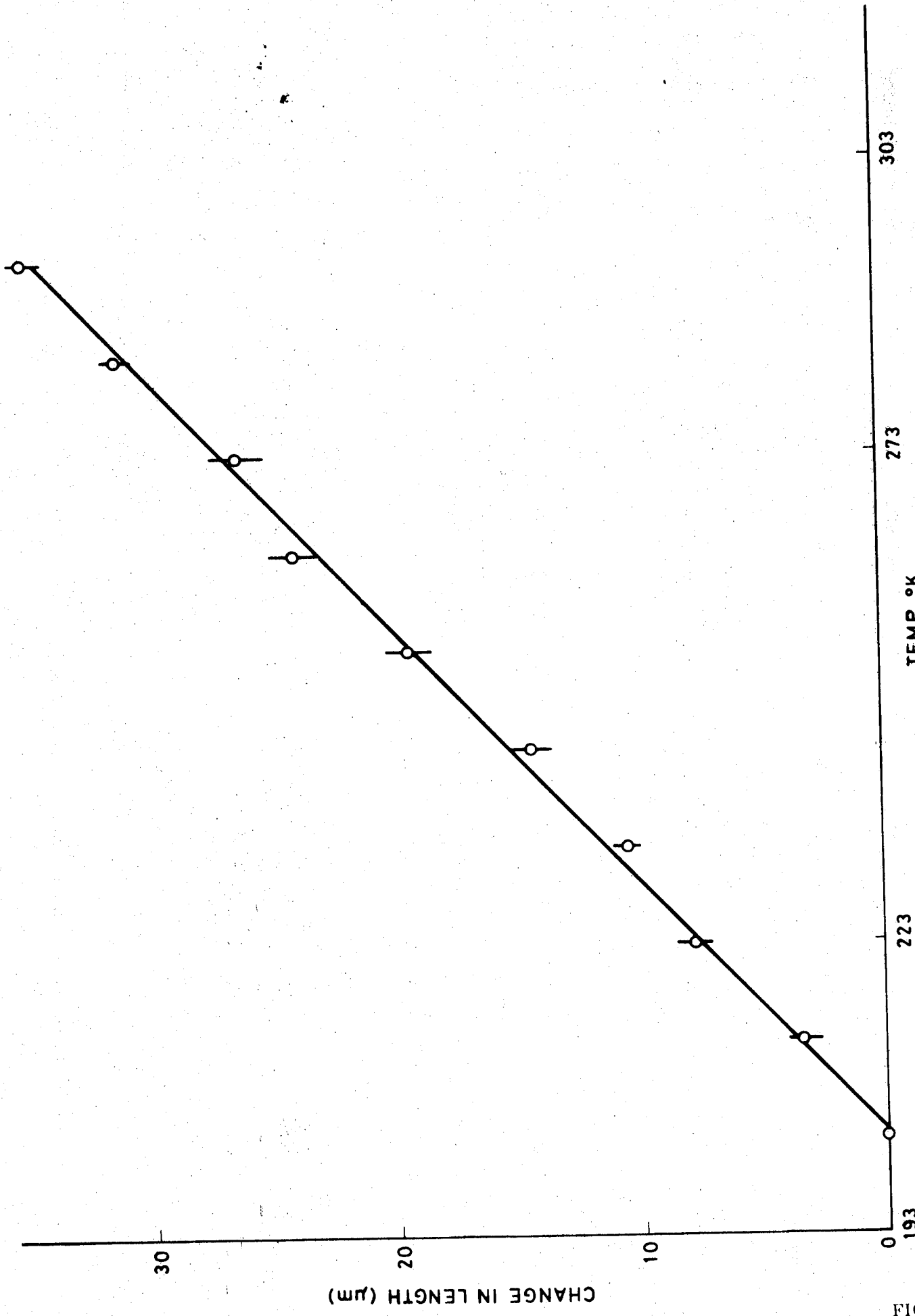


FIG. 35

4. FULL PANEL TEST

4.1 Introduction

The full panel test was a re-run of the SR and T programme thermal test as detailed in the BAe document HSD TP 7553. The same aluminium test frame and a similar carbon fibre panel were used and subjected to the same basic test procedure.

The objects of the test were as follows:

- To improve the test arrangement and test procedure in such a way as to minimise differences between the practical situation and the basic theoretical assumptions used by the model. This included such things as fixity and temperature homogeneity.
- To increase confidence in the measured values by improved instrumentation and transducers.
- With increased confidence in the experimental values, as above, to feed back actual behaviour and if necessary apply detail modifications to the theory.

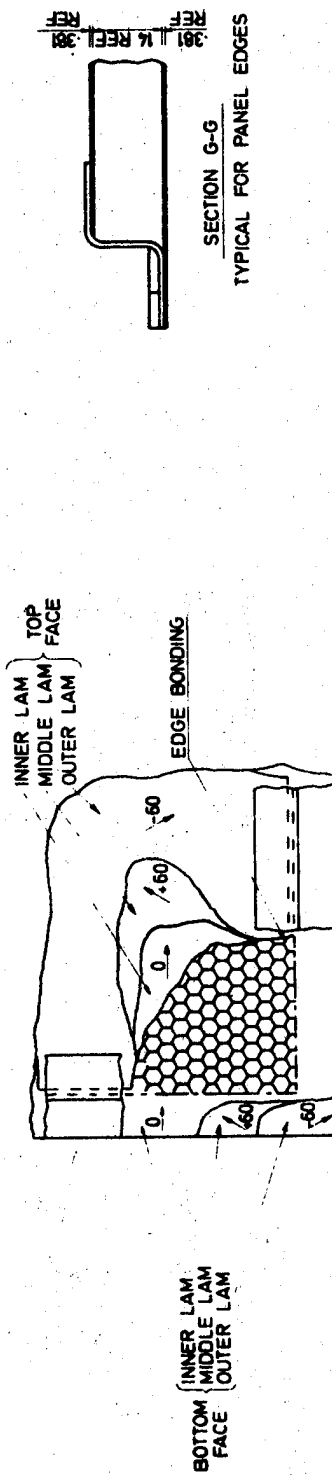
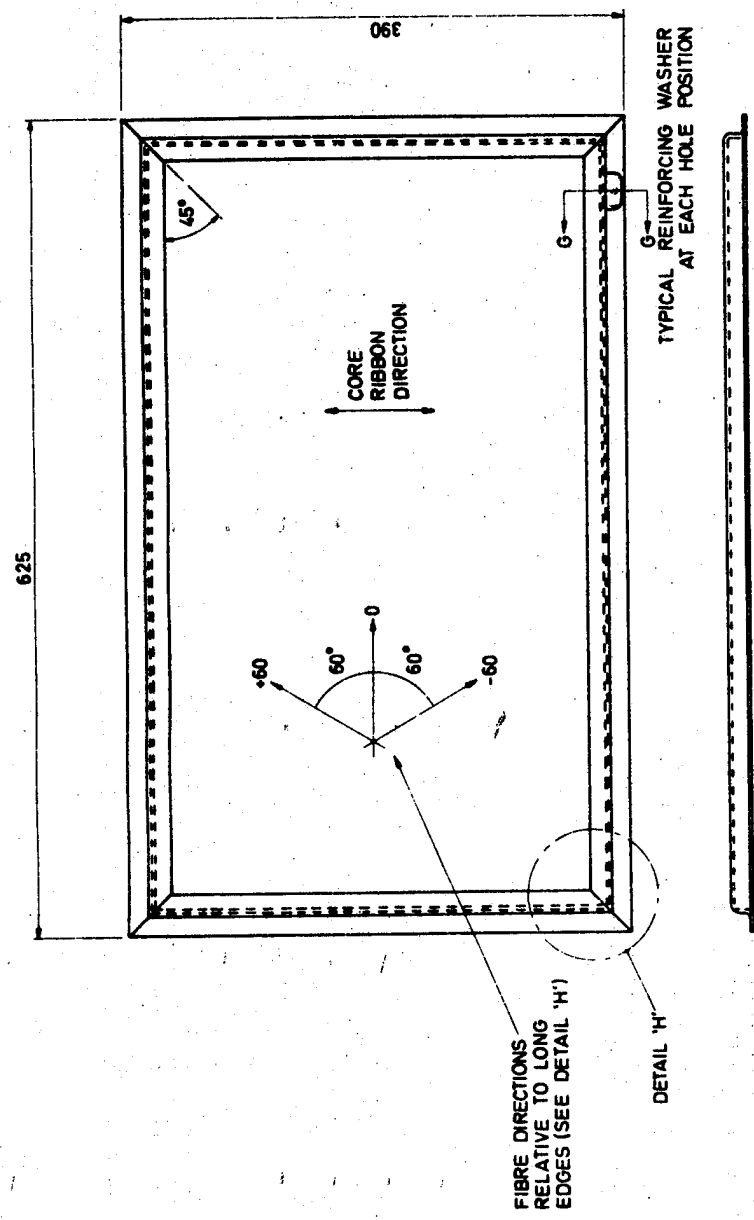
An outline of the improvements to the test arrangement and instrumentation that were proposed and finally used is given in para. 2.2, this section gives a full account of the resulting panel performance.

4.2 Panel Manufacture (Reference Figure 36)

The carbon fibre faced honeycomb panel was manufactured to BAe drawing No. TL 22 109 Basic 01 using the following materials and processes.

4.2.1 Panel Materials

- Carbon Fibre Prepreg in accordance with para. 3.2.1.
- Aluminium honeycomb in accordance with para. 3.2.1.
- Film adhesive in accordance with para. 3.2.1.
- Foam filler adhesive REDUX BSL 212 manufactured by CIBA-GEIGY Limited.
- Titanium reinforcing washers (6Al-4V).



DETAIL 'H'

CUT-AWAY VIEW ON PANEL CORNER.
OTHER CORNERS SIMILAR.

FIG. 36

4.2.2

Processes

See (20) Section 3 for process development.

Faceskins and Z-Section Edge Members

These were press moulded, from the carbon fibre prepreg material, in accordance with BAe specification PSS/GP/50039. The faceskins were moulded between flat caul sheets and the edge members were moulded using a special tool shown in Figure 37.

Faceskins were trimmed to size using a guillotine and edge members were mitred using a 'Dessouter' oscillating circular saw.

Panel Fabrication

Faceskins, core and edgemember were bonded together in one operation using the vacuum bag technique in accordance with BAe specification PSS/GP/50074.

Reinforcing Washer Application

The reinforcing washers were fitted as a separate operation. The titanium was dry blasted to BAe specification DH 215/2 prior to bonding and undersize holes and fixings were used to clamp the mating parts before curing at a temperature of $120 \pm 5^\circ\text{C}$ for 30 minutes.

Hole Finishing

The fixing holes were drilled and reamed to $6 + 0.018$ mm in conjunction with the test frame.

NDT

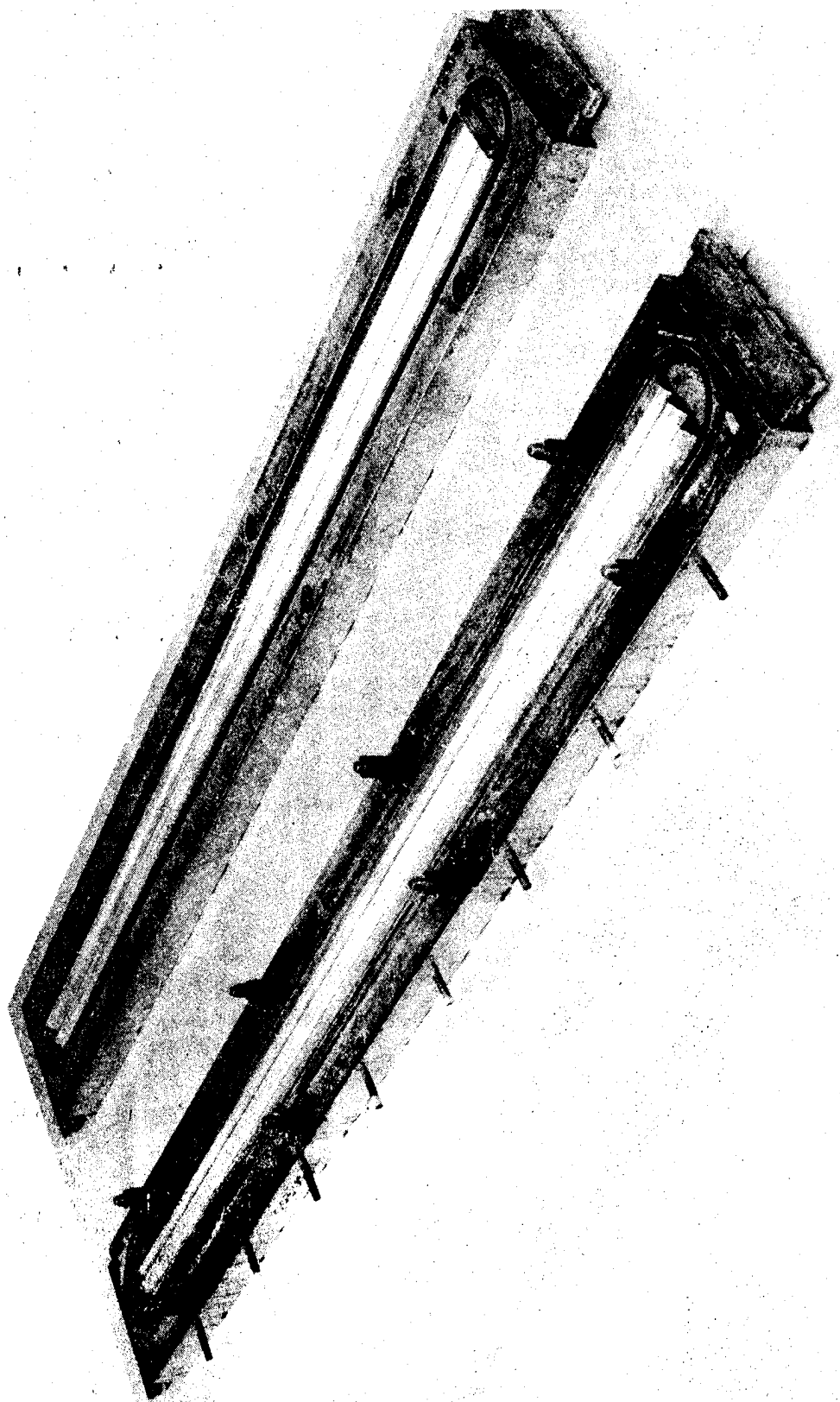
An acoustic bond tester (see Figure 38) was used to detect any disbonds following final finishing. The result of the scan is shown in Figure 39 and indicates the possibility of poor bonding at the extreme corners. The magnitude of the effect was not sufficient to cause concern.

4.3

Test Equipment

The following test equipment was utilised:

- (a) Aluminium test frame, representative of a large spacecraft structure, to BAe drawing No. MST 13594.
- (b) Test oven to BAe drawing No. MST 13607.



67

EDGE MEMBER MOULDING TOOL

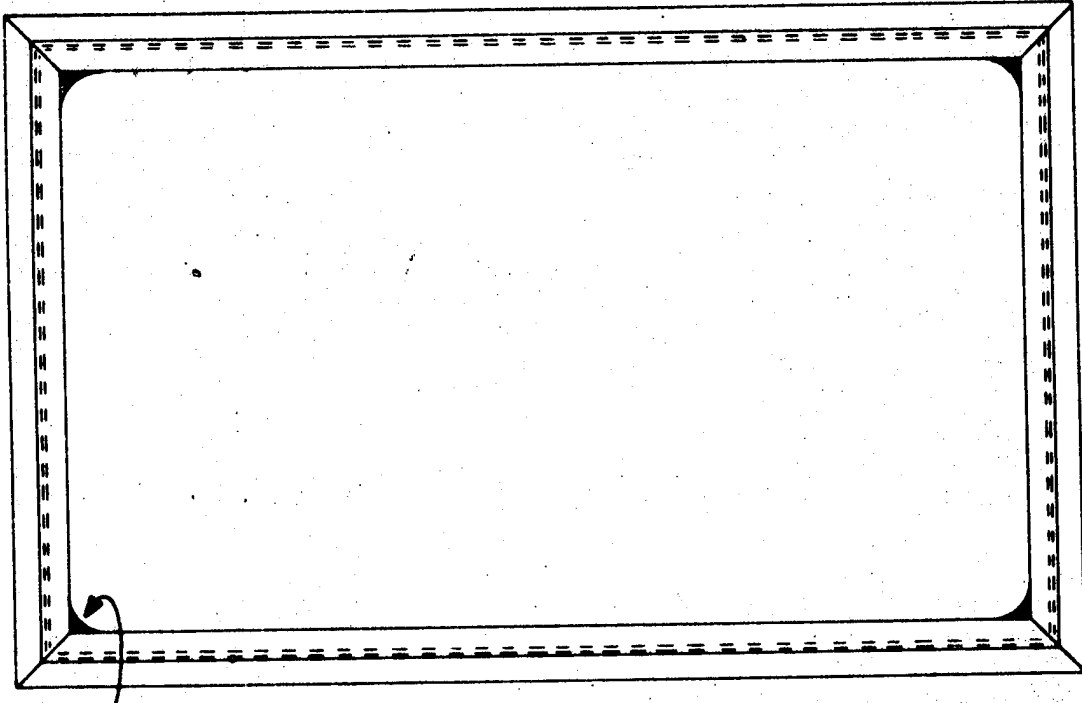
FIG. 37



ACOUSTIC BOND TESTER

FIG. 38

68



SMALL DISCONTINUITIES AT EXTREME CORNERS

**RESULTS OF NDT SCANS. THERE WAS NO DETECTABLE CHANGE
AFTER TESTING.**

ACOUSTIC BOND TESTER RESULTS

FIG. 39

- (c) LN Dewer with an electric pump.
- (d) 200 channel data logger and printer.
- (e) Chromel/Alumel (T1, T2) thermocouples positioned as shown in Figure 40.
- (f) Strain gauges in accordance with para. 2.2.2 and positioned as shown in Figure 40.
- (g) Dial Test Indicators capable of detecting movements of 0.001 inch.
- (h) Dial Test Indicator support frame to BAe drawing No. MST 13608.

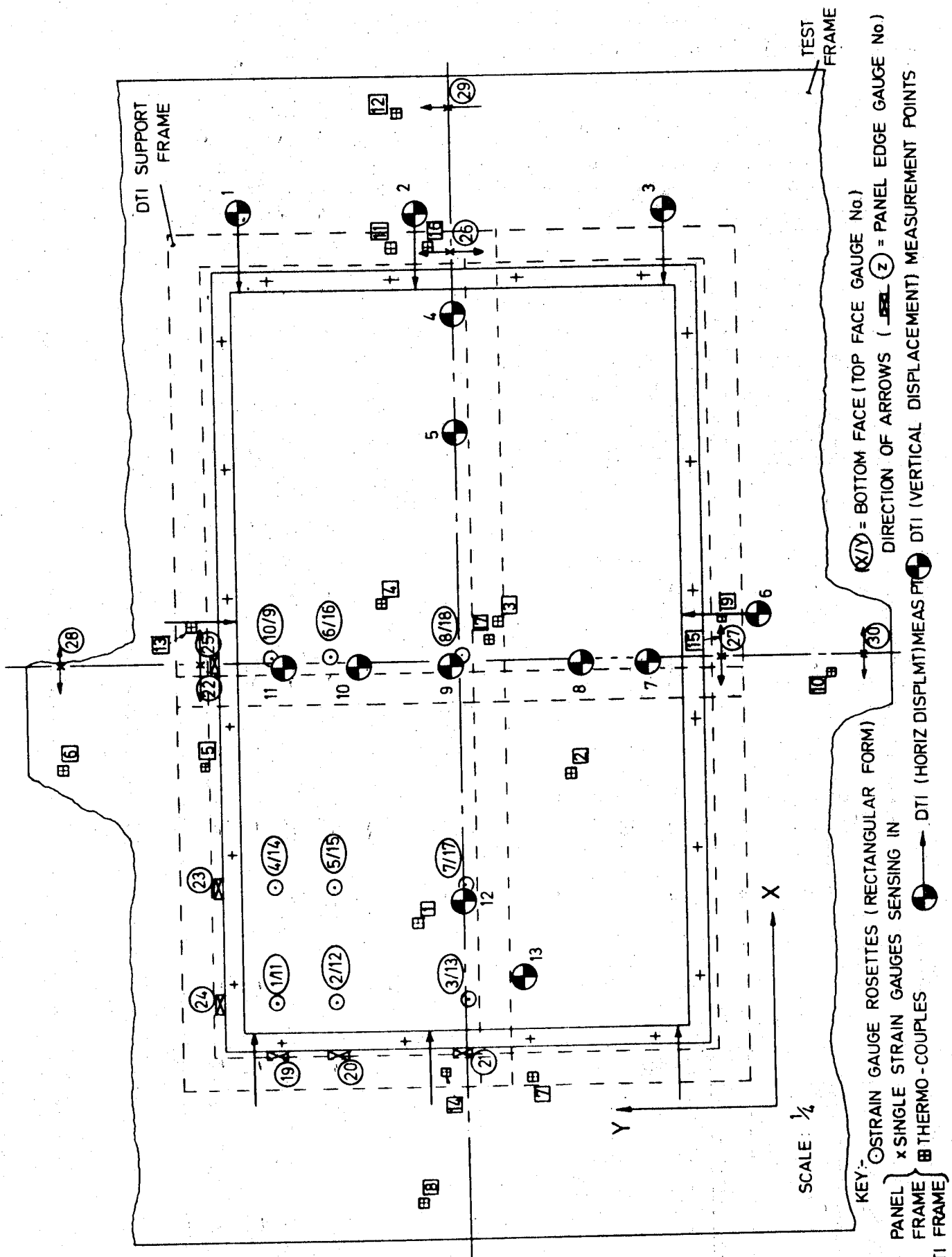
4.4 Test Procedure

Testing was in accordance with BAe specification DTP/GP/50047 Issue 2 (Appendix C).

4.4.1 Deviations from Planned Procedure

The following deviations were made from the planned procedure:

- (a) Para. 2.3.3.2 - additional thermocouples were installed on the DTI support frame.
- (b) Para. 3.1.1.1(d) - ambient temperature was taken as the prevailing ambient (nominally 20°C) at the start and end of each test run.
- (c) Para. 3.1.1.2(h) - the ambient to -75°C thermal cycle was not performed due to timescale limitations. However, transitory -75° DTI and strain gauge readings were taken during the ambient to -100°C cycle.
- (d) Para. 3.1.1.2(m) - initial ambient to minimum achievable temperature thermal cycle was abandoned due to a breakdown of insulation in the test box. The test run was repeated after re-insulation of the box.
- (e) For the duration of tests 1-4 inclusive, a sample piece of CFRP angle-ply laminate 0.07 inches thick x 2 inches x 1.5 inches with carbon fibres orientated at angles 0°, 60° and 120° and instrumented with one strain gauge rosette and a thermocouple, was tested in conjunction with the test panel and frame.



LOCATION OF PANEL AND TEST FRAME
INSTRUMENTATION

Fig. 40.

\times/\circ = BOTTOM FACE (TOP FACE GAUGE No.)
 DIRECTION OF ARROWS (→) = PANEL EDGE GAUGE No.
 1 - 4 = DTI (HORIZ DISPLMT) MEAS PT
 5 - 12 = DTI (VERTICAL DISPLACEMENT) MEAS PT
 13 - 17 = DTI FRAME

- (f) For the duration of test 7 the above specimen together with additional specimens of CFRP/honeycomb composite (identical to test panel lay-up) and L59 aluminium (test frame material) were instrumented with rosette and single strain gauges respectively (one each side of specimen) and thermocouples, and tested in conjunction with the panel and frame assembly.

4. 5 Test Facilities

The test was performed at BAe Stevenage in the Stage 3 Development Test Area.

A 240V 50Hz power supply was utilised to run the Data Logger and printer facility and for operation of the LN pump.

4. 6 Test Details

4. 6. 1 Preparation Activities

The panel and test frame were instrumented in accordance with the procedure except where stated in Section 4. 4. 1. (Figure 40 shows the relative positions of the strain gauges and thermocouples). A pre-test inspection of the test frame and panel was carried out.

Several calibration runs were performed prior to the initial cold cycle in order to verify the performance of the test equipment.

4. 6. 2 Panel Thermal Testing

Two thermal cycles from ambient to -150°C and return (tests 1 and 2) were carried out with the panel free (i.e. decoupled from the test frame). In each case the panel temperature was stabilised at ambient and then at approximately 0°C, -30°C, -60°C, -90°C, -120°C and -150°. Thermocouple, strain gauge and DTI readings were taken at each of these increments. The panel and frame were then allowed to return to ambient taking readings at approximately the same incremental panel temperatures. The panel was attached to the test frame in accordance with the test procedure and the assembly installed in the test chamber.

At the start of each test run the DTI's were zeroed and the ambient thermocouple and strain gauge readings were taken.

The panel and test frame, in the coupled condition, were subjected to five thermal cycles, designated tests 3-7.

DTI, thermocouple and strain gauge readings were taken at each planned cycle temperature and on return to ambient.

Test 3 consisted of ambient to -25°C (nominal panel temperature) and return to ambient.

Test 4 consisted of ambient to -50°C (nominal panel temperature) and return to ambient.

Test 5 consisted of ambient to -100°C (nominal panel temperature), with additional DTI, thermocouple and strain gauge readings being taken at a nominal panel temperature of -75°C , and return to ambient (see para. 4.4.1(c)).

Test 6 was planned as ambient to cryogenic temperatures but due to a failure of the test box insulation the minimum achieved panel temperature was approximately -40°C . DTI, thermocouple and strain gauge readings were taken at this temperature and the assembly then allowed to return to ambient (see para. 4.4.1(d)).

Test 7 was a re-run of test 6 with a minimum achieved panel temperature in this case of -196°C . The assembly was allowed to return to ambient and the panel visually inspected for damage following test completion.

4.7

Discussion of Results

Preliminary analysis of the DTI, thermocouple and strain gauge readings for tests 1-7 yielded the following data:

During thermal cycling the relatively large thermal mass of the test frame compared with the panel tended to cause the frame to 'over-run' at temperatures below -30°C . This resulted in a significant mis-match of frame/panel temperatures when the panel was 'on-condition' for the cycle. It was also found necessary to allow some intermittent circulation of cold nitrogen in order to maintain panel stabilisation, and this further increased temperature differentials.

This effect appeared to worsen when the panel was coupled to the frame, possibly due to the improved thermal contact between the panel and the test frame causing earlier equalising of panel and frame temperatures.

4.7.1 Panel Free Condition

4.7.1.1 DTI Results

Positive value DTI readings were obtained for the panel 'free' case (test 2) indicating an apparent increase in the panel dimensions.

Investigation, however, showed that these readings were biased due to contraction of the DTI support frame, the rate of contraction being greater than that of the panel. The resultant movement of the DTI lever arm pivots relative to the panel edges caused an amplified (2 to 1) compression of the DTI probes with a net positive reading. The actual decrease in panel dimensions for each measured temperature change of the panel, with respect to ambient, was determined by calculating the amount of contraction of the DTI frame for the measured panel temperature (the corresponding DTI frame temperatures were measured for each panel temperature increment) and adding it to the compound DTI reading, carrying all signs. (See Figure 41).

The strains due to thermal effects on the panel along major (X) and minor (Y) axes were then determined for each panel temperature increment (see Figure 41) with the following results:-

- (i) Contraction of the panel along its major axis resulted in a maximum calculated strain value of -1833×10^{-6} at an average panel temperature of -135°C giving a thermal coefficient of expansion of $11.83 \times 10^{-6}/^{\circ}\text{C}$.

The average coefficient of expansion of the panel along the major axis from the dial test indicators was calculated to be $7.92 \times 10^{-6}/^{\circ}\text{C}$.

- (ii) Contraction of the panel along its minor axis resulted in a calculated strain value of 1710×10^{-6} at an average panel temperature of -82°C^* giving a thermal coefficient of expansion of $16.76 \times 10^{-6}/^{\circ}\text{C}$.

The average coefficient of expansion of the panel along the minor axis from the dial test indicators was calculated to be $11 \times 10^{-6}/^{\circ}\text{C}$.

* The maximum calculated strain value of -3874×10^{-6} at -135°C was suspect since there was some evidence of ice formation on the minor axis lever arm pivots at this temperature.

PANEL TEMP. °C	DTI FRAME TEMP DIFF. ΔT _{FRAME}	ΔG _x FRAME FOR ΔTx DTI Posn 2 2	ΔG _x PANEL + FRAME FROM DTI READING 2	ΔG _x PANEL BY SLIM DTI Posn 2 3	STRAIN VALUE Ex × 10 ⁻⁶ 1 1 3	DTI FRAME TEMP DIFF. ΔT _y deg C	ΔG _y FRAME FOR ΔTy DTI Posn 6 6	ΔG _y FRAME + FRAME FROM DTI READING 6	ΔG _y PANEL BY SLIM DTI Posn 6 6	STRAIN VALUE Ey × 10 ⁻⁶ 1 1 3
+0.2	-5.6	-007"	0022"	-0048"	-206	-5.7	-0047"	0003"	-0044"	-312
	-5.4	-0067"	0023"	-0044"	-188					
	-5.6	-007"	0022"	-0048"	-206					
-30.4	-14.5	-018"	0079"	-0101"	-433	-15.2	-0126"	0011"	-0115"	-816
	-13.9	-0173"	0076"	-0097"	-415					
	-14.6	-0181"	0079"	-0102"	-437					
-59.6	-23.0	-0286"	0159"	-0127"	-544	-25.1	-0208"	0026"	-0182"	-1291
	-21.8	-0271"	0133"	-0138"	-591					
	-22.6	-0281"	0139"	-0142"	-608					
-81.9	-32.0	-0391"	0210"	-0187"	-801	-34.8	-0288"	0047"	-0241"	-1710
	-29.8	-0370"	0190"	-0180"	-771					
	-31.8	-0395"	020"	-0195"	-835					
-115.8	-56.2	-0698"	0335"	-0363"	-1555	-62.9	-0521"	0031"	-049"	-3477
	-52.1	-0647"	0269"	-0378"	-1619					
	-55.5	-0689"	0314"	-0375"	-1606					
-134.6	-64.0	-0795"	0470"	-0325"	-1392	-72.0	-0556"	005"	-0546"	-3874
	-59.4	-0738"	0310"	-0428"	-1833					
	-63.5	-0789"	0406"	-0383"	-1641					
-90.5	-22.4	-0278"	0235"	-0043"	-184	-22.6	-0187"	0095"	-0092"	-653
	-21.6	-0268"	0240"	-0028"	-120					
	-22.3	-0277"	0245"	-0032"	-137					
-28.5	-9.7	-012"	002"	-010"	-428	-9.2	-0076"	008"	+0004"	+28
	-9.3	-0116"	003"	-0086"	-368					
	-9.6	-0119"	0019"	-010"	-428					
-5.0	-2.8	-0035"	001"	-0025"	-107	-2.4	-002"	-0003"	-0025"	-163
	-3.7	-0046"	0014"	-0032"	-137					
	-3.8	-0047"	001"	-0031"	-158					

PANEL FREE (TEST 2)

FIG. 41

4.7.1.2 Strain Gauge Results

The 18 strain gauges mounted on the panel were of the self-temperature-compensated type but matched to the expansion coefficient of aluminium. There was therefore an S-T-C mismatch, resulting in the apparent strain output of the gauges being shifted clockwise about the zero strain point. See Figure 9.

The (apparent) strain outputs of three selected gauges on the panel centre line for test 2 are shown in Figure 42.

The corresponding coefficients of expansion are determined from the difference between the strain curves of Figure 42 and the manufacturer's curve of Figure 43 as follows:-

$$\text{Since } \epsilon_{APP\ CF} = \epsilon_{APPAL} - (\alpha_{AL} - \alpha_{CF}) \cdot \Delta T$$

and from Figures 42 and 43 for panel major axis

$$\mu\epsilon_{APP\ CF} - \mu\epsilon_{APPAL} = \Delta\mu\epsilon_x = \Delta\mu\epsilon_1$$

then for gauge 7 in the X direction

$$\Delta\mu\epsilon_x(T) = 1750 + 700 = 2450 \text{ at } -135^{\circ}\text{C} \text{ (average panel temperature)}$$

and, assuming the coefficient of expansion for the S-T-C match to be $23.2 \times 10^{-6}/^{\circ}\text{C}$

$$2450 = (23.2 - \alpha_p) \cdot 155$$

$$\text{giving } \alpha_{PX(T)} = \underline{7.39 \times 10^{-6}/^{\circ}\text{C}}$$

Similarly for gauge 13 in the X direction.

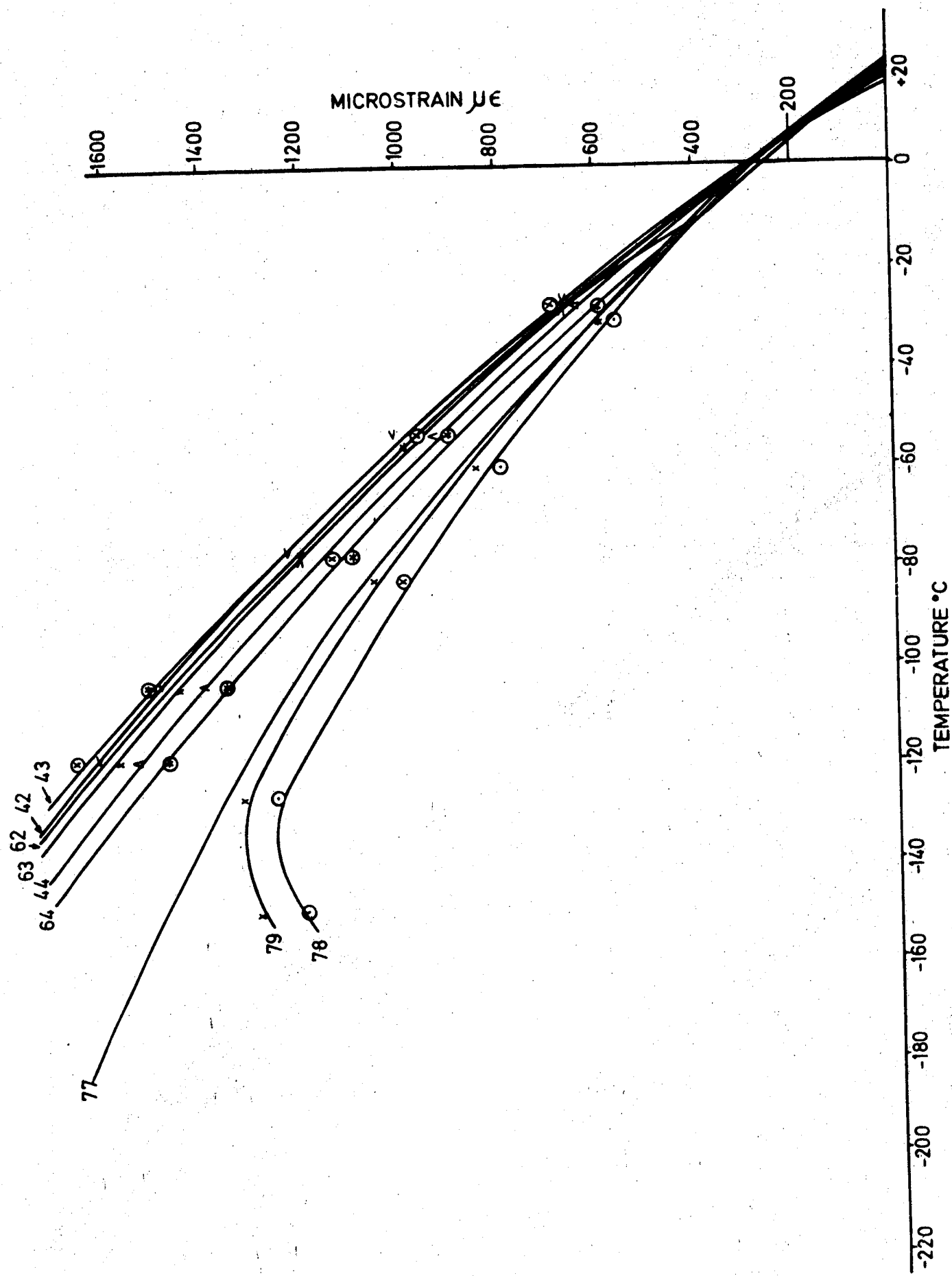
$$\Delta\mu\epsilon_x(13) = 2450 \text{ at } -135^{\circ}\text{C} \text{ (average panel temperature)}$$

$$\text{giving } \alpha_{PX(13)} = \underline{7.39 \times 10^{-6}/^{\circ}\text{C}}$$

For gauge 18 in the X direction

$$\Delta\mu\epsilon_x(18) = 1410 + 700 = 2110 \text{ at } -135^{\circ}\text{C} \text{ (average panel temperature)}$$

$$\text{giving } \alpha_{PX(18)} = \underline{9.59 \times 10^{-6}/^{\circ}\text{C}}$$



S.G. CURVES FOR PANEL FREE CONDITION

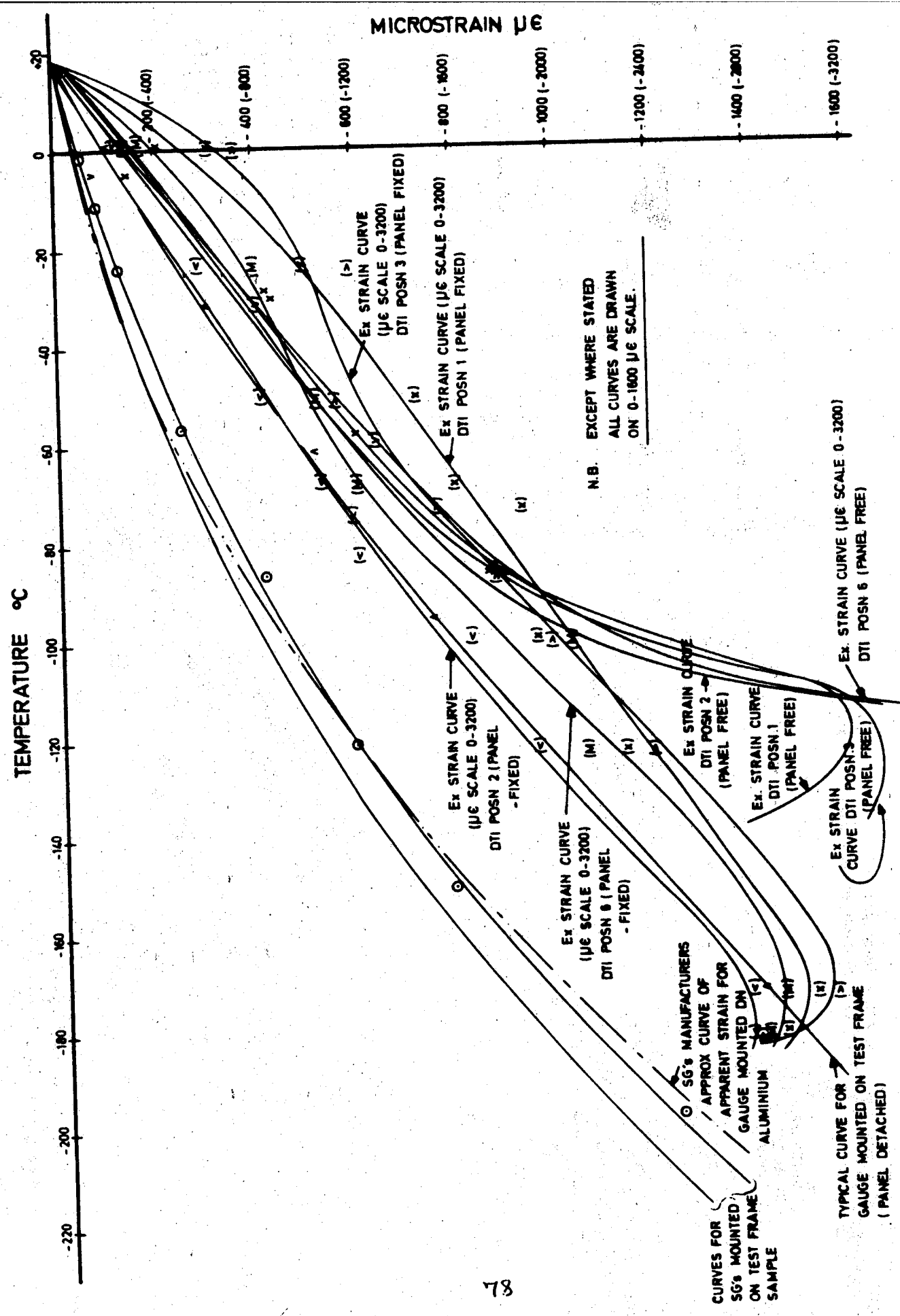


Fig. 43

D.T.I. MEASURED STRAIN⁽¹⁾ EFFECTS ON FREE PANEL

FIG. 43

from Figures 42 and 43 for panel minor axis

$$\mu \epsilon_{APPCF} - \mu \epsilon_{APPAL} = \Delta \mu \epsilon Y = \Delta \mu (\epsilon 2 + \epsilon 3 - \epsilon 1)$$

then for gauge 7 in the Y direction

$$\Delta \mu \epsilon Y(T) = (1790 + 1665 + 1750) + 700 = 2405 \text{ at } -135^{\circ}\text{C}$$

(average panel temperature)

giving $\alpha_{PY}(7) = 7.68 \times 10^{-6}/^{\circ}\text{C}$

for gauge 13 in the Y direction

$$\Delta \mu \epsilon Y(13) = (1730 + 1610 - 1750) + 700 = 2290 \text{ at } -135^{\circ}\text{C}$$

(average panel temperature)

giving $\alpha_{PY}(13) = 8.43 \times 10^{-6}/^{\circ}\text{C}$

for gauge 18 in the Y direction

$$\Delta \mu \epsilon Y(18) = (1260 + 1325 - 1410) + 700 = 1875 \text{ at } -135^{\circ}\text{C}$$

(average panel temperature)

giving $\alpha_{PY(18)} = 11.0 \times 10^{-6}/^{\circ}\text{C}$

α_X and α_Y were calculated from the output of each strain gauge at six (decreasing) incremental panel temperatures. The expansion coefficients were then averaged out for panel top and bottom faces as follows:

$$\alpha_{XPAVE}(\text{top face}) = 7.79 \times 10^{-6}/^{\circ}\text{C};$$

$$\alpha_{YPAVE}(\text{top face}) = 10.5 \times 10^{-6}/^{\circ}\text{C}$$

$$\alpha_{XPAVE}(\text{bottom face}) = 6.56 \times 10^{-6}/^{\circ}\text{C};$$

$$\alpha_{YPAVE}(\text{bottom face}) = 10.19 \times 10^{-6}/^{\circ}\text{C}$$

The outputs from the single gauges mounted around the edge of the panel (on the edge member) averaged out over six decreasing temperature increments produced the following α values:-

$$\alpha_{PY(19)} = \underline{6.52 \times 10^{-6} / ^\circ C}$$

$$\alpha_{PY(20)} = \underline{9.03 \times 10^{-6} / ^\circ C}$$

$$\alpha_{PY(21)} = \underline{12.11 \times 10^{-6} / ^\circ C}$$

$$\alpha_{PX(23)} = \underline{9.09 \times 10^{-6} / ^\circ C}$$

(gauges 22 and 24 became detached from substrate during testing).

Notations as follows:-

$\epsilon_{APP\ CF}$ = Apparent Strain of Carbon Fibre Composite

$\epsilon_{APP\ AL}$ = Apparent Strain of Aluminium

α_{AL} = Expansion Coefficient of Aluminium

α_{CF} = Expansion Coefficient of Carbon Fibre Composite

α_P = Expansion Coefficient of CFRP Panel under test

α_F = Expansion Coefficient of Aluminium Test Frame

α_L = Expansion Coefficient of CFRP Laminate Sample

α_C = Expansion Coefficient of CFRP faced honeycomb Sample

4.7.2 Panel Fixed Condition

4.7.2.1 DTI Results

With the panel coupled to the test frame the DTI's showed negative readings indicating that the rate of contraction of the panel/test frame assembly was now greater than that of the DTI support frame. Corrections were made for the DTI frame contraction as in the 'free' case and the net panel movement is given in Figure 43. The strains due to the compound thermal effects on the panel along major (X) and minor (Y) axes were determined for a series of panel temperatures (see Figure 43) with the following results:-

- (i) The maximum calculated strain value along the panel major axis was calculated to be -3135×10^{-6} at an average panel temperature of $-173^\circ C$.

- (ii) The maximum calculated strain value along the panel minor axis was calculated to be -2923×10^{-6} at an average panel temperature of -173°C .

4.7.2.2 Strain Gauge Results

The strain output of the fixed test panel gauges showed an anti-clockwise rotation about the zero strain point when compared with the same gauges for the free panel. This effect was to be expected since the combined contraction of the panel/test frame assembly was biased towards the aluminium thermal coefficient. The actual compressive strain due to the loading effect of the test frame on the panel was determined by difference between the strain outputs of the gauges for the panel free condition and those for the fixed case at the same panel temperature.

Appendix E gives the real X and Y direction strains and the maximum and minimum strain values and their direction as computed from the data logger outputs of tests 3 to 7. These values were calculated using a specially developed strain gauge programme 'STRAINCAL' details of which are contained in Appendix D. Figures 44 to 55 inclusive show the plots of X and Y direction strains against distance from panel edge for all the gauges on the panel.

4.7.3 Test Frame Behaviour

Panel Free Condition

The outputs from the single gauges mounted on the test frame produced α values for the aluminium, averaged out over six decreasing temperature increments, of the following:-

$$\left. \begin{aligned} \alpha_{FX(25)} &= 26.32 \times 10^{-6} / ^\circ\text{C} \\ \alpha_{FY(26)} &= 26.16 \times 10^{-6} / ^\circ\text{C} \\ \alpha_{FX(27)} &= 26.11 \times 10^{-6} / ^\circ\text{C} \end{aligned} \right\}$$

Inboard edge of frame
- adjacent to panel attachment holes.

$$\alpha_{FX(28)} \quad (\text{Gauge O/C})$$

$$\left. \begin{aligned} \alpha_{FY(29)} &= 25.68 \times 10^{-6} / ^\circ\text{C} \\ \alpha_{FX(30)} &= 25.74 \times 10^{-6} / ^\circ\text{C} \end{aligned} \right\}$$

Outboard edge of frame.

4.7.4 Test Sample Results

4.7.4.1 CFRP Samples

The coefficients of expansion for the CFRP laminate sample and the composite sample tested with the panel were calculated from the outputs of the attached strain gauge rosettes mounted in the same sense (with respect to fibre direction) as for the test panel. The α_x and α_y values were averaged out over eight (decreasing) temperature increments as follows:-

(a) CFRP Laminate

$$\alpha_{XL\ AVE} = \underline{8.46 \times 10^{-6}/^{\circ}C}$$

$$\alpha_{YL\ AVE} = \underline{9.69 \times 10^{-6}/^{\circ}C}$$

(b) CFRP faced aluminium honeycomb

$$\alpha_{XC\ AVE}^{(top\ face)} = \underline{9.36 \times 10^{-6}/^{\circ}C};$$

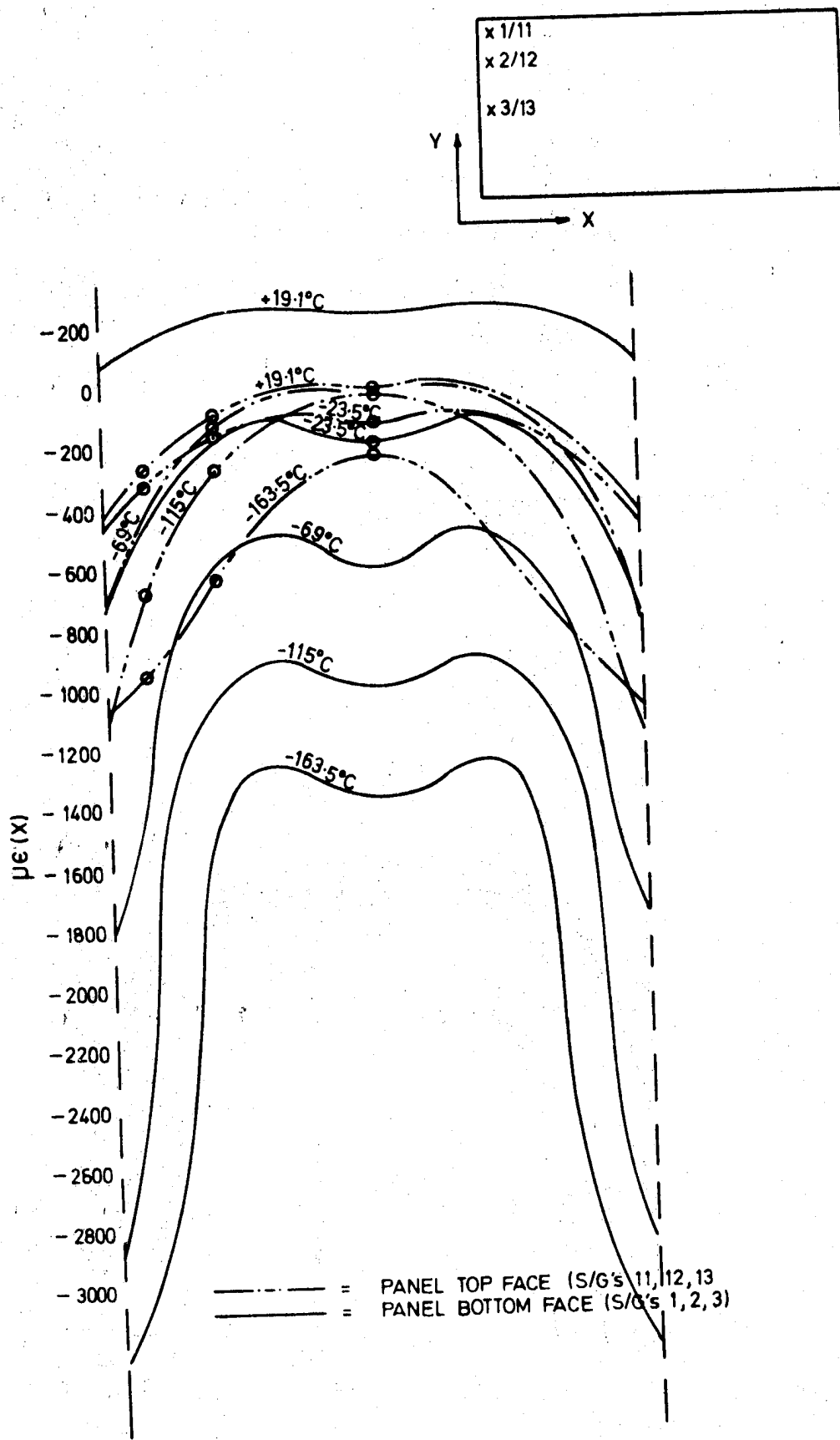
$$\alpha_{YC\ AVE}^{(top\ face)} = \underline{12.08 \times 10^{-6}/^{\circ}C}$$

$$\alpha_{XC\ AVE}^{(bottom\ face)} = \underline{10.19 \times 10^{-6}/^{\circ}C};$$

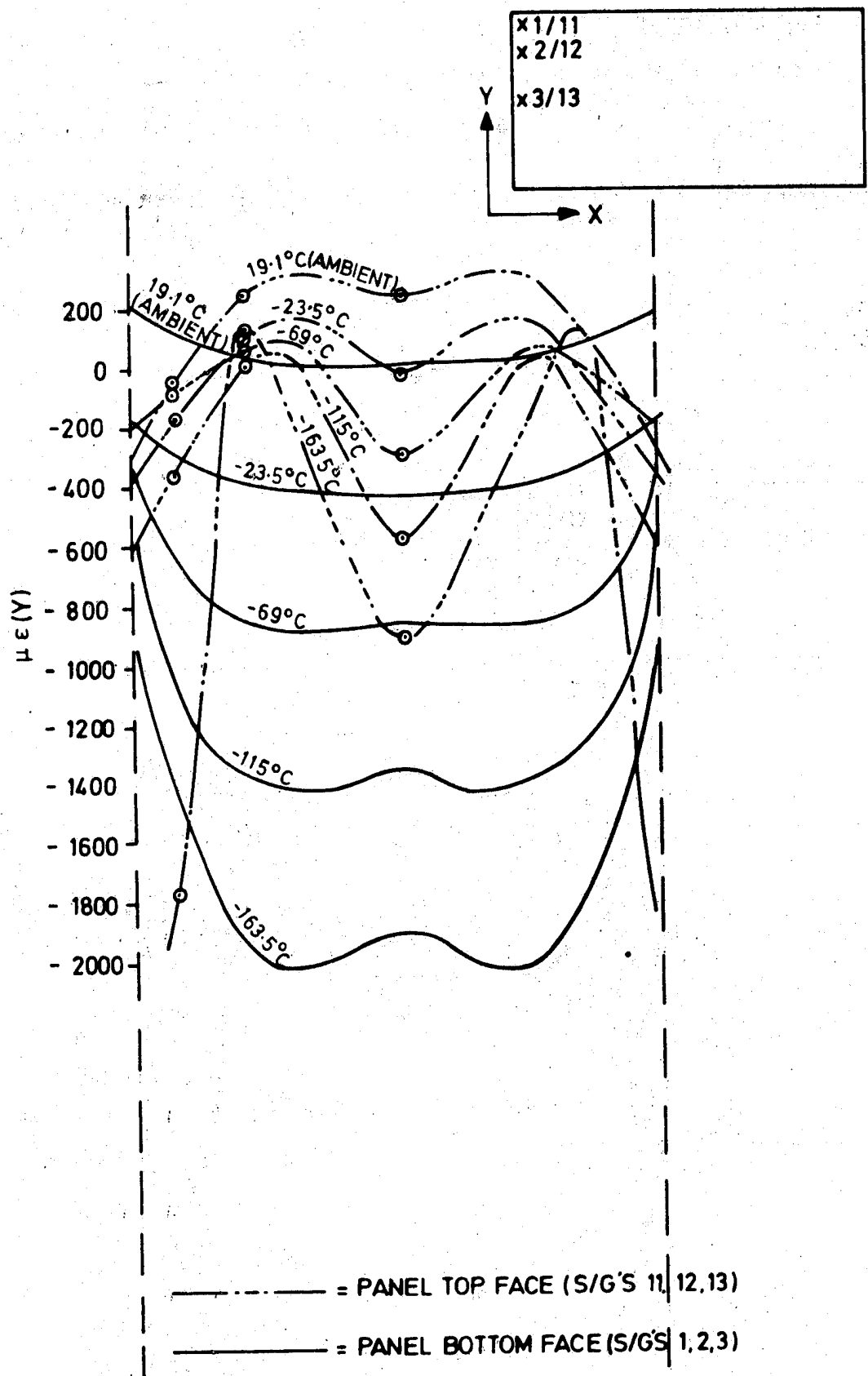
$$\alpha_{YC\ AVE}^{(bottom\ face)} = \underline{10.24 \times 10^{-6}/^{\circ}C}$$

4.7.4.2 Test Frame Sample

Gauges were mounted on a sample of the BS L59 test frame material and outputs showed good correlation with the strain gauge manufacturer's apparent strain curve, indicating an α value for the unstrained material of $\underline{23.2 \times 10^{-6}/^{\circ}C}$.

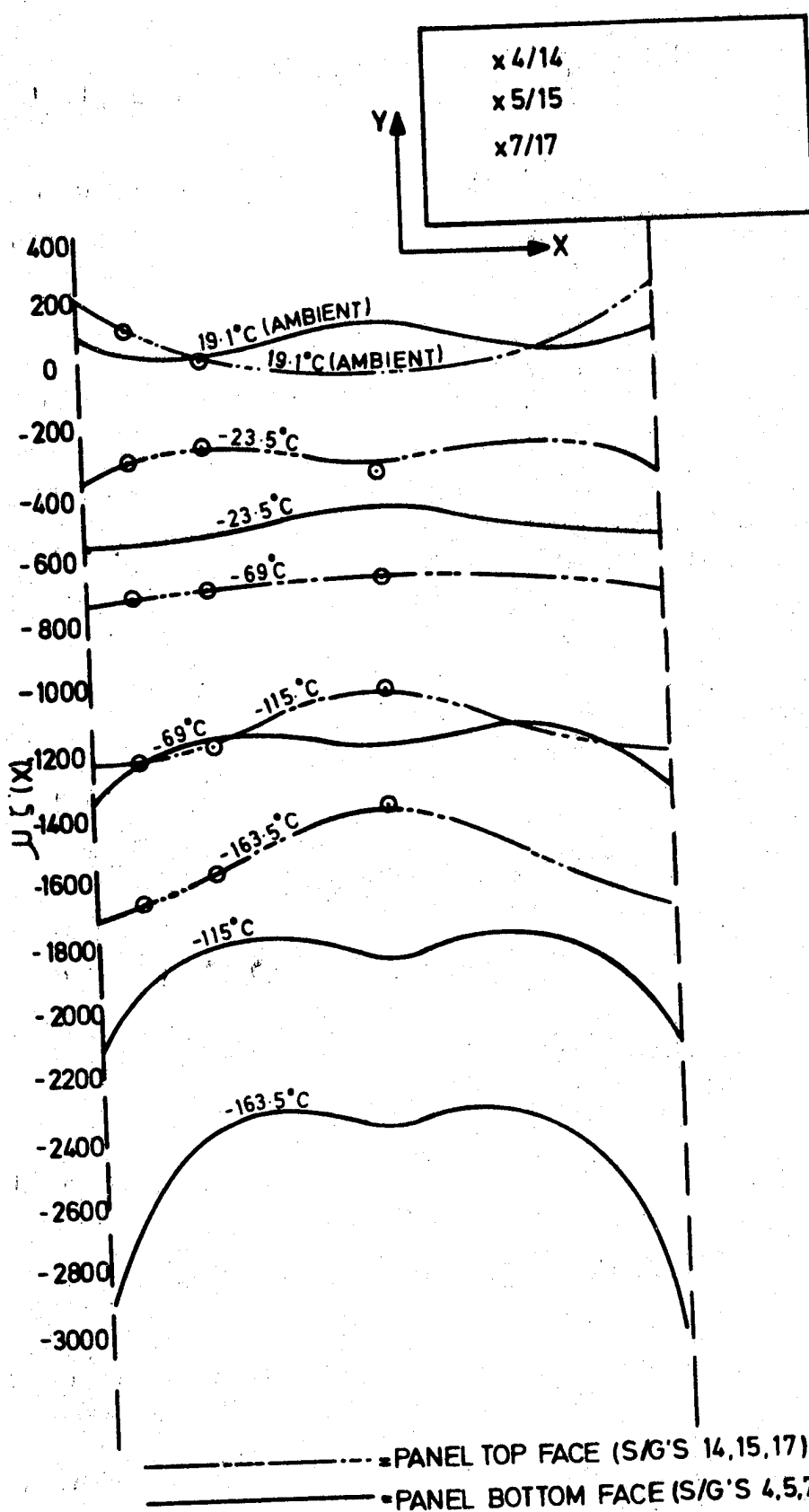


STRAIN DISTRIBUTION MEASURED IN X DIRECTION

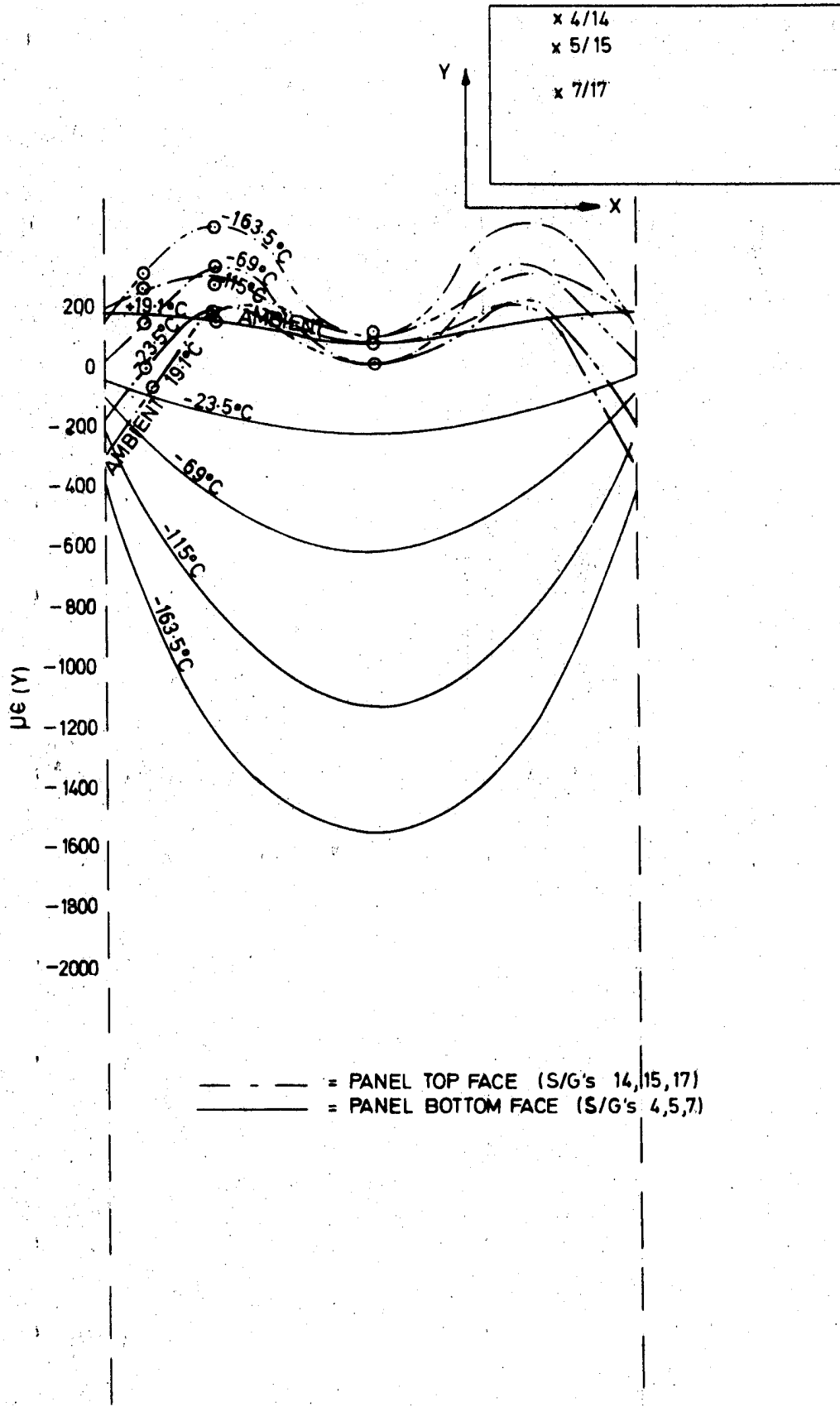


STRAIN DISTRIBUTION MEASURED IN Y DIRECTION.

FIG. 45.



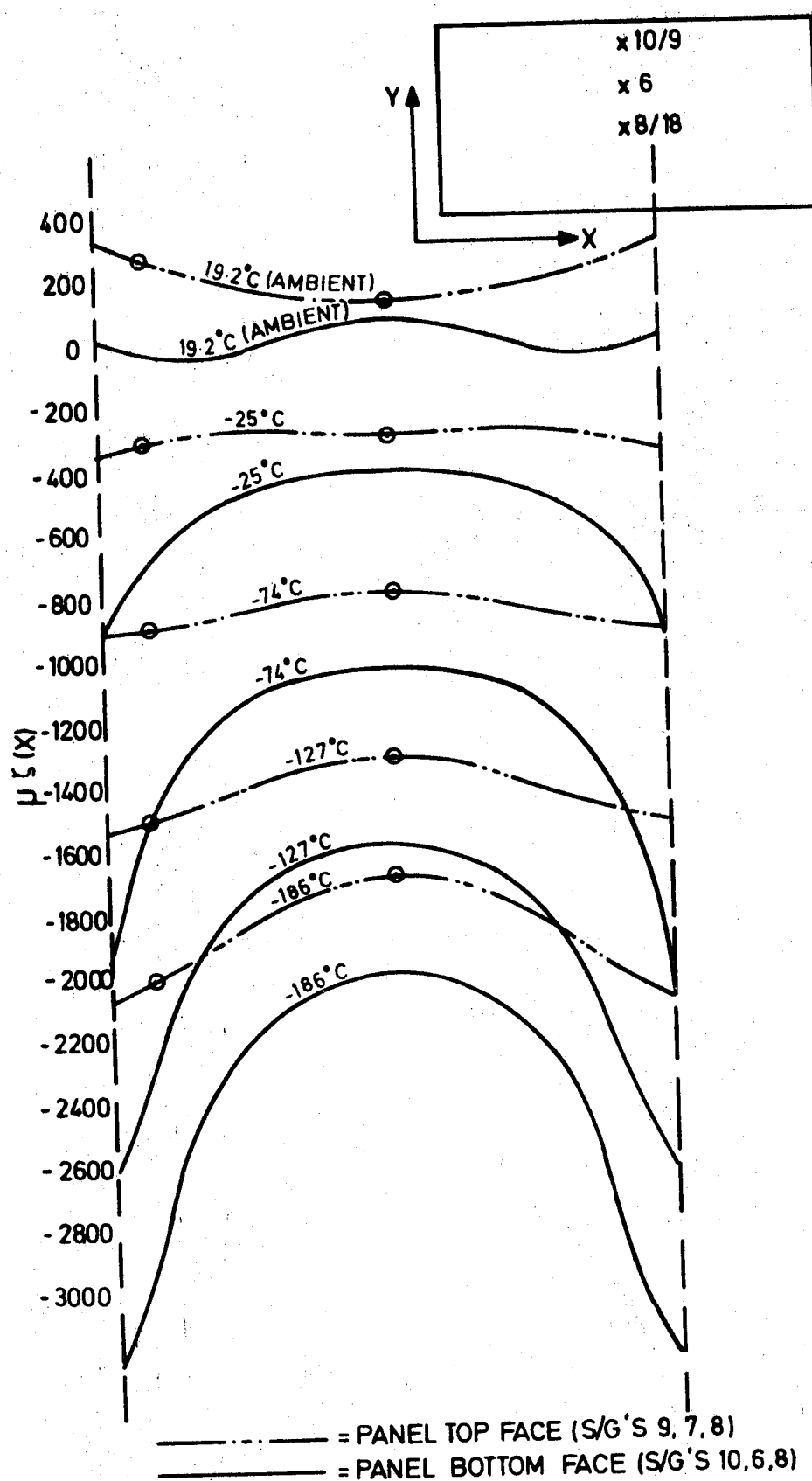
STRAIN DISTRIBUTION MEASURED IN X DIRECTION FIG. 46



STRAIN DISTRIBUTION MEASURED IN Y DIRECTION

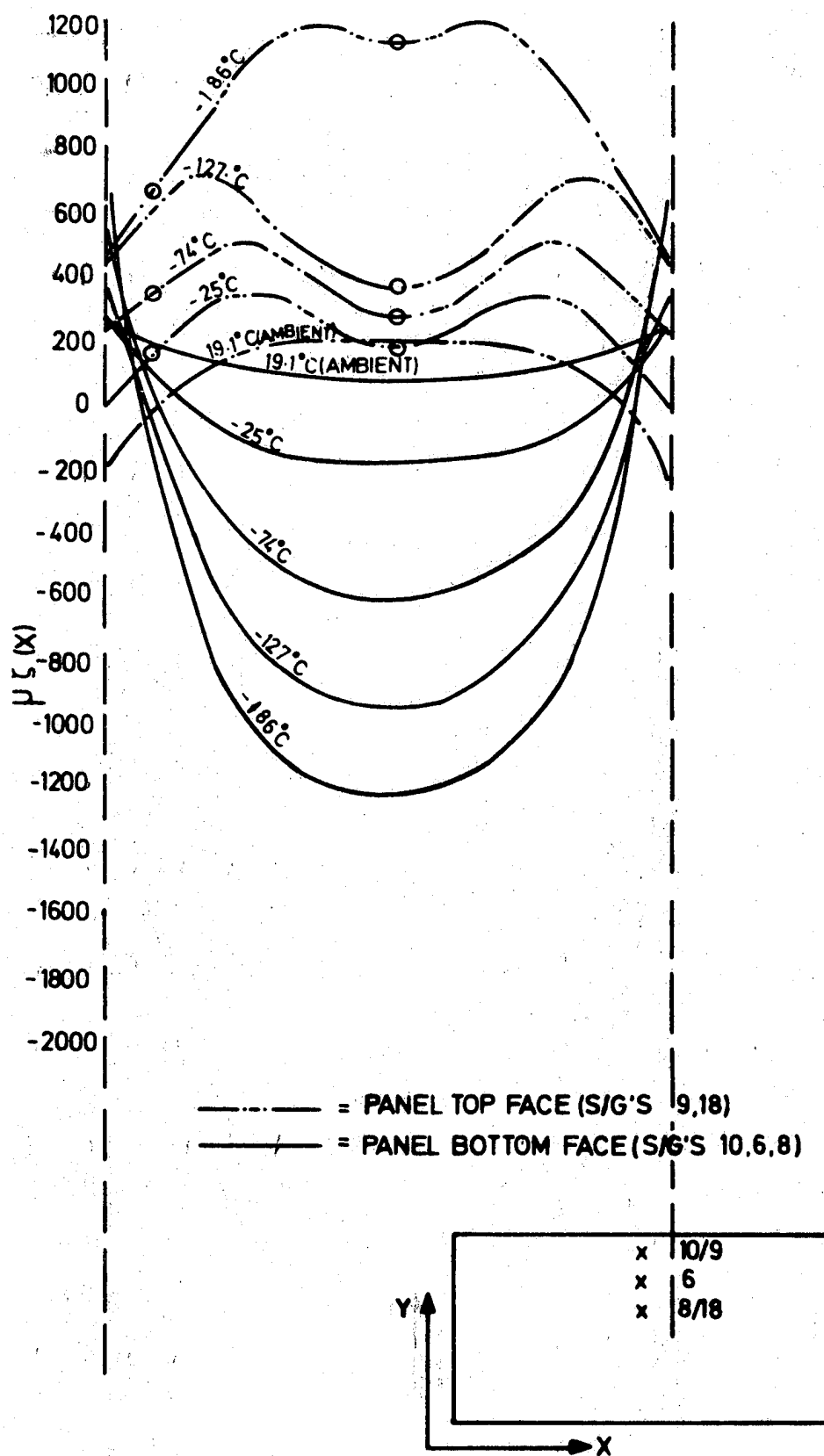
86

Fig. 47.

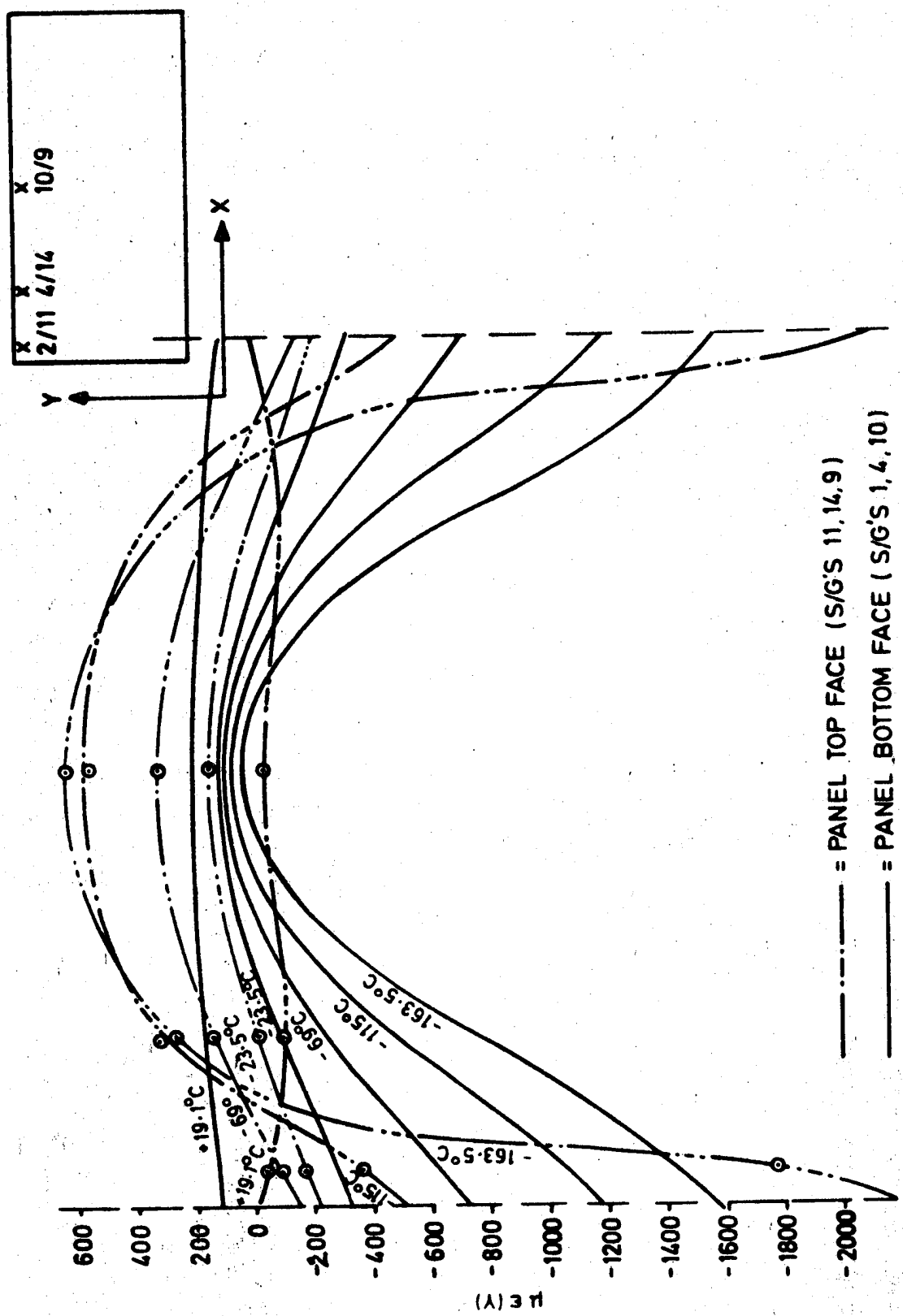


STRAIN DISTRIBUTION MEASURED IN X DIRECTION

FIG. 48

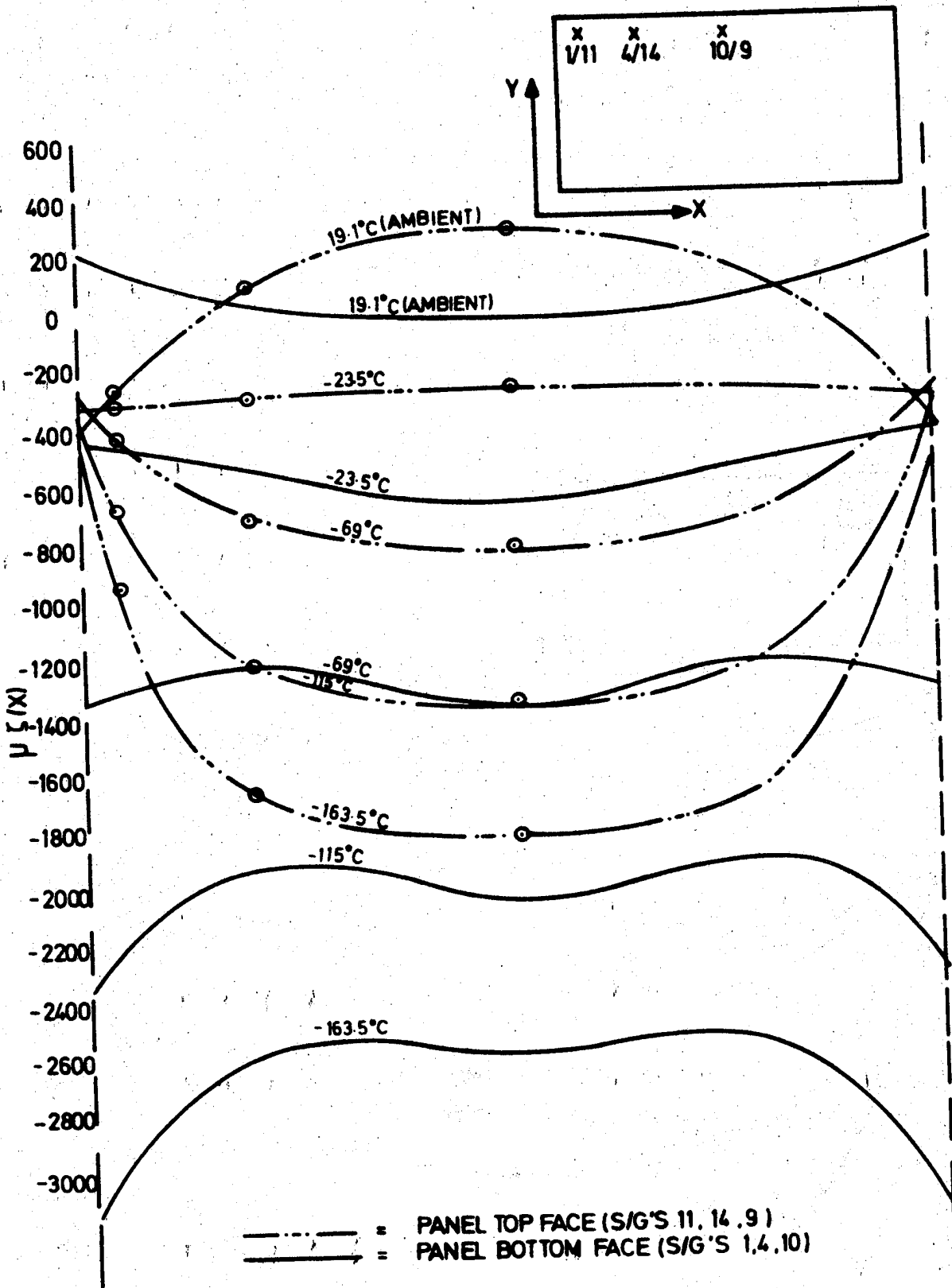


STRAIN DISTRIBUTION MEASURED IN Y DIRECTION FIG. 49



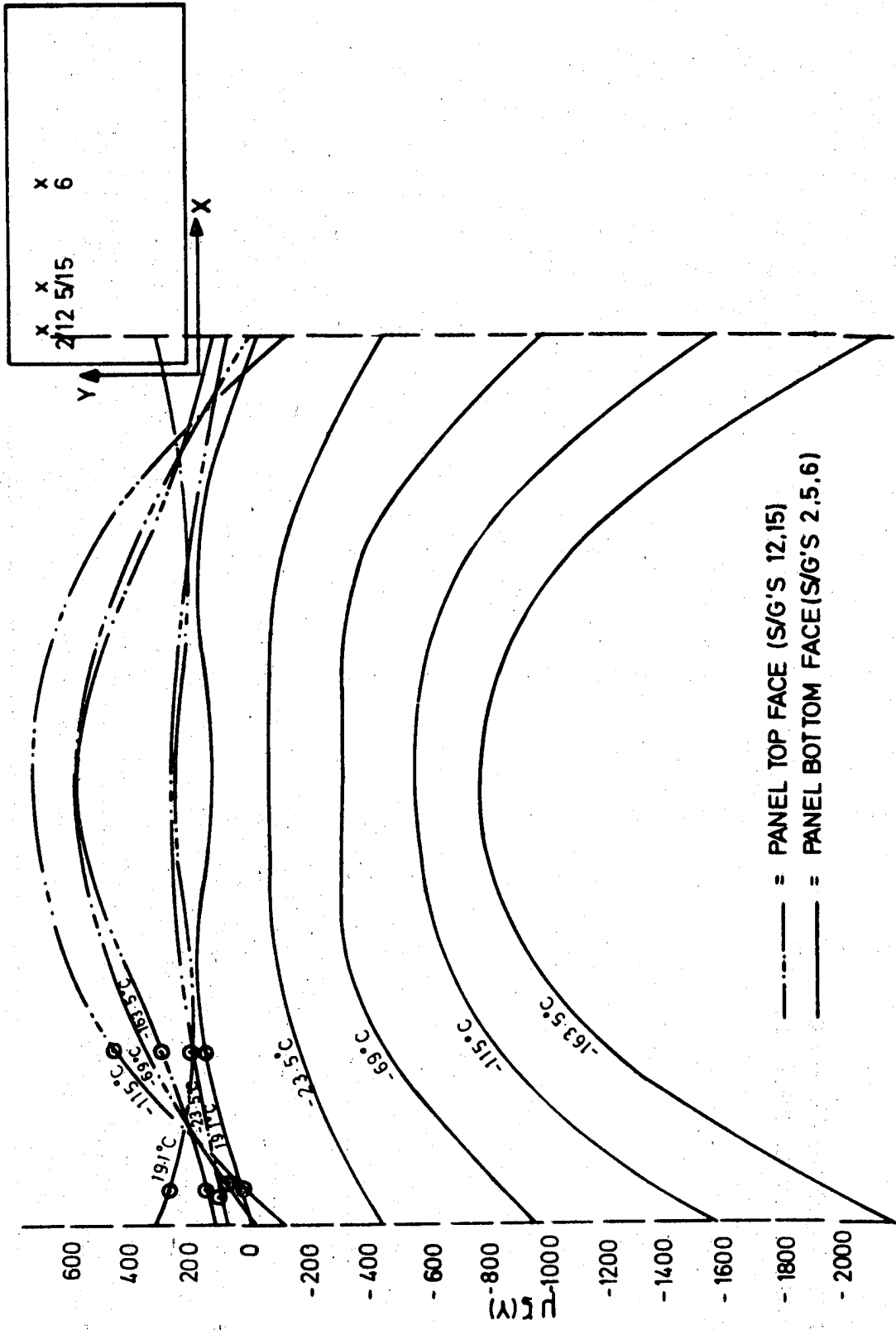
STRAIN DISTRIBUTION MEASURED IN Y DIRECTION

FIG. 50.



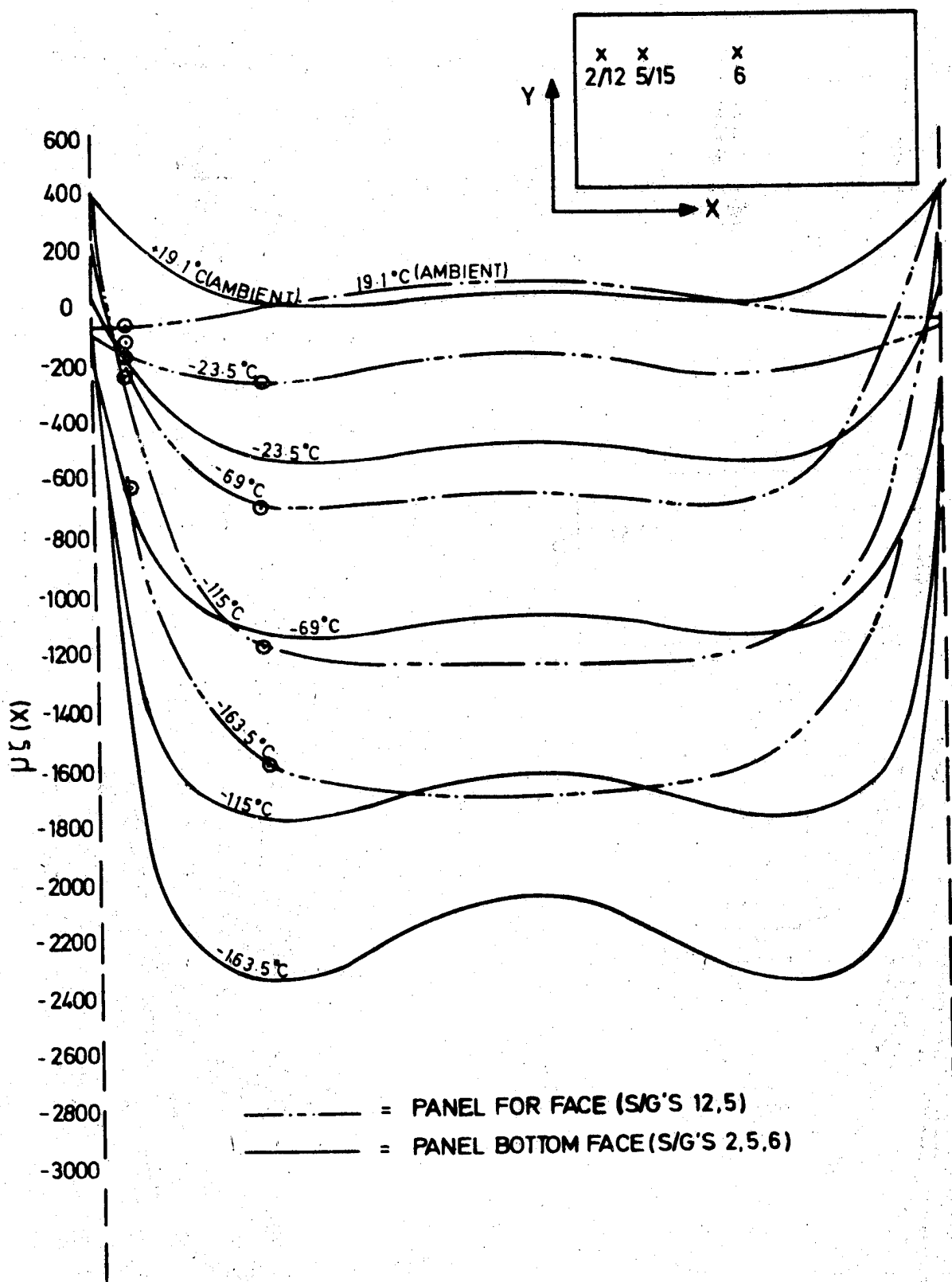
STRAIN DISTRIBUTION MEASURED X DIRECTION

FIG. 51

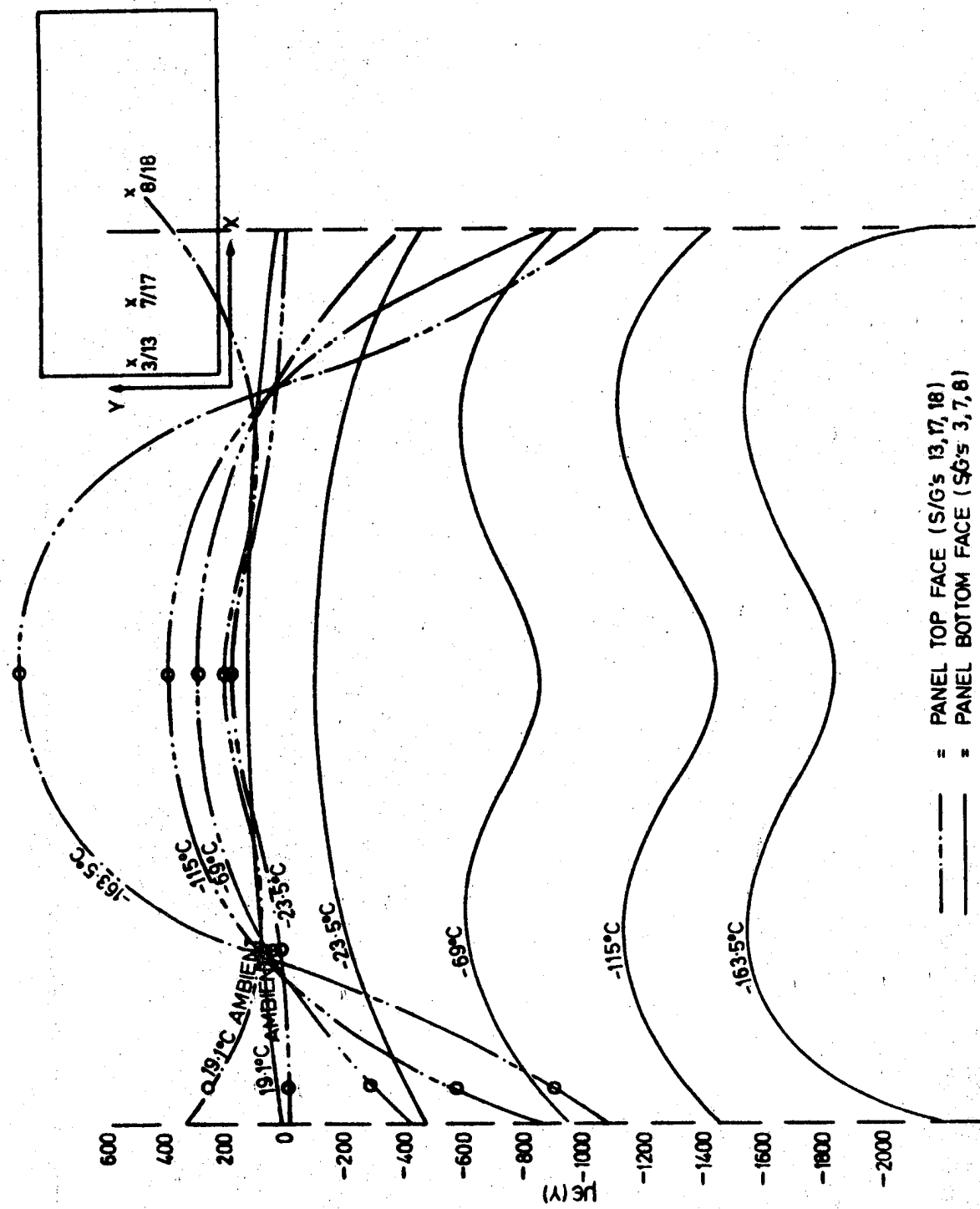


STRAIN DISTRIBUTION MEASURED IN Y DIRECTION

FIG. 52

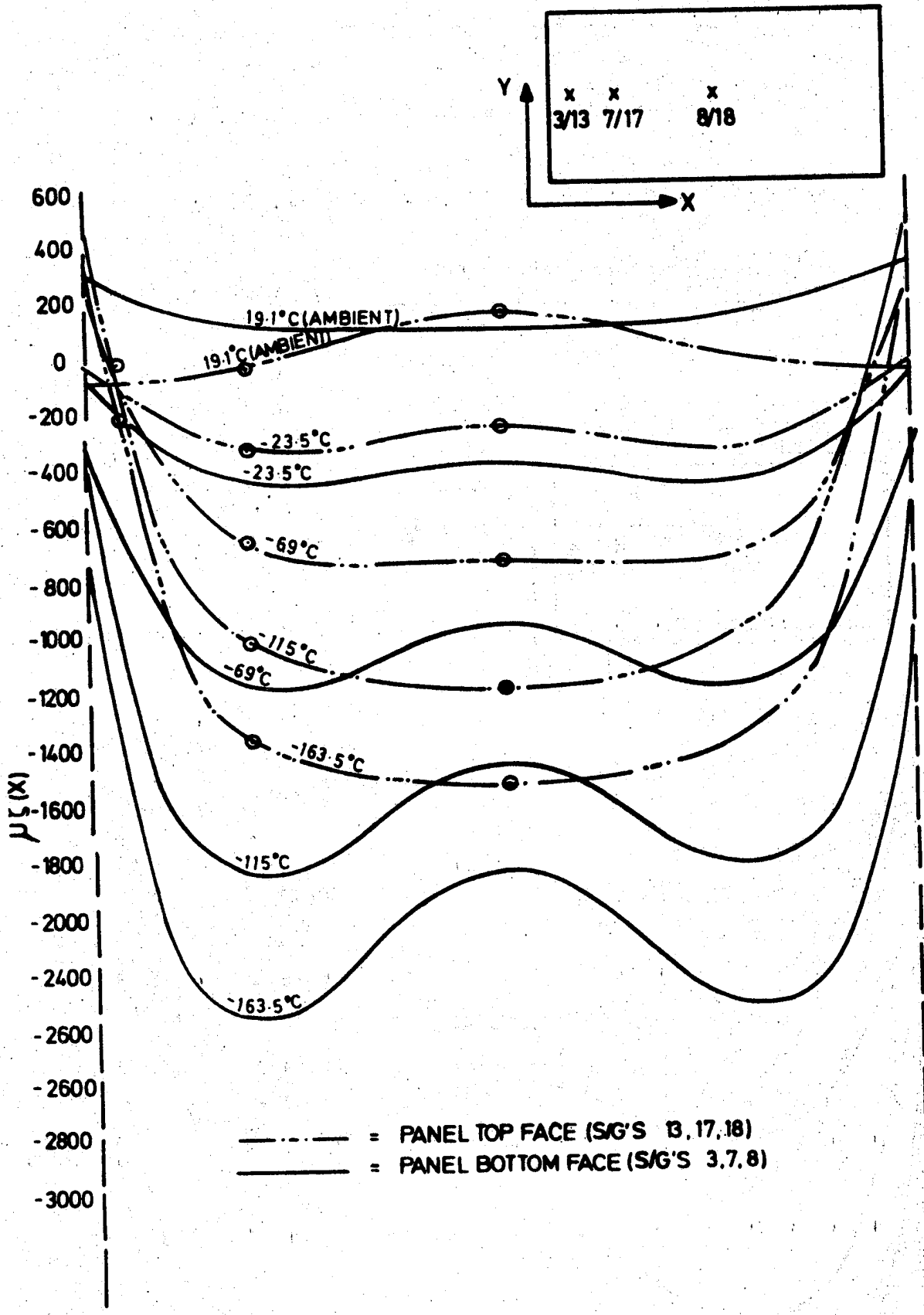


STRAIN DISTRIBUTION MEASURED IN X DIRECTION FIG. 53



STRAIN DISTRIBUTION MEASURED IN Y DIRECTION

Fig. 54.



STRAIN DISTRIBUTION MEASURED IN X DIRECTION FIG. 55

5.

DISCUSSION

The improved model as described in para. 2.1.1 and Appendix F was run using the material properties selected as per para. 3.6. A 50°C temperature decrement was used which gave deflections in the X, Y and Z directions as shown in Figure 56. Corresponding strains predicted by the model for the same decrement are shown in Figures 59 to 62.

5.1

Panel Deflections, Theory vs Practice

Figure 57 gives a comparison between theoretical and practical deflections. The following points emerge:

(a) Normal Deflection along centrelines of Panel

The theoretical model results are seen to be approximately 50% of those measured on test by the Dial Test Indicators.

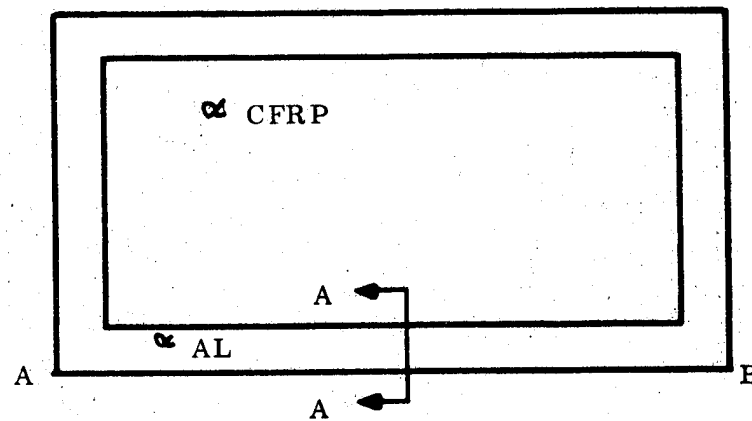
(b) In-Plane Deflections Panel Y-Direction

The theoretical model results are seen to be approximately 30% of those measured by the Dial Test Indicators.

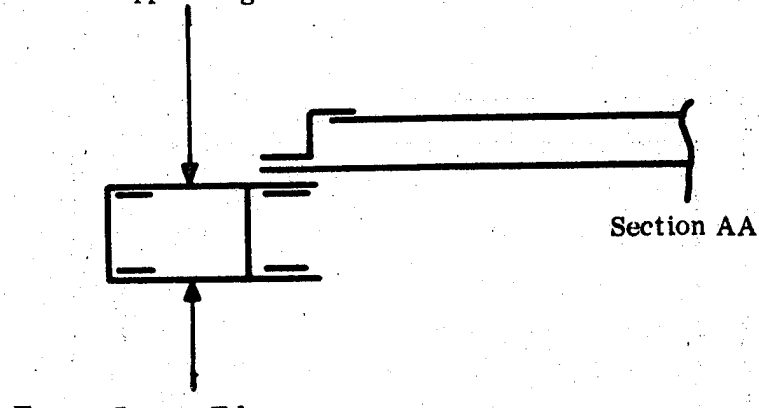
The most significant reason for these discrepancies lies in the differences between overall panel expansion coefficients and those used in the model which were derived from the coupon tests.

The average values determined from the panel tests were 7.0×10^{-6} and 11×10^{-6} per $^{\circ}\text{C}$ for the X and Y directions respectively. A single value of 3.5×10^{-6} per $^{\circ}\text{C}$ was determined in the test programme and subsequently used by the model.

For the 'STARDYNE' Finite Element package used it is not possible to input separate values for X and Y coefficients of expansion for the triangular sandwich elements. If an averaged value of 9×10^{-6} per $^{\circ}\text{C}$ were used in the model, then the theoretical in-plane deflections would be much greater but the theoretical normal deflections would be much smaller. Hypothetical curves for this expansion coefficient are shown in Figure 57. The explanation of this effect is given below.



Frame Upper Edge

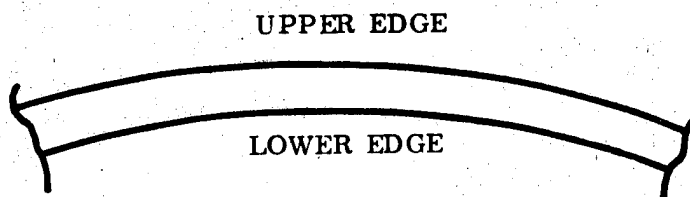


Section AA

α_{CFRP} = CTE of CFRP faced honeycomb panel

α_{AL} = CTE of aluminium

Following a temperature drop, the expected deflected shape of the beam AB where $\alpha_{CFRP} < \alpha_{AL}$ is shown below:



The lower edge is allowed to contract freely but the upper edge of the beam is restrained due to the carbon fibre panel.

If the panel were to be given a hypothetical increase in CTE then the restraint offered by the panel would be reduced and consequently the out of plane deflections would be reduced. It can similarly be seen that a reduction in the restraint would also increase the in plane deflections.

To check whether or not the apparent CTE of the panel remained constant with temperature, a plot (Figure 58) was made of deflection at the centre of the panel against temperature. The linearity of the curve shows that the CTE is constant which is in agreement with the coupon tests.

It is evident that correction of the CTE alone will not give model results that agree exactly with those obtained in practice. Other sources of error are considered below:

- Errors in Dial Gauge Indicator Readings due to the effects of temperature on their mechanisms.
 - Based on then current manufacturer's data an average value of 252 N/mm^2 was used in the model for the honeycomb shear stiffness. Later information gives values of 270 and 170 N/mm^2 for the longitudinal and transverse directions respectively. If an average of these values was used it would be lower than that in the model and would give rise to greater theoretical normal deflections and result in better correlation between theory and practice.
 - Errors in idealisation of box beam frame. Since this beam is of fabricated construction it may not possess a torsion constant as high as that suggested by incorporating the bending normal to the plate. This can be explained by reference to the diagrams following:

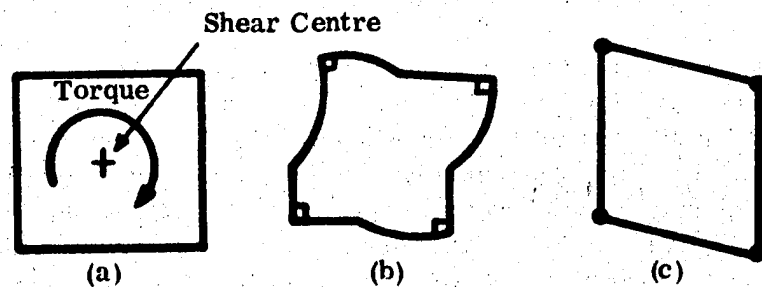
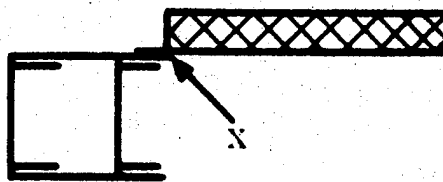


Diagram (a) shows the torque applied to the fabricated aluminium box section. Diagrams (b) and (c) show the effects of the torque applied to the box if the corners of the box are rigidly connected and pinned respectively.

The model utilises quadrilateral plates that conform to (b) rather than (c). For this reason the box may be described too stiffly in torsion giving rise to too great an end restraint, in bending, to the panel. A torsionally less stiff theoretical frame would allow greater out of plane deflections of the panel and hence closer agreement between theory and practice.

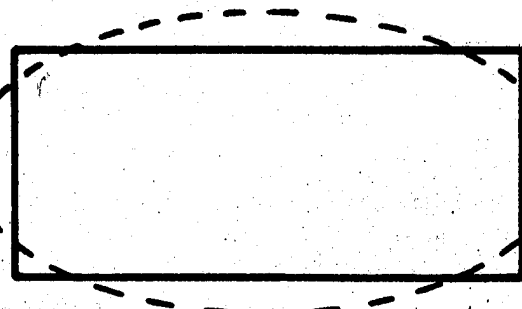
Additionally, because of the type of quadrilateral plate elements used in the model, the joint line 'X', shown below, is also considered to take bending.



This joint line may also be described too stiffly by the model. The effect of this is again to provide too great a theoretical bending restraint and thus smaller out of plane deflections by the panel than are seen in practice.

Although the numerical results from model were not in agreement with those obtained from practical testing, the in-plane and normal deflection gave the expected deflected shape of the structure.

An exaggerated in plane deflected form is given below:



- Errors due to Dial Test Indicator arrangement.

- (a) In-plane Readings.

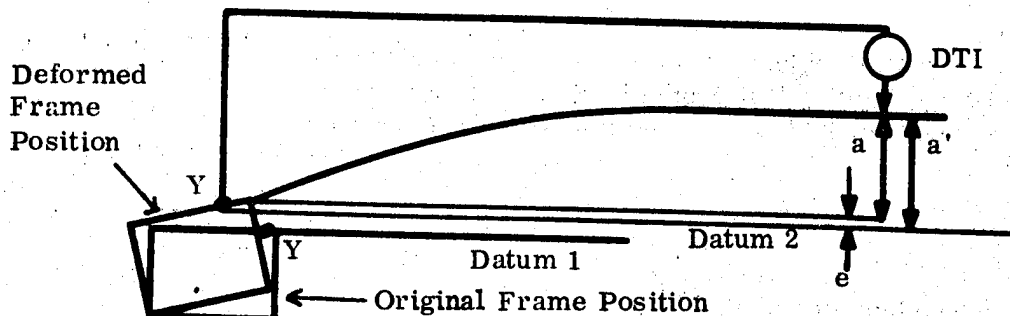
These readings were used to calculate the coefficient of thermal expansion for the panel and give results in the longitudinal (X) and transverse (Y) directions similar to those obtained from the strain gauge readings.

Measurements were, however, subject to large correction factors due to the fact that the DTI's were connected to an aluminium frame which contracted relative to the panel.

(b)

Normal Readings

With reference to the diagram below it can be seen that a minor source of error arises from the fact that the DTI frame was supported on rods which rested on the frame outside the panel perimeter. Measurements taken normal to the panel were thus slightly greater than the actual deflections.



a = actual deflection of panel as given by the model

a' = apparent deflection of panel relative to mounting datum

e = vertical deflection of the panel edge fixing relative to the dial gauge frame fixing.

It follows $a' - e = a$.

Thus for actual deflections of the panel ' e ' should be subtracted from all DTI readings but cannot be obtained from the measurements taken.

From consideration of deflections alone the following conclusions can be drawn.

- Theoretical and practical deflected forms are similar.
- Absolute values are, however, very different, practical values being approximately twice and three times the theoretical values for normal and in plane measurement respectively.

- Differences between the panel CTE's and the coupon CTE's, as used by the model, are significant and must contribute to the differences in absolute deflections. The apparent differences cannot, however, be explained at this time and future research should aim at solving this critical anomaly.
- Discussion has shown that the differing CTE's are not the sole source of error in the absolute deflections. Other sources that have been proposed are associated with local model idealisations and the practical measuring arrangement. The latter is thought to be more significant than the former but both are considered small in comparison with the observed differences.
- For the 'panel free' case the panel CTE's derived from the DTI and strain gauge readings were in close agreement. This would tend to give confidence to the in-plane DTI measurements and the large apparent, panel CTE's.

5.2

Panel Strains, Theory vs Practice

Figures 59, 60, 61 and 62 give the model computed strains together with the practically derived values.

Each of the plots of theoretical and actual strains show the same form and in each case the theoretical results are always greater than those measured in practice.

Bottom surface readings were all greater than top surface readings for the four cases plotted. The reasons for these differences is that the induced bending of the panel produces an additive compressive strain to the bottom surface and a tensile strain to the top surface. These bending strains thus subtract from the end load compressive strain in the top surface and add to the end load compressive strain in the lower surface.

A tendency for the theoretical results to be greater than the actual is compatible with the coefficient of thermal expansion being entered as lower than actual in the model input.

That is if α_{CF} tends towards that of α_{AL} then there will be less relative strain between the two panels.

The correct CTE value would only lower the strains by about 28%. The maximum actual strain values are seen to be up to 50% less than the theoretical maximum strains. The minimum strains are seen to be up to 80% less than the minimum theoretical strains.

An additional discrepancy will be due to the fact that the panel in the 'fixed' condition was not free from strain at ambient temperature (+19.1°C). This strain shown on Figures 44-55 inclusive was induced by panel and/or frame irregularities in geometry and was accentuated by the close tolerance fixings.

For the plots 59-62 the actual curves were derived from a reading at -23.5°C by correcting with strains induced in assembly at +19.1°C, then factoring by $\frac{50}{19.1 + 23.5}$ to compare with the strain output from model for a 50°C drop in temperature.

The above does not result in a direct comparison between actual and theoretical strains as the strains induced at ambient will influence the panel loading but are not taken into account by the model.

The induced strains are due to the clamping of the panel to the frame and thus their effect should be reduced towards the centre of the panel.

Other reasons for discrepancies between actual and theoretical values may be in local model idealisations as discussed in para. 5.1. They are not, however, considered to be a significant source of error.

Overall conclusions based on analysis of strains are as would be expected very similar to those obtained from the deflection analysis para. 5.1. Trends and forms are similar but absolute values are different. Differences are not, however, so marked as they were for the deflections. The primary source of error appears to be the anomalous CTE values although again this is not considered the sole source of error.

5.2.1

Failure Prediction

Maximum stresses identified by the model for a 50°C drop in temperature were 51.54 and 49.33 N/mm² for the X and Y directions respectively. These correspond to values of 46.4 and 37.4 N/mm² obtained from the fixed panel test for a similar temperature drop. (See Appendix G).

Coupon testing showed a local buckling failure of 107.0 N/mm² at -100°C for the honeycomb sandwich which would give a predicted failure at -89°C. In practice there was no evidence of failure at this temperature and the panel was still intact at the lowest temperature reached on test which was -166°C. Recorded panel stresses at this temperature were 197 and 137 N/mm² for the X and Y directions respectively.

Neglecting errors between theory and practice the two practically derived stresses differ by almost 2 to 1 and could at panel failure differ by more. It can only be concluded that the coupon test arrangement did not simulate the panel mode of failure by developing a premature failure peculiar to itself.

Certainly the measured failure stress is significantly below that found during other test programmes albeit with different layups.

Further work, see para. 5.3, is required to investigate the relationship between coupon and panel instability modes.

5.3

Recommendations

The most significant sources of error that have been identified in this Study are differences between coupon derived CTE and failure stresses and those found for the overall panel. Before any further improvements to the modelling or measuring arrangements are made it is imperative that a better understanding of these differences is obtained. It is therefore recommended that test programmes be instigated to investigate the following:

(1) CFRP faced honeycomb sandwich CTE's.

- standard coupons, and samples with edge member cut from the panel
- laser interferometric methods to be employed
- local measurements to be made within perimeter of large panel to reduce edge effects.

(2) CFRP faced honeycomb sandwich in-plane compressive failure

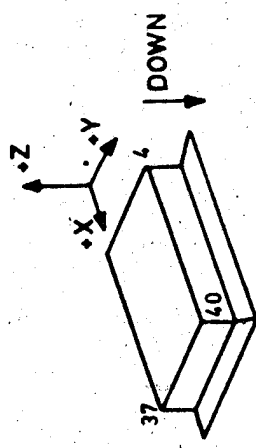
- overall and local instability failure
- faceskin material failure
- effects of combined loading
- edge member effects

Once these areas have been investigated the panel/frame analysis should pursue the following course:

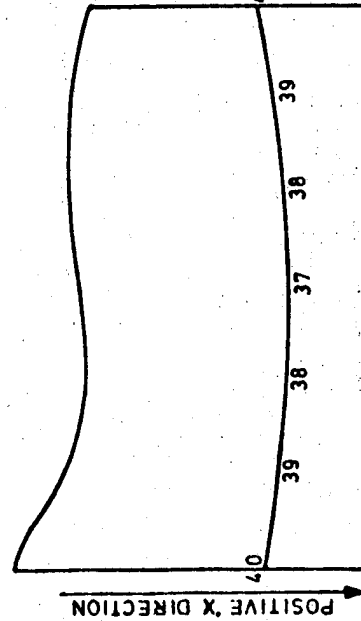
(1) Model the frame alone and subject it to a temperature drop (consideration could perhaps be given to using a solid aluminium frame to ease the analysis at this stage)

- (2) Model the panel alone and subject it to a temperature drop
 - (3) Test frame by subjecting it to a temperature drop
 - (4) Test panel by subjecting it to a temperature drop. For all practical tests the following should be observed:
 - (a) All necessary deflections should be measured optically
 - (b) Strain gauges calibrated for the material on which they are intended to measure strains should be used
 - (c) It should be ensured that the surfaces to be bolted are flat and that there is no likelihood of strain being induced when the two structures are bolted together.
 - (5) Alter stiffness of elements in models (1) and (2) and/or idealisation, for example add more elements to produce a more accurate model.
- When a satisfactory correlation between theory and practice is achieved the panel and frame should be bolted together and tested as such.
- (6) Model the structure complete using the same idealisations as for the sub-structures and subject it to a temperature drop.

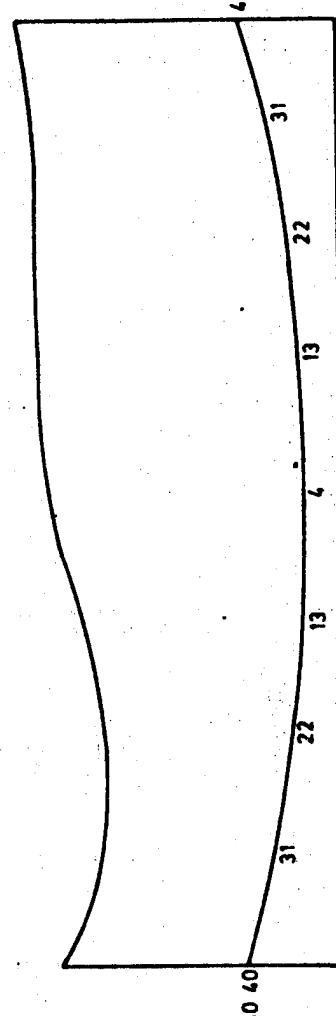
This should generate a close approximation between theory and practice and will certainly give a better understanding of the relative interactions that are involved.



END CONTRACTION IN X DIRECTION

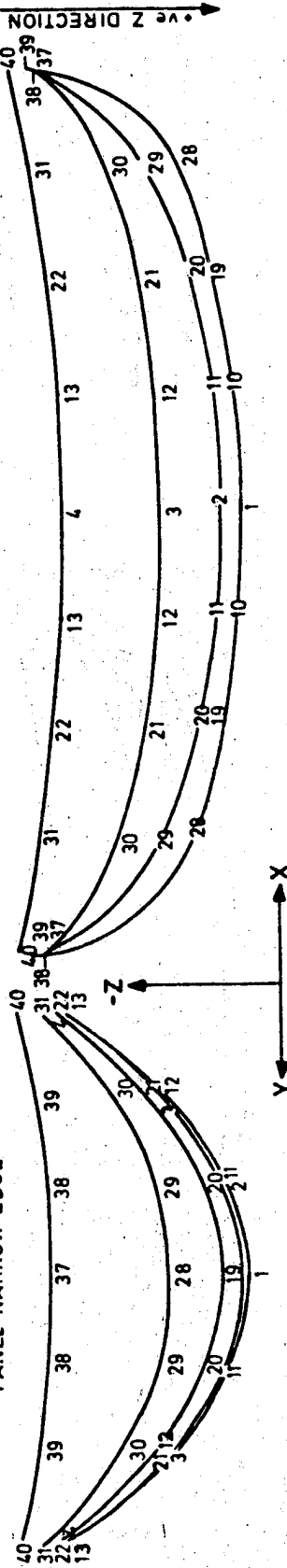


SIDE CONTRACTIONS IN Y DIRECTION

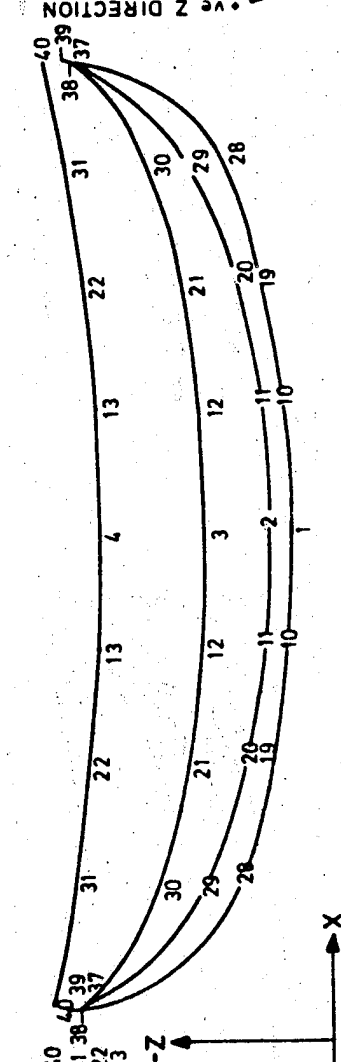


END DEFLECTIONS IN Z DIRECTION (X100)

PANEL NARROW EDGE



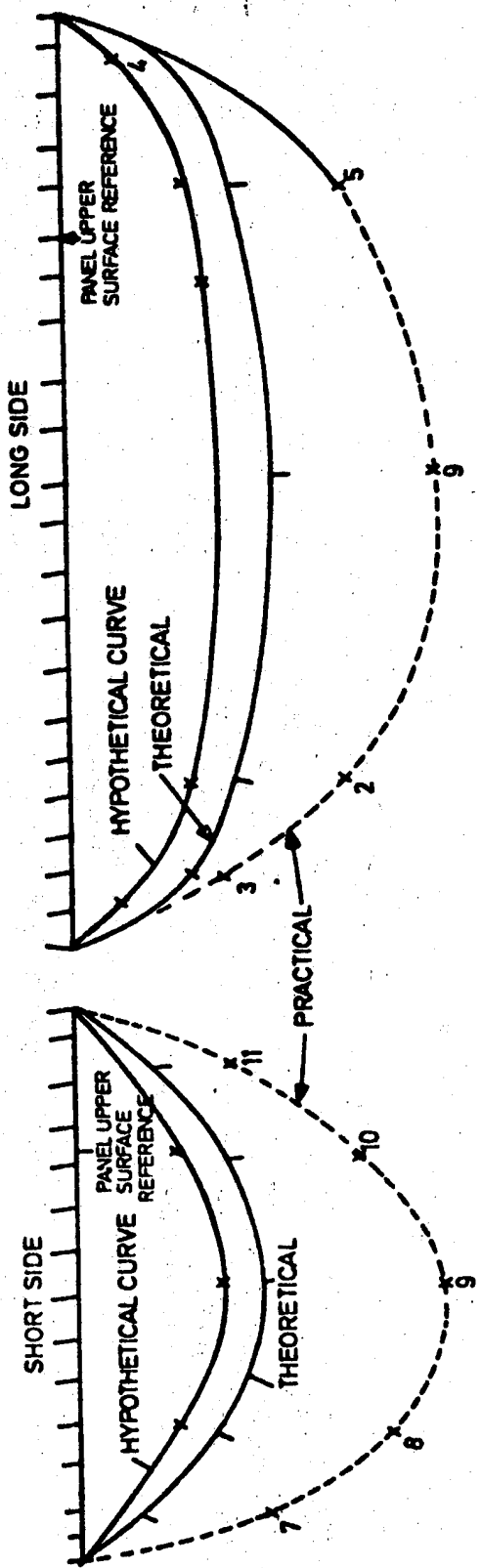
SIDE DEFLECTIONS IN Z DIRECTION (X100)



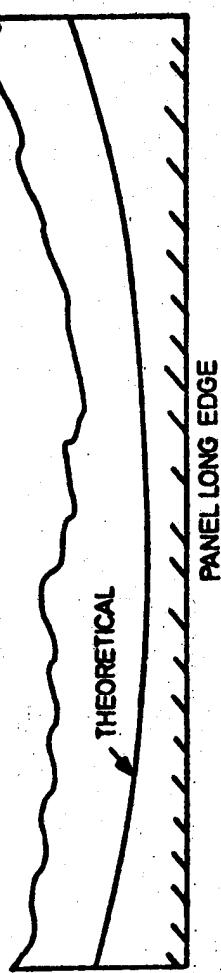
•VE Y DIRECTION

•VE Z DIRECTION

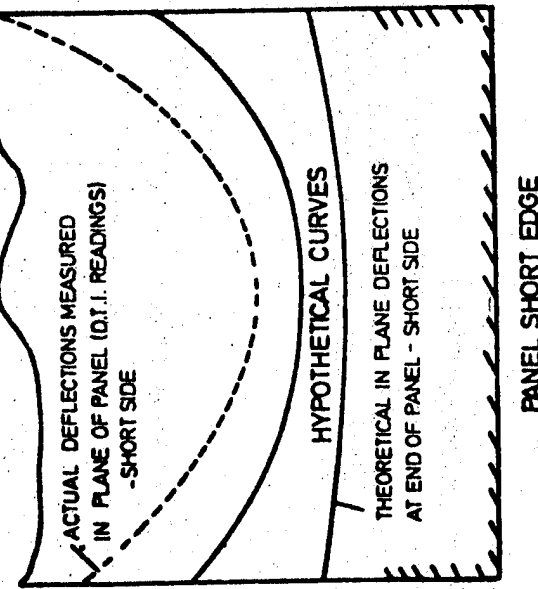
THEORETICAL DEFLECTIONS OF CARBON FIBRE PANEL WHEN THE
PANEL IS ATTACHED TO THE ALLUMINIUM FRAME 50°C DROP IN TEMP. FIG.56.



PANEL DEFLECTIONS MEASURED NORMAL TO THE SURFACE ALONG THE CENTRE LINES. PANEL FIXED AND SUBJECTED TO 50°C TEMPERATURE DROP DEFLECTIONS X 100. DIMENSIONS X0.25.



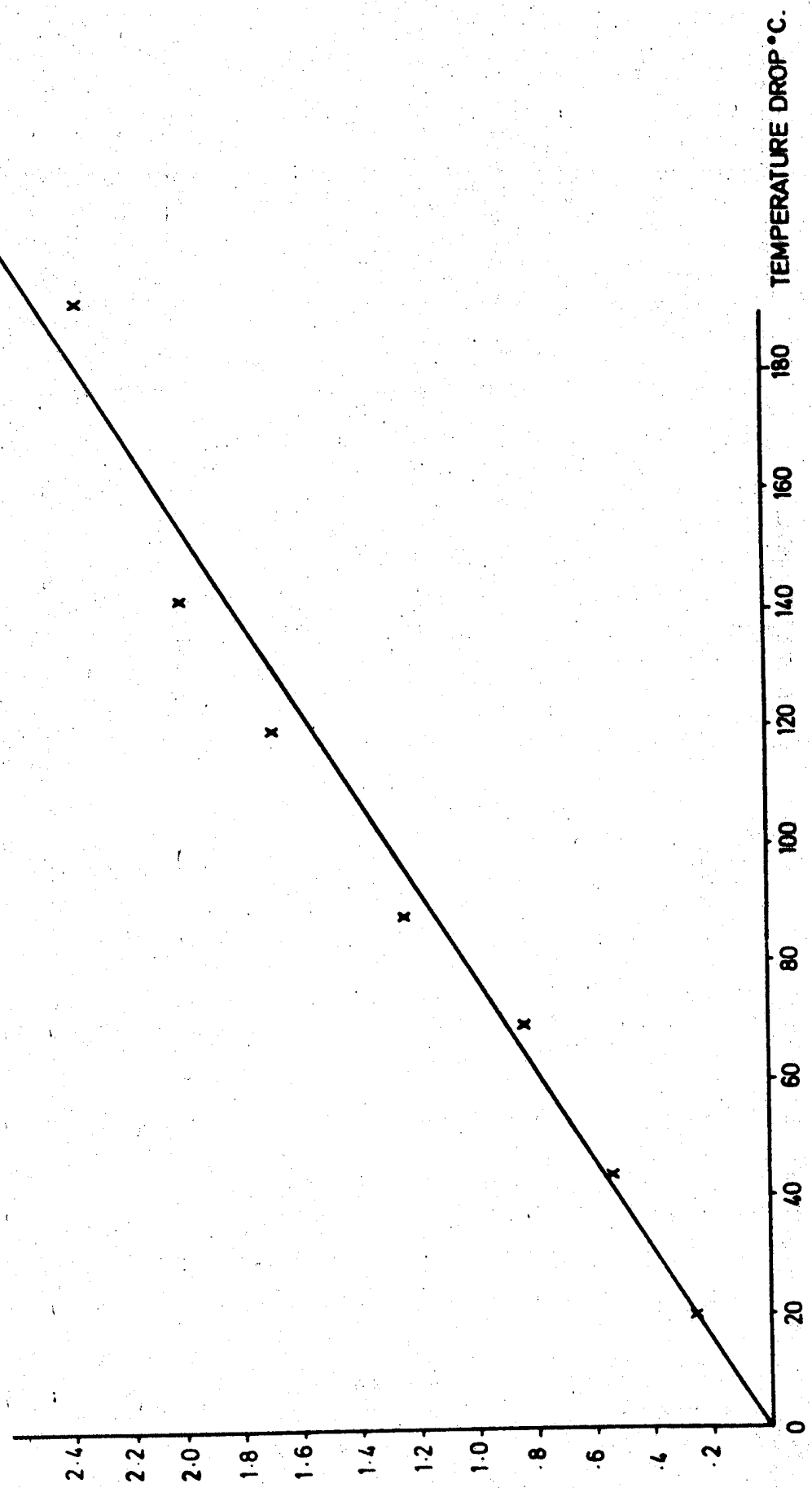
PANEL DEFLECTIONS MEASURED IN PLANE ALONG PANEL EDGES. PRACTICAL DEFLECTIONS FOR PANEL LONG EDGE NOT SHOWN SINCE THERE WAS ONLY A SINGLE POINT MEASUREMENT.



PANEL SHORT EDGE

PLOT OF THEORETICAL AND ACTUAL DEFLECTIONS OF CARBON FIBRE PANEL WHEN ATTACHED TO ALUMINIUM FRAME

FIG. 57.

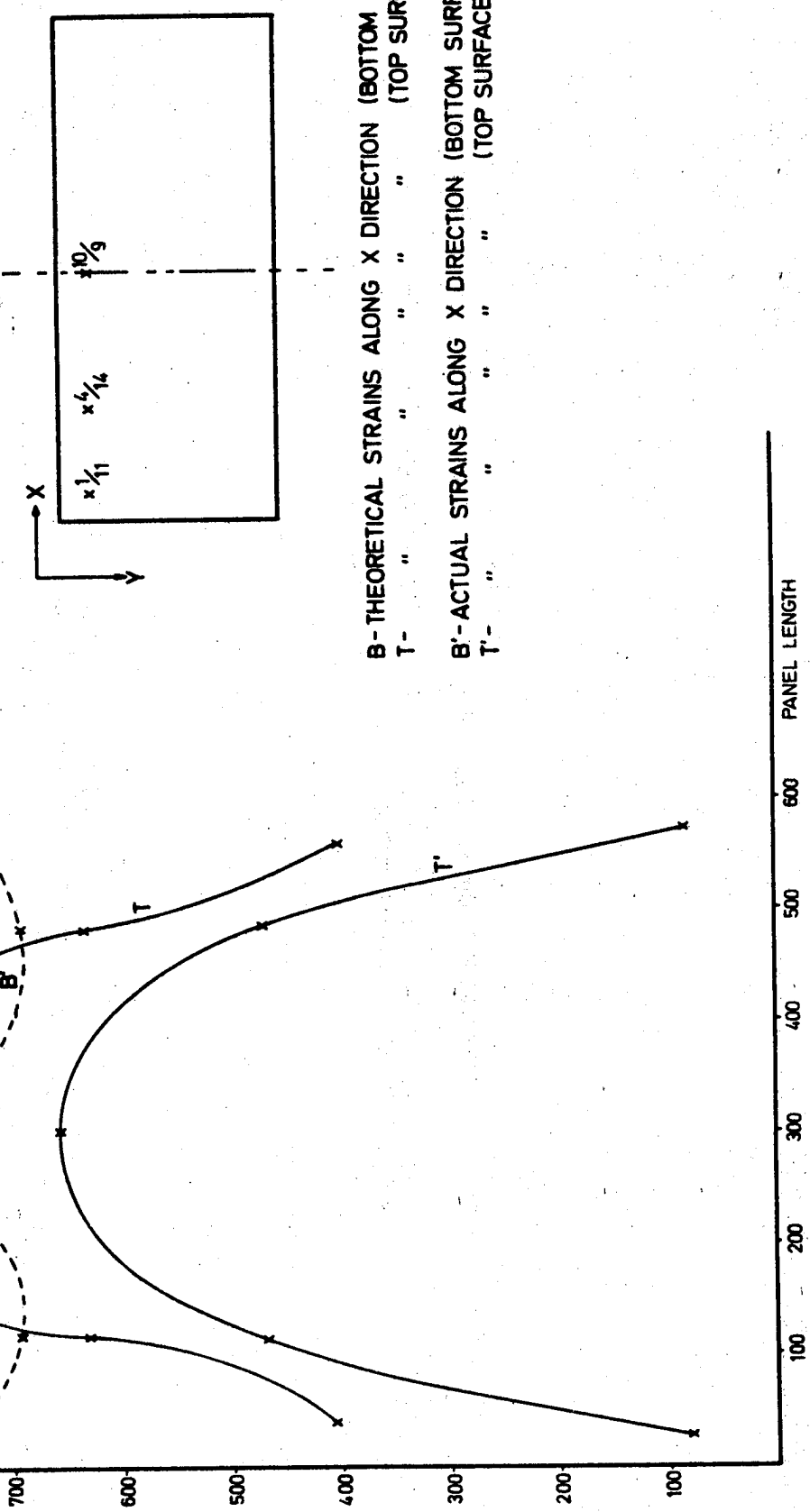


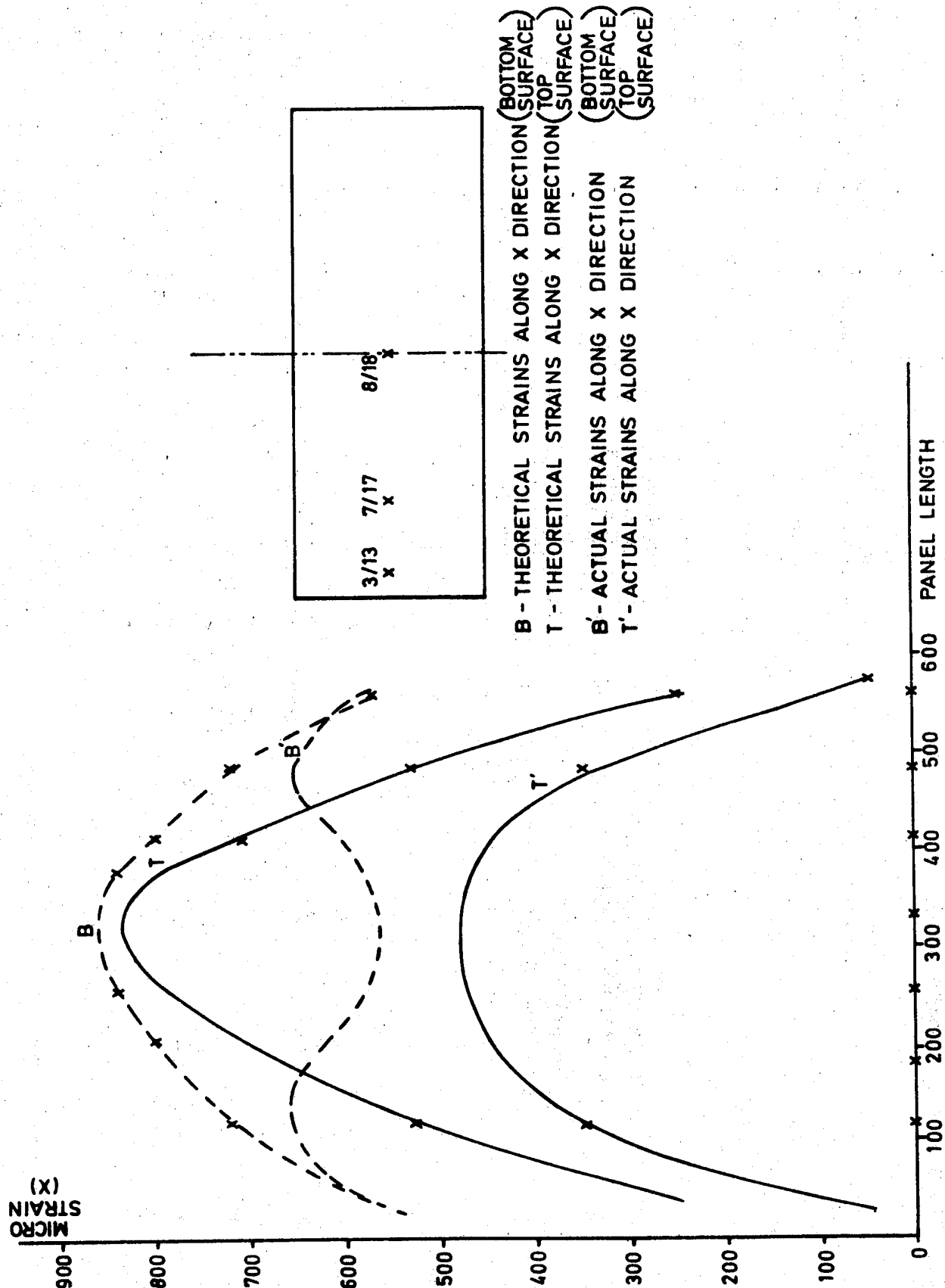
PLOT OF DIAL TEST INDICATOR READING (9)v TEMPERATURE DROP
NB. D.T.I.9 READING NORMAL DEFLECTION AT PANEL CENTRE.

FIG. 58

PLOT OF THEORETICAL AND ACTUAL STRAINS FOR TOP AND BOTTOM SURFACES OF CARBON FIBRE
PANEL. STRAINS MEASURED AT POSITIONS 1,4,10, FOR BOTTOM SURFACE
11,14,9, FOR TOP SURFACES

FOR 50°C DROP IN TEMPERATURE





PLOT OF THEORETICAL & ACTUAL STRAINS FOR TOP & BOTTOM SURFACES OF
 CARBON FIBRE PANEL. STRAINS MEASURED AT POSITIONS 3,7,8, FOR BOTTOM SURFACE
 13,17,18 FOR TOP SURFACE
 FOR 50°C DROP IN TEMPERATURE

FIG. 60.

PLOT OF THEORETICAL AND ACTUAL STRAINS FOR TOP AND BOTTOM SURFACES OF CARBON FIBRE PANEL. STRAINS MEASURED AT POSITIONS 1,2 AND 3 FOR TOP SURFACE 11,12 AND 13 FOR BOTTOM SURFACE FOR 50°C DROP IN TEMPERATURE

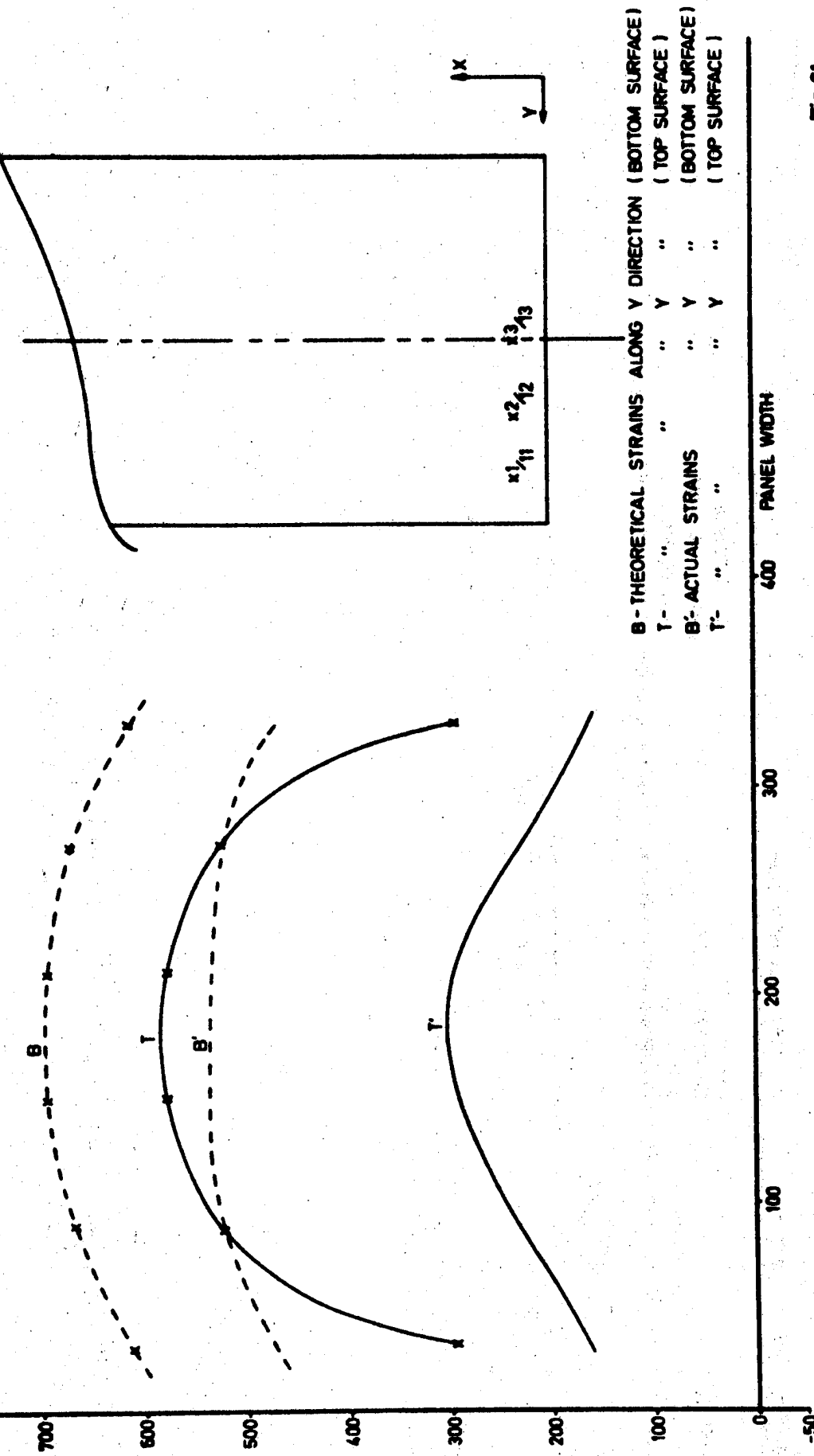
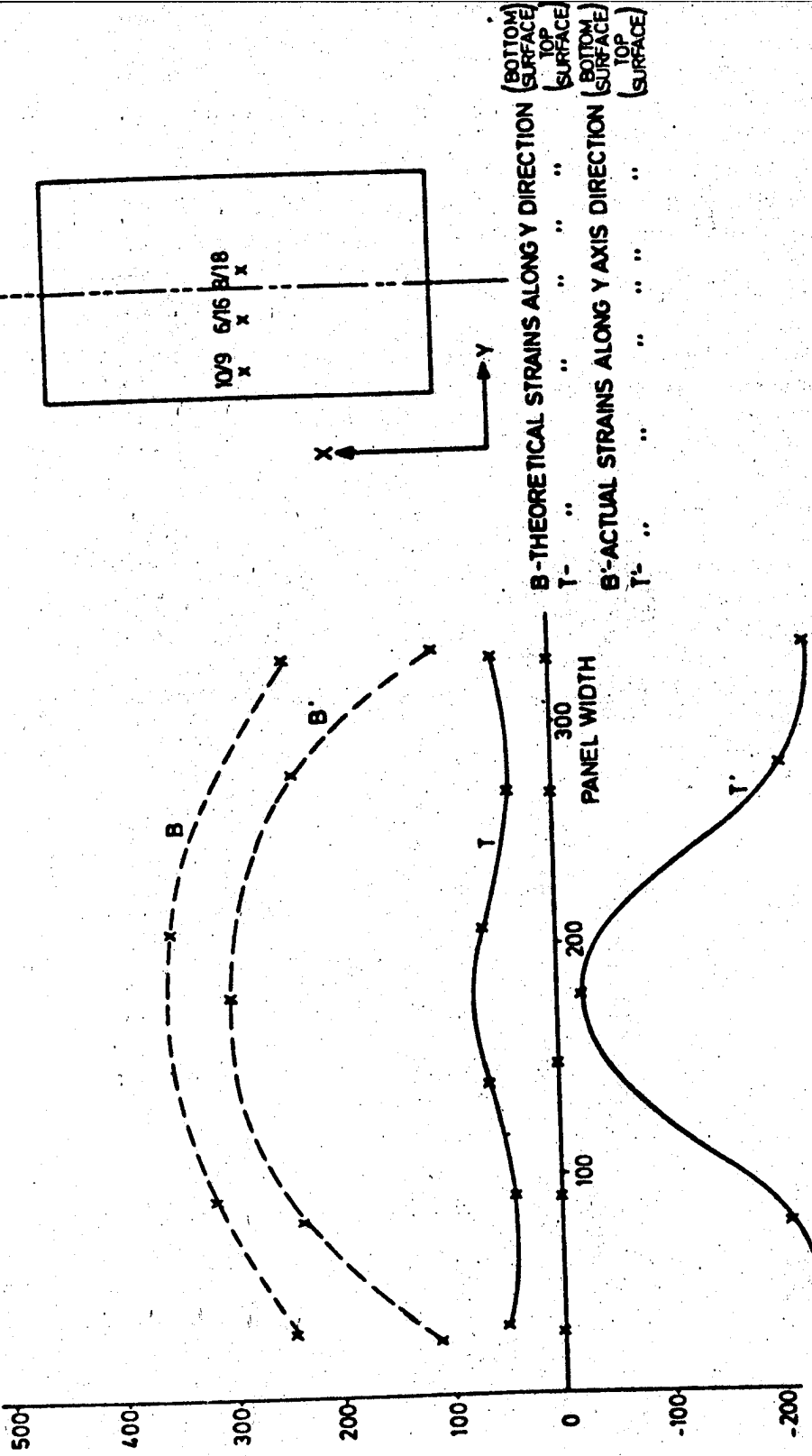


Fig. 61.



PLOT OF THEORETICAL AND ACTUAL STRAINS FOR TOP AND BOTTOM SURFACES OF CARBON FIBRE PANEL. STRAINS MEASURED AT POSITIONS 10, 6, 8 (BOTTOM SURFACE) 9, 16, 18 (TOP SURFACE)

110

9, 16, 18 (TOP SURFACE)

FIG. 62

6. CONCLUSION

An improved mathematical model backed by coupon test results has still not been able to fully simulate the effect of low temperature excursions on a CFRP panel/aluminium frame combination.

The reasons for the lack of correlation between theoretical and actual results are due to unknown factors both in the development of the model and in the production of the CFRP panel/frame assembly.

Better agreement between the results could be achieved. This would require more practical testing, together with computer idealisations of the panel and frame as separate problems. The structural behaviour of the assembly is of such a complexity as to require deeper investigation both practically and theoretically.

The results to date do not reveal enough data to solve the problem but do show more clearly the source of some of the discrepancies. Comparing the practical and model results, there is good agreement in form and would certainly be better absolute agreement if the larger thermal expansion coefficients were fed into the model.

Major problems lie in relating the coupon test CTE's and failure levels with those of the panel. The expansion coefficients for the panel appeared to be 300% up on those measured from the coupons and failure stresses were greater than 200% up since no failure was observed even at the lowest temperature reached on test. No reasons are offered for these discrepancies but suggestions for a future test programme to investigate the problems have been put forward.

Coupon testing has provided an important range of low temperature performance data which will be useful to applications outside this study. Generally moduli tended to increase with decreasing temperature, but the strength behaviour was subject to greater variability. The strength and modulus properties of the angle ply laminates were similar in the longitudinal and transverse directions. The thermal expansion of the unidirectional materials was small and constant with decreasing temperature along the fibre axis, but was much larger and decreased with falling temperature in the transverse direction. The thermal expansions for the angle ply material were small and the same in the two orthogonal directions.

Doubts expressed during the SR and T programme concerning the performance of a CFRP panel/aluminium frame combination at low temperatures have again not been realised. Confidence in CFRP for this and similar applications remains at a high level but it remains that some further research be undertaken to finally align theory with practice.

REFERENCES

- (1) N.L. Hancox, D.C.C. Minty, D.J. Baker, R.A.O. Hall, M.J. Mortimer, and D.L. McElroy. Vol 1 ESRO CR-(P)-597-1976
- (2) N.L. Hancox and D.C.C. Minty, J. Brit. Interplanetary Soc., 30, 391-99, 1977.
- (3) M.B. Kasen, ASTM STP 580, 586, 1975.
- (4) R.E. Schramm and M.B. Kasen, Met. Sci. Eng., 30 197-204, 1977.
- (5) A.A. Fahmy et al. Investigation of Thermal Fatigue in Fiber Composite Materials, NASA CR-2641, 1976.
- (6) M.F. Rickett, Hawker Siddeley Dynamics Technical Paper TP 7567, Volume 2, Appendix A. ESA CR(P) - 803(2) 1976.
- (7) W.R. Goggin. Thermomechanical Stability of Graphite/Epoxy Composites. Applied Optics, Volume 13, No. 2, 1974.
- (8) A.S.D. Wang et al. Humidity Effects on the Creep Behaviour of an Epoxy Graphite Material. AIAA, 1975, 1.
- (9) Welwyn Strain Measurement Ltd. Basingstoke, England. Strain Gauge Temperature Effects, Bulletin No. TN-128-2.
- (10) P.D. Ewins, Composites, Standards, Testing and Design, 144-153. Nat. Phys. Lab. (UK) Conf., April 1974.
- (11) N.L. Hancox, J. Mat. Sci., 7, 1030-36, 1972.
- (12) J.A. Dickinson Final Report for Phase 1 of a Study on the Use of CFRP in Satellite Structures, ESTEC CR331, 1974.
- (13) N.L. Hancox and D.C.C. Minty, AERE, G876, 1977.
- (14) N.L. Hancox, J. Mat. Sci., 10, 234-42, 1975.
- (15) E.de Lamatte and A.J. Perry, Fibre Sci. and Tech., 3, 157, 1970.
- (16) J.E. Ashton, J.C. Halpin and P.H. Petit, Primer on Composite Materials, Analysis, Technomic Pub. Co. Stanford, Conn. USA.
- (17) G.P. Dean and P. Turner, Composites, 4, 174, 1973.
- (18) L.R. Calcote, The Analysis of Laminated Composite Structures, Van Nostrand Reinhold Co., NY. 1969.

- (19) S.W. Tsai, Strength Characteristics of Composite Materials,
NASA CR 224, 1965.
- (20) Hawker Siddeley Dynamics. Report on the Carbon Fibre Faced
Honeycomb Panels for the Spacelab Pallet. HSD TP7553, 1975.

APPENDIX A

CALCULATION OF CTE FOR CFRP FACED ALUMINIUM HONEYCOMB SANDWICH

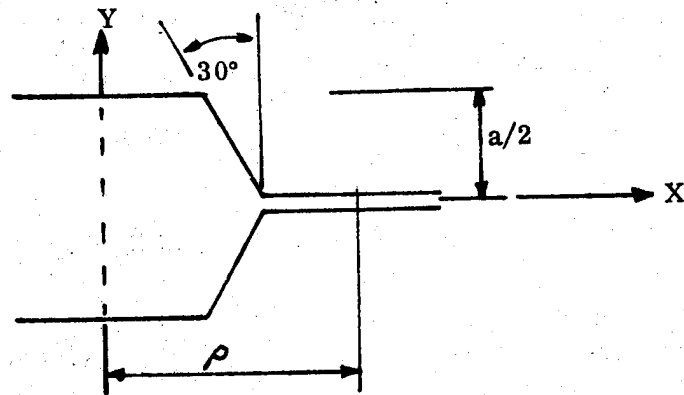
APPENDIX A
CALCULATION OF CTE FOR CFRP-FACED
ALUMINIUM HONEYCOMB SANDWICH

Coefficient of Expansion of Composite Sandwich

The effective coefficient of expansion of the sandwich construction is a function of the coefficients of expansion of the core and the facings and also of their stiffness properties.

Honeycomb Core:

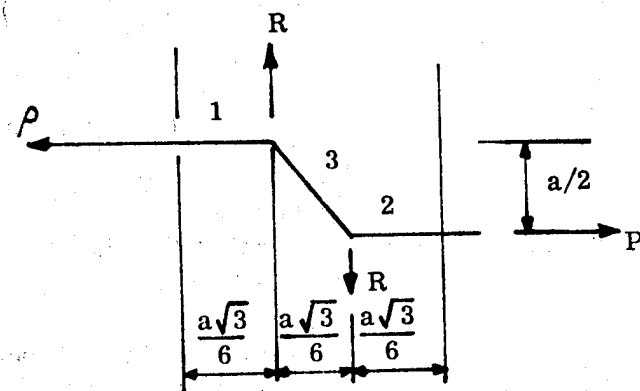
Consider a typical section of the core:



Let
 t = ribbon thickness
 a = cell size across flats
 c = core depth

$$\begin{aligned} \text{Side length} &= a/\sqrt{3} \\ p &= a/\sqrt{3} + a/2\sqrt{3} = \frac{\sqrt{3}a}{2} \end{aligned}$$

Consider the loading on part of one cell



For Moment equilibrium

$$R = \frac{Pa}{2} \cdot \frac{6}{a\sqrt{3}} = \sqrt{3}P$$

Consider an imposed strain in the x direction only
(i.e. $\epsilon_y = 0$).

For sides (1) and (2), increase in length, δ , is given by

$$\delta_{1,2} = \frac{P_1}{EA} = \frac{P}{E} \cdot \frac{a}{2\sqrt{3}} \cdot \frac{1}{ct}$$

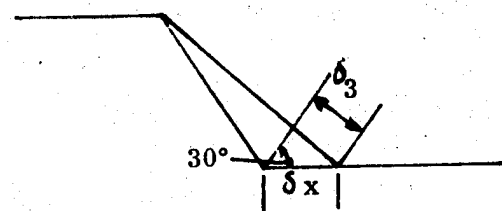
For side (3), load T is derived from

$$T \sin 30 = P$$

$$T \cos 30 = R = P\sqrt{3}$$

From either equation $T = 2P$

$$\therefore \delta_3 = \frac{2P}{E} \cdot \frac{a}{\sqrt{3}} \cdot \frac{1}{ct}$$



$$\text{Axial deflection, } \delta_x = \frac{\delta_3}{\sin 30} = 2\delta_3$$

$$\therefore \text{Total axial deflection} = \frac{Pa}{Ect} \left\{ \frac{1}{\sqrt{3}} + \frac{4}{\sqrt{3}} \right\}$$

$$= \frac{Pa}{Ect} \cdot \frac{5}{\sqrt{3}}$$

$$\text{Strain } \epsilon_x = \frac{\delta}{a} = \frac{10P}{3Ect}$$

The effective stresses are:-

$$\sigma_x = \frac{2P}{ac}$$

$$\sigma_y = \frac{R}{\rho c} = \frac{2P}{ac}$$

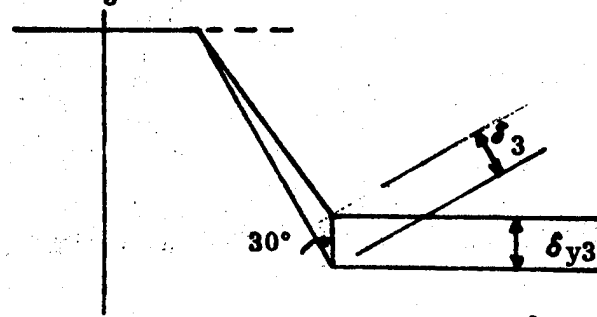
$$\therefore \frac{\sigma_x}{\epsilon_x} = \frac{\sigma_y}{\epsilon_x} = 0.6 \frac{Et}{a}$$

Now consider an imposed strain in the Y direction (i.e. $\epsilon_x = 0$)

$$\text{As above } \delta_1 = \delta_2 = \frac{P}{E} \cdot \frac{a}{2\sqrt{3}} \cdot \frac{1}{ct}$$

$$\sigma_{3.} = \frac{2P}{E} \cdot \frac{a}{\sqrt{3}} \cdot \frac{1}{ct}$$

δ_{y3} due to δ_3



δ_y due to δ_1 and δ_2

$$\delta_{y3} = \delta_3 / \cos 30 = \frac{4Pa}{Ect}$$

If the load/mm is denoted by N_x , N_y thus for the core we have:-

$$\begin{bmatrix} N_x \\ N_y \end{bmatrix} = 69 \times 10^3 \times 14 \begin{bmatrix} .0048 & .0048 \\ .0048 & .0048 \end{bmatrix} \begin{bmatrix} \epsilon_x \\ \epsilon_y \end{bmatrix} \quad \text{N/mm}$$

$$= 4637 \begin{bmatrix} 1 & 1 \\ 1 & 1 \end{bmatrix} \begin{bmatrix} \epsilon_x \\ \epsilon_y \end{bmatrix} \quad \text{N/mm}$$

Carbon Fibre Facings:

$$t = .762 \text{ mm} \quad (\text{for two faces})$$

$$E = 50 \text{ GN/m}^2$$

$$\nu = 0.04$$

$$\begin{bmatrix} N_x \\ N_y \end{bmatrix} = \frac{50 \times 10^3 \times .762}{(1 - 0.04)^2}$$

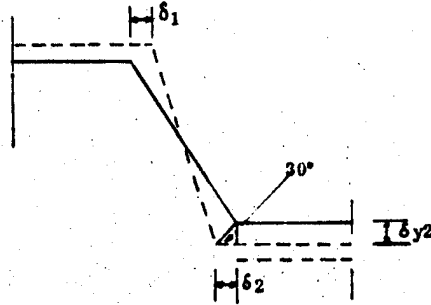
$$\begin{bmatrix} 1 & .04 \\ .04 & 1 \end{bmatrix} \begin{bmatrix} \epsilon_x \\ \epsilon_y \end{bmatrix}$$

$$= 41340 \begin{bmatrix} 1 & .04 \\ .04 & 1 \end{bmatrix} \begin{bmatrix} \epsilon_x \\ \epsilon_y \end{bmatrix} \text{ N/mm}^2$$

Sandwich panel

$$= \text{aluminium} = 23 \times 10^{-6} /^\circ\text{C}$$

$$= \text{C.F.} = 1.3 \times 10^{-6} /^\circ\text{C} \quad (\text{Average value over temp. range } -180 \text{ to } 100^\circ\text{C}).$$



$$\delta_{y2} = \delta_2 \tan 30 \quad \delta_{y1} = \delta_1 \tan 30$$

$$\therefore \delta_y = \delta_{y1} + \delta_{y2} + \delta_{y3}$$

$$= \frac{\text{Pa}}{\text{Ect}} + \frac{1}{3} + \frac{4 \text{ Pa}}{3 \text{ Ect}} = \underline{\underline{\frac{5}{3} \frac{\text{Pa}}{\text{Ect}}}}$$

$$\epsilon_y = \frac{2\delta}{a} = \frac{10}{3} \frac{\text{P}}{\text{Ect}}$$

$$\frac{\delta_x}{\epsilon_y} = \frac{\delta_y}{\epsilon_y} = \underline{\underline{\frac{0.6 \text{ Ect}}{a}}}$$

For 2.0 - 3/16 - .7 core

$$t = .002", \quad a = 1/4"$$

$$\therefore \frac{t}{a} = .008, \quad \frac{\delta}{\epsilon} = .0048E$$

For aluminium alloy $E = 69 \times 10^9 \text{ N/m}^2$

$$\text{Core depth} = 14\text{mm.}$$

$$N_\alpha \text{ aluminium} = 10^{-6} \begin{bmatrix} 4637 & 4637 \\ 4637 & 4637 \end{bmatrix} \begin{bmatrix} 23 \\ 23 \end{bmatrix}$$

$$= 10^{-6} \begin{bmatrix} 213300 \\ 213300 \end{bmatrix}$$

$$N_\alpha C = 10^{-6} \begin{bmatrix} 41340 & 1654 \\ 1654 & 41340 \end{bmatrix} \begin{bmatrix} 1.3 \\ 1.3 \end{bmatrix}$$

$$= 10^{-6} \begin{bmatrix} 55890 \\ 55890 \end{bmatrix}$$

The stiffness matrix for the complete sandwich is:

$$K = \begin{bmatrix} 45977 & 6291 \\ 6291 & 45977 \end{bmatrix}$$

$$N_\alpha \text{ aluminium} + N_\alpha CF = \begin{bmatrix} 269190 \\ 269190 \end{bmatrix} \times 10^{-6}$$

Under Free expansion

$$\begin{bmatrix} N_x \\ N_y \end{bmatrix} = 0 = K \epsilon_\alpha - N_\alpha$$

$$\therefore \epsilon_x = \begin{bmatrix} \epsilon_x \\ \epsilon_y \end{bmatrix} = K^{-1} \begin{bmatrix} 269190 \\ 269190 \end{bmatrix} \times 10^{-6}$$

$$K^{-1} = 10^{-6} \begin{bmatrix} 22.2 & -3.0 \\ -3.0 & 22.2 \end{bmatrix}$$

$$\therefore \begin{bmatrix} \epsilon_x \\ \epsilon_y \end{bmatrix} = 10^{-6} \begin{bmatrix} 5.2 \\ 5.2 \end{bmatrix}$$

Hence effective coefficient of expansion of the sandwich is
 $5.2 \times 10^{-6} /^{\circ}\text{C}$ in any direction.

APPENDIX B

MASTER LIST OF SPECIMENS

APPENDIX B

MASTER LIST OF SPECIMENS

1. INTRODUCTION

This Appendix details the total specimen requirements for the Study.

All specimens have been given a purely numerical reference for immediate identification.

2. FAILURE CRITERIA AT CRYOGENIC TEMPERATURES

2.1 Unidirectional Specimens

Specimen No.	Drawing No. TL	Test No.	Test Description	Test Temperature °C
001	22037 - 05	01	LTM	20
002	22037 - 05	01	LTM	20
003	22037 - 05	01	LTM	t1 -60
004	22037 - 05	01	LTM	-60
005	22037 - 05	01	LTM	t2 -100
006	22037 - 05	01	LTM	-100
007	22037 - 05	01	LTM	t3 -170
008	22037 - 05	01	LTM	-170
009	22037 - 05	01	LTM	-190
010	22037 - 05	01	LTM	-190
011	22037 - 05	01	LTM	SPARE
012	22037 - 05	01	LTM	SPARE
013	22037 - 04	02	LTS	20
014	22037 - 04	02	LTS	20
015	22037 - 04	02	LTS	-60
016	22037 - 04	02	LTS	-60
017	22037 - 04	02	LTS	-100
018	22037 - 04	02	LTS	-100
019	22037 - 04	02	LTS	-170
020	22037 - 04	02	LTS	-170
021	22037 - 04	02	LTS	-190
022	22037 - 04	02	LTS	-190
023	22037 - 04	02	LTS	SPARE
024	22037 - 04	02	LTS	SPARE
025	22038 - 04/1	03	TTM	20
026	22038 - 04/1	03	TTM	20
027	22038 - 04/1	03	TTM	-60
028	22038 - 04/1	03	TTM	-60
029	22038 - 04/1	03	TTM	-100
030	22038 - 04/1	03	TTM	-100
031	22038 - 04/1	03	TTM	-170

2.1 Unidirectional Specimens (continued)

Specimen No.	Drawing No. TL	Test No.	Test Description	Test Temperature °C
032	22038 - 04/1	03	TTM	-170
033	22038 - 04/1	03	TTM	-190
034	22038 - 04/1	03	TTM	-190
035	22038 - 04/1	03	TTM	SPARE
036	22038 - 04/1	03	TTM	SPARE
037	22038 - 05	04	TTS	20
038	22038 - 05	04	TTS	20
039	22038 - 05	04	TTS	-60
040	22038 - 05	04	TTS	-60
041	22038 - 05	04	TTS	-100
042	22038 - 05	04	TTS	-100
043	22038 - 05	04	TTS	-170
044	22038 - 05	04	TTS	-170
045	22038 - 05	04	TTS	-190
046	22038 - 05	04	TTS	-190
047	22038 - 05	04	TTS	SPARE
048	22038 - 05	04	TTS	SPARE
049	22039	05	LCS	20
050	22039	05	LCS	20
051	22039	05	LCS	-60
052	22039	05	LCS	-60
053	22039	05	LCS	-100
054	22039	05	LCS	-100
055	22039	05	LCS	-170
056	22039	05	LCS	-170
057	22039	05	LCS	-190
058	22039	05	LCS	-190
059	22039	05	LCS	SPARE
060	22039	05	LCS	SPARE
061	22040	06	TCS	20
062	22040	06	TCS	20

2.1 Unidirectional Specimens (continued)

Specimen No.	Drawing No. TL	Test No.	Test Description	Test Temperature °C
063	22040	06	TCS	-60
064	22040	06	TCS	-60
065	22040	06	TCS	-100
066	22040	06	TCS	-100
067	22040	06	TCS	-170
068	22040	06	TCS	$t_3 -170$
069	22040	06	TCS	-190
070	22040	06	TCS	-190
071	22040	06	TCS	SPARE
072	22040	06	TCS	SPARE
073	22041	07	SM	20
073	22041	08	SS	20
074	22041	07	SM	20
074	22041	08	SS	20
075	22041	07	SM	-60
075	22041	08	SS	-60
076	22041	07	SM	-60
076	22041	08	SS	-60
077	22041	07	SM	-100
077	22041	08	SS	-100
078	22041	07	SM	-100
078	22041	08	SS	-100
079	22041	07	SM	-170
079	22041	08	SS	-170
080	22041	07	SM	-170
080	22041	08	SS	-170
081	22041	07	SM	-190
081	22041	08	SS	-190
082	22041	07	SM	-190
082	22041	08	SS	-190

2.1 Unidirectional Specimens (continued)

Specimen No.	Drawing No. TL	Test No.	Test Description	Test Temperature °C
083	22041	07	SM	SPARE
083	22041	08	SS	SPARE
084	22041	07	SM	SPARE
084	22041	08	SS	SPARE
085	23266	09	LCE	20
086	23266	09	LCE	20
087	23266	09	LCE	-60
088	23266	09	LCE	-60
089	23266	09	LCE	-100
090	23266	09	LCE	-100
091	23266	09	LCE	-170
092	23266	09	LCE	-170
093	23266	09	LCE	-190
094	23266	09	LCE	-190
095	23266	09	LCE	SPARE
096	23266	09	LCE	SPARE
097	23267	10	TCE	20
098	23267	10	TCE	20
099	23267	10	TCE	-60
100	23267	10	TCE	-60
101	23267	10	TCE	-100
102	23267	10	TCE	-100
103	23267	10	TCE	-170
104	23267	10	TCE	-170
105	23267	10	TCE	-190
106	23267	10	TCE	-190
107	23267	10	TCE	SPARE
108	23267	10	TCE	SPARE

2.2 Angle Ply Specimens

Specimen No.	Drawing No. TL	Test No.	Test Description	Test Temperature °C
109	22114-01	11	LTM	20
109	22114-01	12	LTS	20
110	22114-01	11	LTM	20
110	22114-01	12	LTS	20
111	22114-01	11	LTM	-100
111	22114-01	12	LTS	-100
112	22114-01	11	LTM	-100
112	22114-01	12	LTS	-100
113	22114-01	11	LTM	-190
113	22114-01	12	LTS	-190
114	22114-01	11	LTM	-190
114	22114-01	12	LTS	-190
115	22114-01	11	LTM	SPARE
115	22114-01	12	LTS	SPARE
116	22114-02	13	TTM	20
116	22114-02	14	TTS	20
117	22114-02	13	TTM	20
117	22114-02	14	TTS	20
118	22114-02	13	TTM	-100
118	22114-02	14	TTS	-100
119	22114-02	13	TTM	-100
119	22114-02	14	TTS	-100
120	22114-02	13	TTM	-190
120	22114-02	14	TTS	-190
121	22114-02	13	TTM	-190
121	22114-02	14	TTS	-190
122	22114-02	13	TTM	SPARE
122	22114-02	14	TTS	SPARE
123	23271	15	LCS	20
124	23271	15	LCS	20
125	23271	15	LCS	-100

2.2 Angle Ply Specimens (continued)

2.3 Angle Ply Honeycomb Specimens

2.4 Creep Specimens

Test Description Terms

LTM	=	Longitudinal Tensile Modulus
LTS	=	Longitudinal Tensile Strength
TTM	=	Transverse Tensile Modulus
TTS	=	Transverse Tensile Strength
LCS	=	Longitudinal Compressive Strength
TCS	=	Transverse Compressive Strength
SM	=	Shear Modulus
SS	=	Shear Strength
LCE	=	Longitudinal Coefficient of Linear Expansion
TCE	=	Transverse Coefficient of Linear Expansion
C	=	Creep Test
LFM	=	Longitudinal Flexural Modulus
LFS	=	Longitudinal Flexural Strength

APPENDIX C
COMPLETE PANEL TEST PROCEDURE
(BAe Specification DTP/GP/50047)

Procedure No. DTP/GP/50047

CONTENTS

1. SCOPE

- 1.1 Equipment to be Tested**
- 1.2 Purpose of Test**

2. CONDITIONS

- 2.1 Personnel**
- 2.2 Special Hazards/Precautions**
- 2.3 Preparation**
 - 2.3.1 Test Equipment**
 - 2.3.2 Test Equipment Preparation**
 - 2.3.3 Test Article Preparation**
 - 2.3.3.1 Strain Gauge Installation**
 - 2.3.3.2 Panel Preparation**

3. PROCEDURE

- 3.1 Procedure Performance**
 - 3.1.1 Test Sequence**
 - 3.1.1.1 Thermal Cycling (Panel Free)**
 - 3.1.1.2 Thermal Cycling (Panel Attached)**

4. DATA REQUIREMENTS

- 4.1 Data Reporting**

Figure 1 Strain Gauge and Thermocouple Positions

1. SCOPE

1.1 Equipment to be Tested

A carbon fibre honeycomb panel dimensioned in accordance with HSD Drawing No. TL 22109 Basic 01.

The panel will be attached to a test frame of a large spacecraft structure. The HSD drawing number of the frame is MST 13594.

1.2 Purpose of Test

The purpose of the tests detailed in this document are to subject the panel/test frame assembly to thermal cycling and investigate the effects of differential thermal expansion and how this coincides with the theoretical analysis.

2. CONDITIONS

2.1 Personnel

The Test Conductor shall be responsible for supplying an adequate number of qualified personnel to carry out the activities associated with the test.

2.2 Special Hazards/Precautions

Safety precautions associated with the test facility and equipment shall be the responsibility of the Test Conductor. During the test, the panel will be inside a chamber and any potential failure will be contained.

2.3 Preparation

2.3.1 Test Equipment

- MST 13607 Insulated Test Box
- Liquid Nitrogen Bowser - self pressurising from which cold gaseous nitrogen at temperatures approaching that of liquid nitrogen is piped into the test box.
- 200 Channel Data logger to MST 14223/2 plus printer.
- T1. T2. Thermocouples taped to the panel and aluminium frame in the positions shown in Figure 1 of this document.
- Strain gauges positioned on the panel and frame as shown in Figure 1.

Procedure No. DTP/GP/50047

2.3.1 Cont'd.

- Dial Test Indicators (DTI's) (for use with the insulated test box) plus support frame and attachment rods as shown on HSD Drawing No. MST 13608.
- Ultrasonic test probe.

2.3.2 Test Equipment Preparation

All thermocouples, strain gauges, dial test indicators and other measuring and recording equipment shall be supplied, fitted or connected by the Test Conductor. Sufficient calibration runs and checks shall be performed by the Test Conductor to verify the performance of the test equipment.

2.3.3 Test Article Preparation

2.3.3.1 Strain Gauge Installation

Micro-Measurements series WK (temperature compensated) 350 ohm strain gauges (rosette and single) will be fitted to the panel and frame.

The gauges used will have an accuracy of 0.3 - 0.4% and all changes in gauge resistance will be referred to a fixed stable resistance with applied correction factors for apparent strain and non-matching coefficients of expansion.

2.3.3.2 Panel Preparation

Carry out a pre-test inspection of the test frame and panel for planarity and record bolt hole sizes in the panel and their positions, and record any surface damage.

Install the strain gauges and thermocouples in the positions indicated in Figure 1.

3. PROCEDURE

3.1 Procedure Performance

3.1.1 Test Sequence

Tests shall be conducted in the sequence specified herein.

3.1.1.1 Thermal Cycling (Panel Free)

- (a) Carry out a check and record the overall dimensions of the test frame and include a check for planarity.
- (b) Install strain gauges, and thermocouples in the positions indicated in Figure 1.
- (c) Install the test frame in the test chamber.
- (d) Install the Dial Test Indicators (DTI) complete with support frame as indicated in Figure 1.
- (e) Subject the frame and panel (disconnected) to a thermal cycle, from an ambient temperature of 15°C down to -150°C and return to ambient as follows:-
 - (i) Stabilise the panel temperature at approximately 30°C increments.
 - (ii) Record the DTI and strain gauge readings at each of these increments.
- (f) Repeat (e).
- (g) Analyse the results by plotting graphically strains against temperature. Assess the results of this analysis with regard to the characteristics of the gauges. If these characteristics display significant anomalies subject the frame and panel to further thermal cycles until these anomalies are minimised.

3.1.1.2 Thermal Cycling (Panel Attached)

- (a) Attach the panel to the test frame using M6 Titanium bolts and steel nuts and torque tighten to 4.5Nm. Record the temperature at which the panel attachment is made.
- (b) Install the assembly in the test chamber.
- (c) Record DTI and strain gauge and thermocouple readings.
- (d) Subject the assembly to a thermal cycle from an ambient temperature of + 15°C down to approximately -25°C and return to ambient..
- (e) Record the strain gauge readings at achieved minimum temperature.
- (f) Subject the assembly to a thermal cycle from an ambient temperature of 15°C down to approximately -50°C and return to ambient.
- (g) Record the DTI and strain gauge readings at achieved minimum temperature.
- (h) Subject the assembly to a thermal cycle from an ambient temperature of 15°C down to approximately -75°C and return to ambient.
- (i) Record the DTI and strain gauge readings at achieved minimum temperature.
- (k) Reduce the temperature of the assembly, by allowing cold nitrogen to circulate in the chamber, to approximately -100°C and return to ambient.
- (l) Record DTI and strain gauge readings at achieved minimum temperature.
- (m) Reduce the temperature in steps of 25°C to the limit of the test equipment's capability or until a significant failure to the panel occurs.
- (n) Record DTI and strain gauge readings at each of these temperatures.

Procedure No. DTP/GP/50047

3.1.1.2 Cont'd.

- (p) Shut off the supply of cold nitrogen and allow the assembly to return to ambient temperature.
- (q) Remove the assembly from the cold box and inspect for visible signs of damage.
- (r) Inspect the panel for damage and bolt hole shape, size and position.

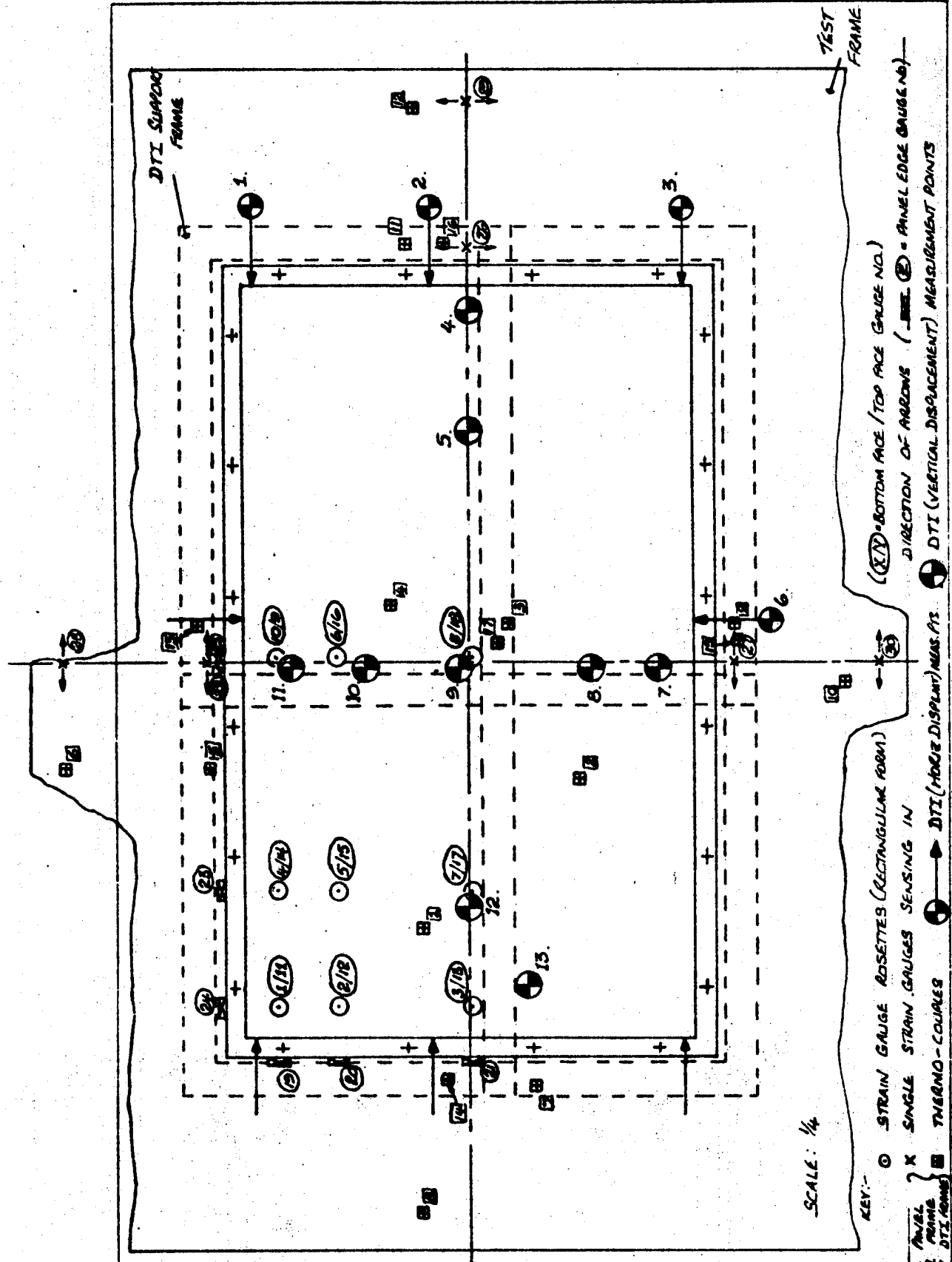
4. DATA REQUIREMENTS.

4.1 Data Reporting

Tabulate all results obtained.

Analyse the results as strain in geometric axes against temperature.

Photographs of the test specimen will be taken before the test and also of any damage that occurs during the testing.



Title: LOCATION OF PANEL AND TEST FRAME
INSTRUMENTATION

British Aerospace, Dynamics Group

Figure: 1 Issue: 2

Document No.

DTP/GP/50047

APPENDIX D
'STRAINCAL COMPUTER PROGRAM'

CONTENTS

- 1. INTRODUCTION**
- 2. THEORY**
- 3. PROGRAM DESCRIPTION**
- 4. INPUT DESCRIPTION**
- 5. OUTPUT DESCRIPTION**
- 6. PROGRAM USAGE**

SIMPLIFIED FLOW CHART

APPENDIX

- | | |
|-----------------------------|-------------------------|
| D1. Calibration Data | a. Sample Input |
| | b. Sample Output |
| D2. Test Data | a. Sample Input |
| | b. Sample Output |

1.

INTRODUCTION

When using certain types of strain gauges a zero error is introduced into the readings which varies with temperature. This is corrected for by varying the temperature of the body under test without any artificial strain imposed upon it. The strain gauges attached to the points of interest give results forming calibration curves of temperature against strain. From these curves the artificial zero point, or nominal value for each strain gauge may be determined for any value of temperature. If the body is now put under strain and the temperature varied, the nominal value may be calculated from the calibration curves, and subtracted from the strain measurement giving the true strain.

The program considers two configurations of strain gauge, the rosette type and the single type. The single type only requires calibration as it only reads strain in one direction, but the rosette type measures strain in three directions and from this the maximum and minimum strain values may be calculated and also their directions.

The program has two modes:

- (i) Calibration mode and
- (ii) Test mode

During the calibration mode the calibration curves are input and stored by the program. During the test mode, the test data is read in which contains measured strain and temperature. This test data is then calibrated and resolved as described above.

2.

THEORY

The calibration curves are sorted out in the form of temperature against strain and each run contributes a point on the curve for each channel number.

Test Mode

When the test data has been read in the nominal strain is obtained from the calibration data by linear interpolation with respect to temperature. The equation used is shown below:

$$S_x = CS_1 + (T_x - CT_1) \frac{(CS_2 - CS_1)}{(CT_2 - CT_1)} \quad \dots \dots 2.1$$

where S_x is the nominal strain

T_x is the temperature of the test period

(CT_1, CS_1) and (CT_2, CS_2) are two points on the calibration curve which are closest to the test point.

The calibration curve is of the hysteresis type and thus the two points used on the calibration curve must be on the same part of the curve as the test data. For example if the temperature of the test data is being reduced then calibration data must be from the downward path and similarly if the temperature is being increased then the calibration data must be from the upward path.

The calibrated test data is then scaled by multiplying by the variable SCALE input as data.

The results of the single strain gauge type are now ready for output, but the rosette type strain gauge still requires some resolving. The rosette strain gauge groups the channel numbers into sets of threes. Let three channel numbers of one strain gauge have the corrected strain values ϵ_1 , ϵ_2 , and ϵ_3 . These values are used to calculate the full output for the rosette type strain gauge.

$$\epsilon_x = \epsilon_1 \quad \dots \dots 2.2$$

$$\epsilon_y = \epsilon_2 + \epsilon_3 - \epsilon_1 \quad \dots \dots 2.3$$

$$\gamma_{xy} = \epsilon_3 - \epsilon_2 \quad \dots \dots 2.4$$

$$\epsilon_{\max} = \frac{\epsilon_x + \epsilon_y}{2} + \frac{1}{2}\sqrt{(\epsilon_x - \epsilon_y)^2 + \gamma_{xy}^2} \quad \dots \dots 2.5$$

$$\epsilon_{\min} = \frac{\epsilon_x + \epsilon_y}{2} - \frac{1}{2}\sqrt{(\epsilon_x - \epsilon_y)^2 + \gamma_{xy}^2} \quad \dots \dots 2.6$$

$$\phi_p = \frac{1}{2} \tan^{-1} \left| \frac{\gamma_{xy}}{\epsilon_x - \epsilon_y} \right| \quad \dots \dots 2.7$$

To determine the maximum and minimum direction of the strain the following tests have to be done:

(I) If ratio $\frac{\gamma_{xy}}{\epsilon_x - \epsilon_y} = \frac{+ve}{+ve}$ then angle of max. princ. strain $\phi_{p \max.} = (\phi_p)^0$
 and angle of min. princ. strain $\phi_{p \min.} = (\phi_p + 90)^0$

(II) If ratio $\frac{\gamma_{xy}}{\epsilon_x - \epsilon_y} = \frac{+ve}{-ve}$ then angle of max. princ. strain $\phi_{p \max.} = (90 - \phi_p)^0$
 and angle of min. princ. strain $\phi_{p \min.} = (180 - \phi_p)^0$

(III) If ratio $\frac{\gamma_{xy}}{\epsilon_x - \epsilon_y} = \frac{-ve}{+ve}$ then angle of max. princ. strain $\phi_{p \max.} = (180 - \phi_p)^0$
 and angle of min. princ. strain $\phi_{p \min.} = (90 - \phi_p)^0$

(IV) If ratio $\frac{\gamma_{xy}}{\epsilon_x - \epsilon_y} = \frac{-ve}{-ve}$ then angle of max. princ strain $\phi_{p \max.} = (90 + \phi_p)^0$
 and angle of min. princ strain $\phi_{p \min.} = (\phi_p)^0$

These results are then output.

3.

PROGRAM STRUCTURE

The basic program structure can be seen using the simplified flow chart , see Fig. 1.

First of all the user must read in the calibration data which is signified by the second card of the data pack. The calibration data is stored in a single three dimensional array having references of channel number, run number and strain/temperature. The data read in at the beginning of the data file is checked for consistency, e.g. the ranges specified for the rosettes to check that exact grouping of threes is possible allowing for inconsistencies when channel numbers are not used. If inconsistencies are input in the ranges specified for single strain gauge readings then this will be picked up and the program will be halted.

The channel numbers are also checked that they follow on in steps of one. Even if a certain channel number is never used, the data file must include the channel number with two other numbers after it, the last number (the temperature reading) being set to -999 , indicating reading is to be ignored.

The program then searches through the calibration data in the ranges specified for rosette type strain gauges , to find any reading with the temperature set to -999 . On finding one, the program sets the other two temperature readings of the same rosette type strain gauge , and same run to -999 .

When all the calibration data has been input and checked it is listed out with all the readings for each channel grouped together.

The calibration curves are now set and as long as the program is not re-loaded then the information will be stored for use when running the test data.

The test data may now be input for calibration and resolving. This data is stored in a similar way to the calibration data, i.e. a single three dimensional array. As the data is being read in the channel numbers are checked that they increment in steps of one in the same way as the calibration data.

The first stage of the test mode section of the program , after the data has been input , is to calibrate the test data. This is done by first obtaining the nominal strain from the calibration data, by linear interpolation with respect to temperature, using the equation (2.1) given in section 2. This nominal value is then subtracted from the measured value and the new calibrated value is then stored in the test data array over-writing the original measured value.

Not all the test data requires calibration thus this correction is only applied upto the maximum channel number of the calibration data, or upto the last channel number of the test data.

The test data now calibrated is resolved according to its strain gauge type as described in section 2. For the single strain gauge type, the data only requires to be multiplied by SCALE (input as data), to scale the reading before being output on the line printer. The rosette type strain gauge groups the channel numbers into threes and after scaling, as in the single type test data, uses equation 2.2 to 2.7 in section 2 to produce the value ϵ_x , ϵ_y , ϵ_{xy} , ϵ_{max} , ϵ_{min} , p_{max} and p_{min} ready to output on the line printer.

4.

INPUT DESCRIPTION

The data for the program is input on cards and was peripheral * CRO. Free format is used by the program, thus adjacent numbers must be separated by at least one space, if any other separator is used by the program then this will cause an error.

The data for the program is listed below in tabular form:

Card No.	Description	Format
1.	TITLE(I), I = 1,10 Input the title to be printed at the top of the output file. Must be within the first 30 columns.	10A8
2.	ICAL Flag to define program mode i.e. ICAL = 0 Calibration mode ICAL = 1 Test mode If ICAL = 1 then go to data cards 3b	10
3a.	SCALE Scaling factor of the strain readings	F0.0
4a.	NR Number of runs of the calibration data Minimum value 2. Maximum value 20.	10
5a.	RUNTEMP(I), I = 1, NR where RUNTEMP(I) is the overall temperature of the Ith run.	NR F0.0
6a.	ROSING(I), I = 1, 4 This defines two ranges of channel numbers to be grouped in threes for rosette type strain gauges. The ranges are ROSING(1) to ROSING(2) and ROSING(3) to ROSING(4)	4I0
7a.	ROSING(I), I = 5, 8 This defines two ranges of single type strain gauges. The ranges are ROSING(5) to ROSING(6) and ROSING(7) to ROSING(8)	4I0

Card No.	Description	Format
8a.	IDUD No. of inconsistencies in the channel numbers for the rosette type strain gauges. Maximum value = 5. If IDUD = 0 miss card 9a.	10
9a.	ROSING(I), I = 9, JJ Where JJ = 8 + IDUD * 2 This defines a maximum of 5 ranges of channel numbers not to be used in calculations when considering rosette type strain gauges. The ranges defined are ROSING(9) to ROSING(10) etc. and indicate the numbers to be ignored. ROSING(I) is included in the range to be ignored, and for cases where only one number is to be ignored ROSING(I) will equal ROSING (I + 1).	10I0
10a to NC + 9a	CH STRAIN TEMP CH = Channel Number STRAIN = Strain reading TEMP = Temperature at time of measurement. For Run 1 where NC is the number of channel numbers in each run. Maximum value of NC = 100	10, 2F0.0
NC + 10a .. to 2 NC + 9a	CH STRAIN TEMP For Run 2 and similarly for each run upto card number NR*NC + 9a, which is the last card of the calibration data.	10, 2F0.0
3b.	NRTEST where NRTEST is the number of test runs. Maximum value = 20	10
4b.	RUNTEMP(I), I = 1, NRTEST where RUNTEMP(I) is the overall temperature of Ith run of the test data.	NRTEST 10
5b to NCTEST + 4b	CH STRAIN TEMP For Run 1 where NCTEST is the number of channel numbers in each run. Maximum value of NCTEST = 120.	10, 2F0.0
NCTEST + 5b	CH STRAIN TEMP For Run 2 and similarly for each run upto card number NRTEST*NCTEST + 4b which is the last card in the test data.	10, 2F0.0

The channel numbers of each run must start and finish on the same number and rise in steps of one. The first channel number of each set of data must be the same as that of the calibration data run previously. The last channel number may be different for each set of data. In the data file the channel numbers must be incremented in steps of one, including those not actually used by the program. If any channel number is missed then this will be signified by a halted message as follows:

Halted: Data Error Channel numbers inconsistent

In cases where no data is available for a channel then this will be signified by inputting a temperature of -999.

The program checks the ranges of channel numbers set for the rosette type strain gauge and if it is found that exact grouping of threes is not possible (allowing for the inconsistencies) then this is signified by a halted message as follows:

Halted: Data Error in strain gauge distinctions

The program also halts with the above message if the user attempts to read in an inconsistency in the range set for the single strain gauge type.

5.

OUTPUT DESCRIPTION

For both the calibration and test mode the title of the output file as input as data and a listing of overall temperature against run number are printed on the first page of the output file.

For the calibration mode the information for each channel number is output in blocks. Each block is headed by its channel number and underneath this are three columns headed by RUN, TEMPERATURE, and STRAIN. The temperature column gives the temperature of the strain gauge at the time of the strain measurement. For runs of that channel number where the temperature of the data file has been set to -999 is indicated by the message "No data available for this channel on this run".

For the test mode the rest of the output is again in blocks but these blocks can take two forms depending whether it is associated with a rosette type strain gauge or the single strain gauge. For the single type strain gauge the block is headed by the channel number and below has two columns headed TEMPERATURE and CORRECTED STRAIN. The temperature applies to the temperature of the strain gauge at the time of measurement. The corrected strain is the measured strain after calibration, where applicable, and scaling. The other type of output format for the rosette type strain gauge has each block headed by the three channel numbers associated with that rosette strain gauge. Below this are 8 columns headed by TEMP, E(x), E(y), GAMMA (xy), E(max), E(min), PHI(max) and PHI(min) where TEMP is the temperature of the strain gauge at the time of measurement the other variables are as determined in section 2, where E signifies ϵ , brackets signify subscript and PHI signifies ϕ_p .

For runs where the temperature has been set to -999 then this is signified by "Information not available". On rare cases where there is not enough calibration data on a channel number then this is signified by "Not enough calibration data available".

6.

PROGRESS USAGE

The program requires a core size of 22656 words and the name of the binary image is STRAINCALBIN and uses peripheral *CRO and *LPO. An estimation of time required by the program is 20 seconds per 1000 lines of data plus 5 seconds.

Assume that the calibration data is held in CALDATA, and two sets of test data are held in TESTDATA1 and TESTDATA2, then the George III statements required to run the program are as follows:

JT	150
MZ	23000
LO	STRAINCALBIN
AS	*CRO, CALDATA
AS	*LPO, CALOP
TI	50
EN	
RL	*CRO
RL	*LPO
LF	CALOP, *LP, AL
AS	*CRO, TESTDATA1
AS	*LPO, TESTOP1
TI	50
EN	
RL	*CRO
RL	*LPO
LF	TESTOP1, *LP, AL
AS	*CRO, TESTDATA2)
AS	*LPO, TESTOP2)
TI	50)
EN)
RL	*CRO)
RL	*LPO)
LF	TESTOP2, *LP, AL)

The last part may be repeated for as many test data files as is required, as long as STRAINCALBIN is not re-loaded. If the program is re-loaded then the calibration data is lost.

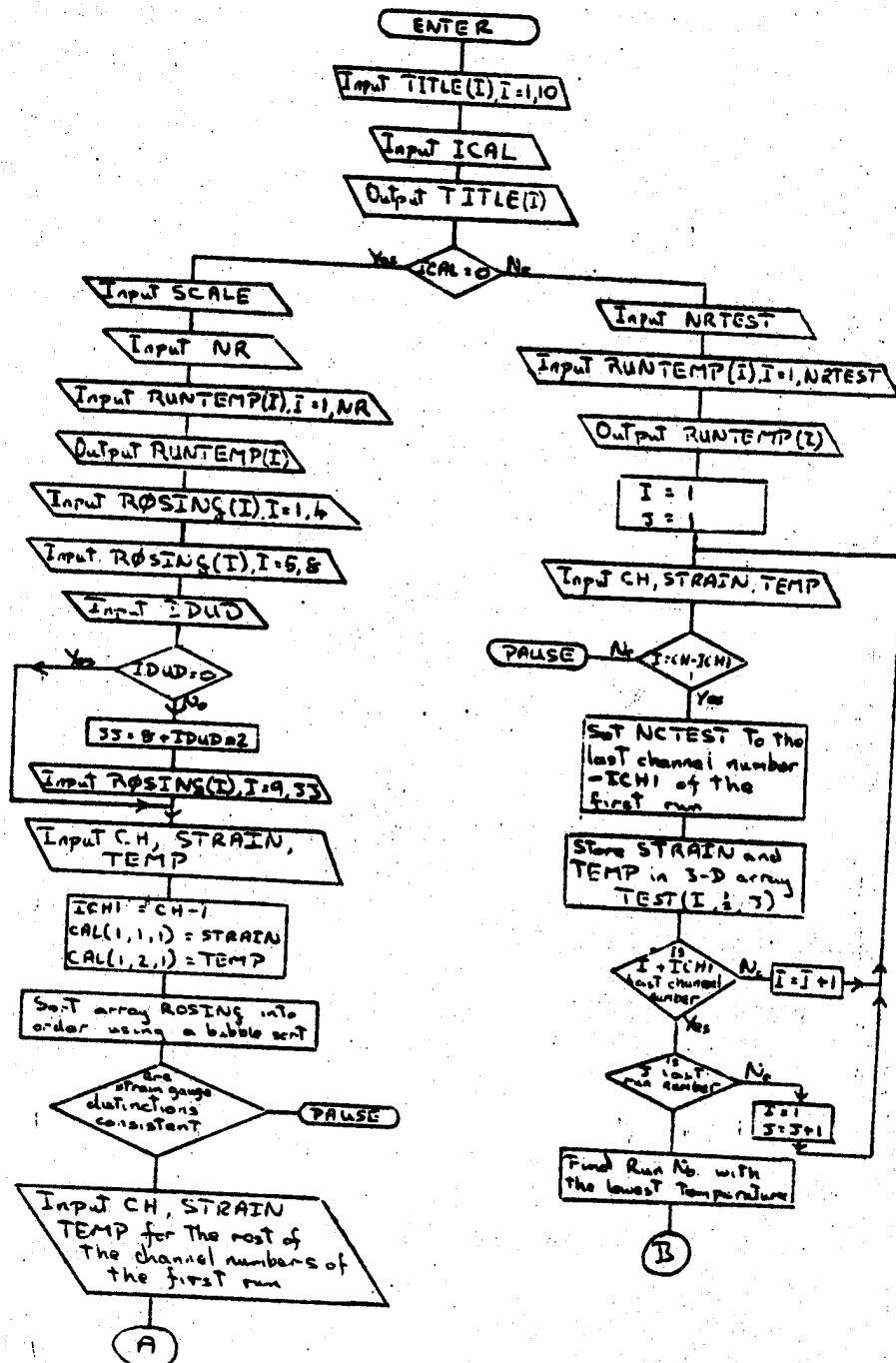


Fig 1a
Simplified flowchart of program STRAINCHL

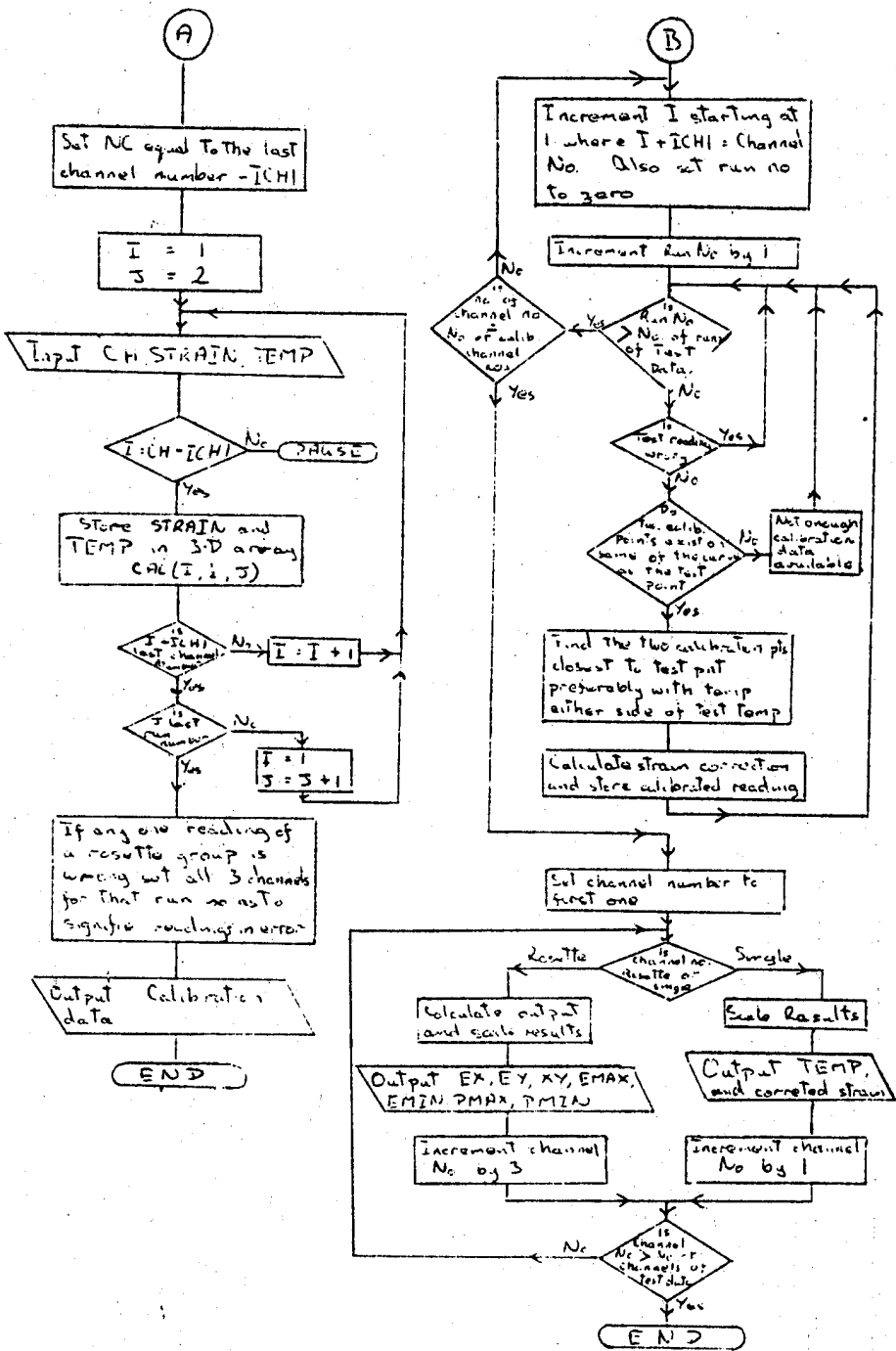


Fig 1 b

APPENDIX D1

CALIBRATION DATA

- a. Sample Input**
- b. Sample Output**

200487C.EU053

LISTING OF 10E.CALDATA21913 PRODUCED ON MAR27 AT 10.22.36
OUTPUT BY LISTFILE IN "200487C.EU053" ON MAR27 AT 10.26.36 USZ06 17

DOCUMENT CALDATA2

3 TEST DATA 2 CALIBRATION
1 0
2 100.0
3 6
4 20 0 -20 -40 0 20
5 9 10 14 16
6 11 12 17 18
7 1
8 7 7
9 1 0 15
10 2 2 25
11 3 0 35
12 4 1 -640
13 5 2 15
14 6 3 15
15 7 3 20
16 8 2 20
17 9 2 20
18 10 0 15
19 11 1 20
20 12 0 15
21 1 0 5
22 2 0 5
23 3 0 5
24 4 1 5
25 5 1 5
26 6 4 5
27 7 4 0
28 8 4 0
29 9 4 0
30 10 0 0
31 11 3 0
32 12 6 0
33 1 6 -15
34 2 0 -15
35 3 0 -15
36 4 2 -15
37 5 2 -15
38 6 1 -15
39 7 0 -15
40 8 0 -20
41 9 0 -20
42 10 0 -20
43 11 15 -20
44 12 0 -20
45 1 0 -40
46 2 0 -40
47 3 0 -40
48 4 0 -40
49 5 6 -40
50 6 7 -30
51 7 10 -35
52 8 15 -40
53 9 18 -40
54 10 0 -999
55 11 20 -40 -2
56 12 0 -40
57 1 0 0
58 2 1 0
59 3 0 0
60 4 2 -5
61 5 2 -5
62 6 5 -5
63 7 5 -5
64 8 6 -5
65 9 3 -5
66 10 0 0
67 11 10 -2
68 12 0 0
69 1 0 20
70 2 0 20
71 3 0 20
72 4 1 10
73 5 0 20
74 6 0 20
75 7 0 20
76 8 2 10
77 9 3 10
78 10 0 20
79 11 1 20
80 12 0 20
81 *****
82

ORIGINAL PAGE IS
OF POOR QUALITY

GGGGGGGGGGGGGG

66666666666666

6.666666666666666

666666666666
666666666666

Digitized by srujanika@gmail.com

© 2007 by the author

DE487C-EUH53

LISTING OF :PE.CALOP1(1) PRODUCED ON 9MAR78 AT 10.26.52

OUTPUT MY LISTFILE IN '0E487C.EUE53' ON 9MAR78 AT 10.26.54 USING 17

DOCUMENT : CALCP1

TEST DATA 2 CALIBRATION

THE OVERALL TEMPERATURE OF EACH RUN

RUN	TEMPERATURE
1	20.00
2	0.00
3	-20.00
4	-40.00
5	0.00
6	20.00

CHANNEL NUMBER 1

RUN	TEMPERATURE	STRAIN
1	15.00	0.00
2	5.00	0.00
3	-15.00	0.00
4	-40.00	0.00
5	0.00	0.00
6	20.00	0.00

CHANNEL NUMBER 2

RUN	TEMPERATURE	STRAIN
1	25.00	0.00
2	5.00	0.00
3	-15.00	0.00
4	-40.00	0.00
5	0.00	0.00
6	20.00	0.00

CHANNEL NUMBER 3

RUN	TEMPERATURE	STRAIN
1	15.00	0.00
2	5.00	0.00
3	-15.00	0.00
4	-40.00	0.00
5	0.00	0.00
6	20.00	0.00

CHANNEL NUMBER 4

RUN	TEMPERATURE	STRAIN
1	NO DATA AVAILABLE FOR THIS CHANNEL ON THIS RUN	
2	5.00	1.00
3	-15.00	2.00
4	-40.00	8.00
5	-5.00	2.00
6	10.00	1.00

CHANNEL NUMBER 5

RUN TEMPERATURE STRAIN

1.	NO DATA AVAILABLE FOR THIS CHANNEL ON THIS RUN	
2	5.00	1.00
3	-15.00	2.00
4	-40.00	6.00
5	-5.00	2.00
6	20.00	0.00

CHANNEL NUMBER 6

RUN TEMPERATURE STRAIN

1.	NO DATA AVAILABLE FOR THIS CHANNEL ON THIS RUN	
2	5.00	4.00
3	-15.00	1.00
4	-30.00	3.00
5	-5.00	5.00
6	20.00	0.00

CHANNEL NUMBER 8

RUN TEMPERATURE STRAIN

1	20.00	2.00
2	0.00	4.00
3	NO DATA AVAILABLE FOR THIS CHANNEL ON THIS RUN	
4	NO DATA AVAILABLE FOR THIS CHANNEL ON THIS RUN	
5	-5.00	6.00
6	10.00	2.00

CHANNEL NUMBER 9

RUN TEMPERATURE STRAIN

1	20.00	2.00
2	0.00	4.00
3	NO DATA AVAILABLE FOR THIS CHANNEL ON THIS RUN	
4	NO DATA AVAILABLE FOR THIS CHANNEL ON THIS RUN	
5	-5.00	3.00
6	10.00	3.00

CHANNEL NUMBER 10

RUN	TEMPERATURE	STRAIN
1	15.00	0.00
2	0.00	0.00
3	NO DATA AVAILABLE FOR THIS CHANNEL ON THIS RUN	
4	NO DATA AVAILABLE FOR THIS CHANNEL ON THIS RUN	
5	0.00	0.00
6	20.00	0.00

CHANNEL NUMBER 11

RUN	TEMPERATURE	STRAIN
1	20.00	1.00
2	0.00	5.00
3	-20.00	15.00
4	-40.00	20.00
5	-5.00	10.00
6	20.00	1.00

CHANNEL NUMBER 12

RUN	TEMPERATURE	STRAIN
1	15.00	0.00
2	0.00	0.00
3	-20.00	0.00
4	-40.00	0.00
5	0.00	0.00
6	20.00	0.00

APPENDIX D2

TEST DATA

- a. Sample Input**
- b. Sample Output**

DE 487 C-EU 853

LISTING OF :PE.DATA2SET(1) PRODUCED ON 3MAR78 AT 14.43.38

#OUTPUT BY LISTFILE IN 'DE487C.EUR53' ON 9MAR78 AT 10.28.21 USING 17

DOCUMENT DATASET

C	TEST DATA 2	SETT
1	1	
2	2	
3	20 0	
4	1 1 16	
5	2 2 16	
6	3 2 16	
7	4 5 20	
8	5 7 20	
9	6 9 20	
10	7 8 15	
11	8 8 15	
12	9 8 15	
13	10 4 20	
14	11 7 15	
15	12 0 15	
16	13 1 15	
17	14 1 15	
18	15 0 15	
19	16 0 15	
20	17 5 16	
21	18 10 20	
22	1 15 -999	
23	2 15 0	
24	3 15 0	
25	4 2 -10	
26	5 8 -10	
27	6 2 -10	
28	7 10 -15	
29	8 5 -15	
30	9 10 -15	
31	10 10 16	
32	11 12 -10	
33	12 0 -999	
34	13 0 -999	
35	14 5 0	
36	15 5 0	
37	16 5 0	
38	17 12 -1	
39	18 18 0	
40	***	
41		

TEST DATA 2 SET1

THE OVERALL TEMPERATURE OF EACH RUN

RUN	TEMPERATURE
1	20.00
2	C-50

CHANNEL NUMBERS 1 2 3

TEMP.	E(X)	E(Y)	GAMMA(XY)	E(MIN)	E(MAX)	PHI(MIN)	PHI(MAX)	
16.00	0.1000E 03	0.3000E 03	0.0000E 00	0.3000E C3	0.1000E 03	90.0	180.0	
RUN 2	. INFORMATION NOT AVAILABLE							

CHANNEL NUMBERS 4 5 6

TEMP.	E(X)	E(Y)	GAMMA(XY)	E(MIN)	E(MAX)	PHI(MIN)	PHI(MAX)
20.00	0.4750E 03	0.4750E 03	0.4000E 03	0.6750E C3	0.2750E 03	45.0	135.0
-10.00	0.2500E 02	0.6250E 03	0.6000E 03	0.7493E 03	-0.5926E 02	67.5	157.5

CHANNEL NUMBERS 8 9 10

TEMP.	E(X)	E(Y)	GAMMA(XY)	E(MIN)	E(MAX)	PHI(MIN)	PHI(MAX)
15.00	0.3500E 03	0.4000E 03	0.1500E 03	0.5811E C3	0.1689E 03	22.5	112.5
-15.00	-0.5000E 02	0.1500E 04	-0.5500E 03	0.1547E C4	-0.9734E 02	99.8	9.8

CHANNEL NUMBER 11

TEMPERATURE CORRECTED STRAIN

15.00	0.5000E 03
-10.00	0.2000E 03

CHANNEL NUMBER 12

TEMPERATURE CORRECTED STRAIN

15.00	0.0000E 00
RUN 2	INFORMATION NOT AVAILABLE

CHANNEL NUMBERS 14 15 16

TEMP.	E(X)	E(Y)	GAMMA(XY)	E(MAX)	E(MIN)	PHI(MAX)	PHI(MIN)
15.00	0.1000E 03	-0.1000E 03	0.0000E 00	0.1000E 03	-0.1000E 03	0.0	90.0
C.CD	0.5000E 03	0.5000E 03	0.0000E 00	0.5000E 03	0.5000E 03	0.0	0.0

CHANNEL NUMBER 17

TEMPERATURE CORRECTED STRAIN

16.00	0.5000E 03
-1.00	C.1200E 04

CHANNEL NUMBER 18

TEMPERATURE CORRECTED STRAIN

20.00	0.1000E 04
0.00	0.1800E 04

APPENDIX E

COMPUTED STRAIN VALUES FOR TEST 7

(Refer to Table E1 in conjunction with Fig. 40)

THERMO - COUPLE NO.	CHANNEL NO.	STRAIN GAUGE (ROSETTE) NO.	CHANNEL NO.			REPRESENTED BY: THERMO-DUO	STRAIN GAUGE (SINGLE) NO.	CHANNEL NO.	REPRESENTED BY: THERMO-CUPP E
			(E ₁)	(E ₂)	(E ₃)				
0(AMBIENT)	0	1(CF PANEL BOTTOM)	24	25	26	1	19(CF PANEL EDGE)	80	1
1(CF PANEL TOP)	1	2(")	27	28	29	1	20(")	81	1
2(")	2	3(")	30	31	32	1	21(")	82	1
3(")	3	4(")	33	34	35	1	22(")	84	4
4(")	4	5(")	36	37	38	1	23(")	85	1
5(TEST FRAME BD)	5	6(")	39	40	41	4	24(")	86	1
6(")	6	7(")	42	43	44	1	25(TEST FRAME TOP)	88	5
7(")	7	8(")	45	46	47	3	26(")	89	11
8(")	8	9(CF PANEL TOP)	48	49	50	4	27(")	90	9
9(")	9	10(CF PANEL BOTTOM)	51	52	53	4	28(")	92	6
10(")	10	11(CF PANEL TOP)	56	57	58	1	29(")	93	12
11(")	11	12(")	59	60	61	1	30(")	94	10
12(")	12	13(")	62	63	64	1			
13(DTI FRAME)	13	14(")	65	66	67	1	35(TEST FRAME SAMPLE BOTTOM FACE)	112	21 (TEST 7)
14(")	14	15(")	68	69	70	1	36(TEST FRAME SAMPLE TOP FACE)	113	21 (TEST 7)
15(")	15	16(")	71	72	73	4			
16(")	16	17(")	74	75	76	1			
17(")	17	18(")	77	78	79	3			
18(CF SKIN SAMPLE)	18								
19(AMBIENT)	19	31(CF SKIN SAMPLE TOP FACE)	96	97	98	18			
20(CF PANEL BOT TEST 6)		32(CF SKIN SAMPLE BOTTOM FACE)	100	101	102	18			
21(CF PANEL SAMPLE 20 TEST 7)		33(CF PANEL SAMPLE TOP FACE)	104	105	106	20 (TEST 7)			
		34(CF PANEL SAMPLE BOTTOM FACE)	108	109	110	20 (TEST 7)			

TABLE E1

20.0°C ± 0.56

LISTING OF 3PL TESTOP7(1) PRODUCED ON 11APR78 AT 10.00.59

ACTUALLY LISTFILE IN 20E487C.EU056 ON 11APR78 AT 10.07.52 USING 17

DOCUMENT TESTOP7

DATA FOR TEST 7 READINGS TAKEN ON 9/2/78 (CALIBRATION DATE 2/2/77)

THE OVERALL TEMPERATURE OF EACH RUN

RUN	TEMPERATURE
1	20.00
2	0.00
3	-25.00
4	-50.00
5	-75.00
6	-100.00
7	-125.00
8	-175.00
9	-190.00
10	-200.00

CHANNEL NUMBERS 24 25 26

TEMP.	E(X)	E(Y)	GAMMA(XY)	E(MAX)	E(MIN)	PHI(MAX)	PHI(MIN)
19.10	0.1622E 03	0.1218E 03	0.6952E 02	0.1622E 03	0.1018E 03	29.9	119.9
-0.30	-0.1129E 03	-0.7506E 02	0.1087E 03	-0.2642E 02	-0.1515E 02	54.6	144.6
-25.50	-C.4724E 03	-0.2790E 03	0.3237E 03	-0.1873E 03	-0.5642E 03	60.5	150.5
-51.50	-0.5158E 03	-0.5055E 03	0.5909E 03	-0.3470E 03	-0.1075E 04	62.4	152.4
-67.00	-C.1504E 04	-0.6204E 03	0.9250E 03	-0.3668E 03	-0.1538E 04	63.2	153.2
-93.70	-C.1750E 04	-0.8262E 03	0.1192E 04	-0.5340E 04	-0.2042E 04	63.9	154.9
-115.00	-0.2185E 04	-0.1059E 04	0.1395E 04	-0.7260E 03	-0.2518E 04	64.5	154.5
-157.50	-C.2897E 04	-0.1377E 04	0.1742E 04	-0.9098E 03	-0.3293E 04	65.5	155.5
-163.50	-C.938E 04	-0.1435E 04	0.1769E 04	-0.1025E 04	-0.335CE 04	65.0	155.0
-17.70	0.2239E 03	0.1786E 03	0.9250E 02	0.2564E 03	0.1505E 03	31.0	121.0

CHANNEL NUMBERS 27 28 29

TEMP.	E(X)	E(Y)	GAMMA(XY)	E(MAX)	E(MIN)	PHI(MAX)	PHI(MIN)
19.10	0.2457E 03	0.2027E 02	-0.4490E 02	0.2479E 03	0.1806E 02	174.4	84.4
-0.30	0.531E 02	-0.1785E 03	-0.1624E 03	0.7918E 02	-0.2641E 03	162.5	72.5
-23.50	-0.1675E 03	-0.3895E 03	-0.2136E 03	-0.1246E 03	-0.4326E 03	158.0	66.0
-51.50	-0.5189E 03	-0.6391E 03	-0.2650E 03	-0.3567E 03	-0.7012E 03	154.9	64.9
-69.30	-0.5759E 03	-0.8471E 03	-0.3701E 03	-0.4621E 03	-0.9409E 03	153.1	63.1
-93.00	-0.8469E 03	-0.1142E 04	-0.4480E 03	-0.7263E 03	-0.1263E 04	151.7	61.7
-115.00	-0.1029E 04	-0.1395E 04	-0.5203E 03	-0.8941E 03	-0.1530E 04	152.6	62.6
-157.50	-3.1409E 04	-0.1874E 04	-0.5611E 03	-0.1270E 04	-0.2004E 04	155.1	65.1
-163.50	-0.1434E 04	-0.1947E 04	-0.5425E 03	-0.1317E 04	-0.2064E 04	156.7	66.7
-17.70	0.3103E 03	0.6115E 02	-0.3600E 02	0.3116E 03	0.5686E 02	175.9	85.9

CHANNEL NUMBERS 30 31 32

TEMP.	E(X)	E(Y)	GAMMA(XY)	E(MAX)	E(MIN)	PHI(MAX)	PHI(MIN)
19.10	0.2340E 03	0.1737E 02	-0.2399E 03	0.2673E 03	-0.3592E 02	156.0	66.0
-0.30	-0.2798E 02	-0.1633E 03	-0.2505E 03	0.8992E 02	-0.2253E 03	153.7	63.7
-23.50	-0.1962E 03	-0.4149E 03	-0.2935E 03	-0.1225E 03	-0.4886E 03	153.4	63.4
-51.50	-0.4376E 03	-0.7004E 03	-0.2581E 03	-0.3839E 03	-0.7521E 03	157.8	67.8
-69.00	-0.6094E 03	-0.8515E 03	-0.2035E 03	-0.5724E 03	-0.8686E 03	160.0	70.0
-93.00	-0.7957E 03	-0.1114E 04	-0.1616E 03	-0.7705E 03	-0.1139E 04	164.4	74.8
-115.00	-0.1044E 04	-0.1559E 04	-0.1603E 03	-0.9871E 03	-0.1377E 04	167.8	77.8
-157.50	-0.1342E 04	-0.1828E 04	-0.1561E 03	-0.1329E 04	-0.1844E 04	171.1	81.1
-163.50	-0.1366E 04	-0.1906E 04	-0.1555E 03	-0.1357E 04	-0.1917E 04	171.9	81.9
-17.70	0.2889E 03	0.6660E 02	-0.2186E 03	0.3336E 03	0.2157E 02	157.8	67.8

CHANNEL NUMBERS 33 34 35

TEMP.	E(X)	E(Y)	GAMMA(XY)	E(MAX)	E(MIN)	PHI(MAX)	PHI(MIN)
19.-10	0.2998E 02	0.1700E 03	0.1831E 03	0.2153E C3	-0.1527E 02	63.7	153.7
-0.-30	-0.2366E 03	0.5635E 02	0.2606E 03	0.8723E C2	-0.2695E 03	72.9	162.9
-23.-50	-0.5560E 03	-0.9522E 02	0.2604E 03	-0.6098E C2	-0.5903E 05	75.3	165.3
-51.-50	-0.9362E 02	-0.2519E 03	0.3639E 03	-0.2066E C3	-0.9316E 03	76.0	166.0
-69.-00	-0.1226E 04	-0.2411E 03	0.4105E 03	-0.2001E C2	-0.1267E 04	78.7	168.7
-93.-00	-0.1591E 04	-0.3568E 03	0.5256E 03	-0.3032E C3	-0.1644E 04	78.5	168.5
-115.-00	-0.1926E 04	-0.4803E 03	0.6025E 03	-0.4201E C3	-0.1988E 04	78.7	168.7
-157.-50	-0.2532E 04	-0.7200E 03	0.7033E 03	-0.6541E C3	-0.2598E 04	79.4	169.4
-163.-50	-0.2582E 04	-0.7616E 03	0.7298E 03	-0.6912E C3	-0.2652E 04	79.1	169.1
-17.-70	-0.1425E 03	0.1941E 03	0.2000E 03	0.2716E C3	-0.6503E 02	52.2	142.2

CHANNEL NUMBERS 36 37 38

TEMP.	E(X)	E(Y)	GAMMA(XY)	E(MAX)	E(MIN)	PHI(MAX)	PHI(MIN)
19.-10	0.1212E 02	0.1491E 03	0.5413E 02	0.1543E C3	0.7024E 01	79.2	169.2
-6.-50	-0.2242E 03	0.3438E 02	0.6039E 01	0.3445E C2	-0.2243E 03	89.1	179.1
-23.-50	-0.5247E 03	-0.1730E 03	-0.5062E 02	-0.1712E C3	-0.5266E 03	94.1	4.1
-51.-50	-0.8922E 03	-0.3361E 03	-0.6254E 02	-0.3333E 03	-0.8940E 02	93.2	3.2
-69.-00	-0.1155E 04	-0.4557E 03	-0.9357E 02	-0.4540E 03	-0.1158E 04	93.8	3.8
-93.-00	-0.1468E 04	-0.6135E 03	-0.1108E 03	-0.6107E 03	-0.1472E 04	93.7	3.7
-115.-00	-0.1747E 04	-0.8555E 03	-0.1572E 03	-0.8191E 03	-0.1799E 04	94.6	4.6
-157.-50	-0.2307E 04	-0.1333E 04	-0.1981E 03	-0.1125E 04	-0.2316E 04	94.8	4.8
-163.-50	-0.2253E 04	-0.1228E 04	-0.4449E 02	-0.1227E 04	-0.2353E 04	91.1	1.1
-17.-70	0.5675E 02	0.1721E 03	0.8370E 02	0.1908E 03	0.7612E 02	66.0	156.0

CHANNEL NUMBERS 39 40 41

TEMP.	E(X)	E(Y)	GAMMA(XY)	E(MAX)	E(MIN)	PHI(MAX)	PHI(MIN)
19.-20	0.3894E 02	0.1175E 03	-0.6951E 02	0.1307E C3	0.2527E 02	110.6	20.8
-6.-40	-0.1960E 03	0.2536E 02	-0.8494E 02	0.3323E C2	-0.2635E 03	100.5	10.5
-23.-50	-0.5033E 03	-0.8768E 02	-0.9810E 02	-0.6197E C2	-0.5000E 03	96.6	6.6
-50.-60	-0.7780E 03	-0.2180E 03	-0.9200E 02	-0.2142E C3	-0.7616E 03	94.7	4.7
-74.-60	-0.1147E 04	-0.3646E 03	-0.1063E 03	-0.3609E C3	-0.1151E 04	94.0	4.0
-103.-00	-0.1447E 04	-0.5203E 03	-0.1161E 03	-0.5168E C3	-0.1470E 04	93.5	3.5
-127.-50	-0.1779E 04	-0.6162E 03	-0.1176E 03	-0.6132E C3	-0.1762E 04	92.9	2.9
-156.-00	-0.2211E 04	-0.6400E 03	-0.1717E 03	-0.8354E C3	-0.2217E 04	93.6	3.6
-196.-50	-0.2242E 04	-0.8644E 03	-0.1689E 03	-0.8593E C3	-0.2247E 04	93.5	3.5
-17.-50	0.3549E 02	0.1525E 03	-0.1079E 03	0.1565E C3	0.1146E 02	114.0	24.0

CHANNEL NUMBERS 42 43 44

TEMP.	E(X)	E(Y)	GAMMA(XY)	E(MAX)	E(MIN)	PHI(MAX)	PHI(MIN)
19.10	0.1051E 03	0.6595E 02	-0.2166E 02	0.1077E 03	0.6330E 02	105.9	75.9
-0.30	-0.1535E 03	-0.6363E 02	-0.1433E 02	-0.2270E 02	-0.1543E 03	95.8	5.8
-21.50	-0.4617E 03	-0.2308E 03	0.1972E 02	-0.2304E 03	-0.4641E 03	87.6	177.6
-51.50	-0.8515E 03	-0.4329E 03	0.7269E 02	-0.4297E 03	-0.8555E 03	85.1	175.1
-69.00	-0.1198E 04	-0.6227E 03	0.3574E 02	-0.6222E 03	-0.1199E 04	88.2	178.2
-93.00	-0.1530E 04	-0.8525E 03	0.4577E 02	-0.8517E 03	-0.1530E 04	86.1	178.1
-115.00	-0.1847E 04	-0.1129E 04	0.4668E 02	-0.1122E 04	-0.1848E 04	88.2	178.2
-157.50	-0.2341E 04	-0.1499E 04	0.2124E 02	-0.1499E 04	-0.2341E 04	69.3	179.3
-163.0	-0.2371E 04	-0.1555E 04	0.3797E 02	-0.1555E 04	-0.2372E 04	88.7	176.7
-17.70	0.1651E 03	0.1613E 03	0.2325E 02	0.1899E 03	0.1566E 03	112.1	112.1

CHANNEL NUMBERS 45 46 47

TEMP.	E(X)	E(Y)	GAMMA(XY)	E(MAX)	E(MIN)	PHI(MAX)	PHI(MIN)
19.20	0.8364E 02	0.7693E 02	-0.8067E 02	0.1206E 03	0.3981E 02	137.4	47.4
-6.40	-0.1398E 03	-0.2611E 02	-0.8076E 02	-0.1312E 02	-0.1516E 03	107.8	17.8
-25.00	-0.4097E 03	-0.1726E 03	-0.8389E 02	-0.1654E 03	-0.4169E 03	99.7	9.7
-49.50	-0.6801E 03	-0.3489E 03	-0.7120E 02	-0.3451E 03	-0.6397E 03	96.1	6.1
-73.00	-0.1026E 04	-0.5966E 03	-0.5146E 02	-0.5551E 03	-0.1027E 04	93.4	3.4
-102.00	-0.1325E 04	-0.7716E 03	-0.5816E 02	-0.7701E 03	-0.1327E 04	93.0	3.0
-125.50	-0.1591E 04	-0.9284E 03	-0.5121E 02	-0.9474E 03	-0.1599E 04	92.3	2.3
-164.50	-0.1928E 04	-0.1244E 04	-0.9067E 02	-0.1241E 04	-0.1945E 04	93.7	2.7
-195.00	-0.2291E 04	-0.1279E 04	-0.8266E 02	-0.1276E 04	-0.2046E 04	93.3	3.3
-17.50	0.7359E 02	0.6788E 02	0.1004E 03	0.1213E 03	0.2062E 02	136.7	46.7

CHANNEL NUMBERS 48 49 50

TEMP.	E(X)	E(Y)	GAMMA(XY)	E(MAX)	E(MIN)	PHI(MAX)	PHI(MIN)
19.20	0.2770E 03	-0.3834E 02	-0.1910E 03	0.3034E 03	-0.6500E 02	164.4	76.4
-6.40	-0.3755E 02	0.3031E 02	-0.1891E 03	-0.1225E 03	-0.6069E 02	136.1	46.1
-25.00	-0.3123E 03	0.1597E 03	-0.2222E 03	-0.1845E 03	-0.3372E 03	102.6	12.6
-50.00	-0.5730E 03	0.2290E 03	-0.2646E 03	0.2502E 03	-0.5542E 03	99.1	9.1
-74.00	-0.8930E 03	0.3468E 03	-0.2644E 03	-0.3629E 03	-0.9091E 03	96.5	6.5
-104.00	-0.1222E 04	0.5062E 03	-0.3152E 03	-0.5204E 03	-0.1237E 04	95.2	5.2
-127.00	-0.1506E 04	0.6253E 03	-0.6502E 03	-0.6375E 03	-0.1517E 04	94.2	4.2
-168.00	-0.2011E 04	0.2971E 03	-0.2971E 03	-0.6645E 03	-0.2611E 04	93.2	3.2
-190.00	-0.2048E 04	0.6296E 03	-0.3244E 03	-0.6394E 03	-0.2058E 04	93.5	3.5
-17.50	0.2322E 03	-0.6031E 02	-0.1643E 03	-0.2574E 03	-0.1055E 03	164.7	76.7

CHANNEL NUMBERS 51 52 53

TEMP.	E(X)	E(Y)	GAMMA(XY)	E(MAX)	E(MIN)	PHI(MAX)	PHI(MIN)
15.-20	-0.-3272E 32	0.-1938E 03	-0.-5117E 02	0.-1967E 02	-0.-3558E 02	96.-4	6.-4
-6.-40	-0.-3045E 03	0.-1456E 03	-0.-3417E 02	0.-1462E 03	-0.-3651E 03	92.-2	2.-2
-25.-00	-0.-6273E 03	0.-1010E 03	-0.-2213E 02	0.-1012E 03	-0.-6875E 03	90.-5	5.-8
-50.-30	-0.-1041E 04	0.-1090E 03	-0.-1206E 02	0.-1095E 03	-0.-1641E 04	90.-3	0.-3
-74.-00	-0.-1466E 04	0.-8928E 02	0.-4614E 02	0.-8961E 02	-0.-490E 04	179.-2	179.-2
-103.-00	-0.-1295E 04	0.-7887E 02	0.-8557E 02	0.-7980E 02	-0.-1296E 04	178.-8	178.-8
-127.-00	-0.-2221E 04	0.-6196E 02	0.-1043E 03	0.-6314E 02	-0.-2226E 04	88.-7	88.-7
-148.-00	-0.-2125E 04	-0.-8449E 01	0.-1089E 03	-0.-7394E 01	-0.-2216E 04	88.-9	88.-9
-156.-00	-0.-2864E 04	-0.-1586E 02	0.-9257E 02	-0.-1511E 02	-0.-2865E 04	179.-1	179.-1
-17.-50	-0.-5194E 02	0.-1969E 03	-0.-1300E 03	-0.-2124E 03	-0.-7790E 02	103.-3	103.-3

CHANNEL NUMBERS 56 57 58

TEMP.	E(X)	E(Y)	GAMMA(XY)	E(MAX)	E(MIN)	PHI(MAX)	PHI(MIN)
19.-10	-0.-2653E 03	-0.-4421E 02	-0.-6583E 03	0.-1925E 03	-0.-5020E 03	125.-7	35.-7
-6.-30	-0.-2628E 02	-0.-1104E 03	-0.-4032E 03	0.-2894E 02	-0.-4021E 03	124.-6	34.-6
-25.-50	-0.-3116E 03	-0.-1663E 03	-0.-9090E 02	-0.-1544E 03	-0.-3268E 03	105.-7	105.-7
-51.-50	-0.-4162E 03	-0.-2997E 03	-0.-3403E 03	-0.-1783E 03	-0.-5381E 05	54.-5	144.-5
-84.-00	-0.-4325E 03	-0.-8215E 02	-0.-6467E 03	-0.-1104E 03	-0.-6252E 05	59.-2	149.-2
-93.-00	-0.-5337E 03	-0.-4508E 02	-0.-1053E 04	-0.-2926E 03	-0.-5939E 03	57.-5	147.-5
-115.-00	-0.-6735E 03	-0.-3623E 03	-0.-1699E 04	-0.-3455E 03	-0.-1382E 04	50.-2	140.-2
-157.-50	-0.-9790E 03	-0.-1582E 04	-0.-3243E 04	-0.-5984E 03	-0.-1995E 04	39.-3	125.-3
-163.-50	-0.-9463E 03	-0.-1773E 04	-0.-3413E 04	-0.-3950E 03	-0.-4116E 04	38.-2	128.-2
-17.-70	-0.-1022E 03	-0.-1732E 03	-0.-6305E 03	-0.-1795E 02	-0.-4550E 03	138.-2	138.-2

CHANNEL NUMBERS 59 60 61

TEMP.	E(X)	E(Y)	GAMMA(XY)	E(MAX)	E(MIN)	PHI(MAX)	PHI(MIN)
19.-10	-0.-7809E 02	0.-2575E 03	-0.-4173E 03	0.-3575E 03	-0.-1780E 03	115.-6	25.-6
-6.-30	-0.-1036E 03	0.-3935E 03	-0.-1387E 03	0.-4030E 03	-0.-1310E 03	97.-8	7.-8
-23.-50	-0.-1630E 03	0.-8717E 02	0.-2343E 03	0.-1334E 03	-0.-2693E 03	68.-4	156.-4
-51.-50	-0.-1807E 03	0.-2504E 02	0.-6043E 03	0.-2413E 03	-0.-3970E 03	54.-4	144.-4
-69.-00	-0.-1213E 03	0.-6977E 02	0.-1064E 04	0.-5146E 03	-0.-5661E 03	50.-1	140.-1
-92.-00	-0.-7279E 02	-0.-3453E 02	0.-1505E 04	0.-6989E 03	-0.-8062E 03	45.-7	135.-7
-115.-00	-0.-2431E 02	0.-5513E 01	0.-1901E 04	0.-8421E 03	-0.-1076E 04	48.-8	138.-8
-157.-50	-0.-5903E 03	0.-1457E 03	0.-2479E 04	0.-1071E 04	-0.-1515E 04	53.-3	143.-3
-163.-50	-0.-6287E 02	0.-1342E 03	0.-2517E 04	0.-1063E 04	-0.-1562E 04	53.-4	143.-4
-17.-70	-0.-2075E 02	0.-2329E 03	-0.-4064E 03	0.-3545E 03	-0.-1335E 02	119.-0	29.-0

CHANNEL NUMBERS 62 63 64

TEMP.	E(X)	E(Y)	GAMMA(XY)	E(MAX)	E(MIN)	PHI(MAX)	PHI(MIN)
14.10	-0.9211E 01	0.2544E 03	-0.6029E 02	0.2578E 03	-0.1261E 02	56.4	6.4
-0.30	-0.3465E 02	0.1185E 03	-0.7726E 02	0.1277E 03	-0.4384E 02	103.4	13.4
-23.50	-0.1175E 03	-0.1451E 02	-0.9175E 02	-0.2952E 01	-0.1550E 03	110.8	20.8
-51.50	-0.1388E 03	-0.2461E 03	-0.1426E 03	-0.1032E 03	-0.2816E 03	153.5	63.5
-66.50	-0.2515E 02	-0.2906E 03	-0.1968E 03	-0.7955E 01	-0.3237E 03	161.6	71.6
-93.00	0.2646E 02	-0.4570E 03	-0.2105E 03	0.5145E 02	-0.4783E 03	168.3	78.3
-111.50	-0.3478E 02	-0.5786E 03	-0.2267E 03	-0.1079E 02	-0.6013E 03	169.7	78.7
-157.50	0.1934E 03	-0.8565E 03	-0.2699E 03	-0.1644E 03	-0.8547E 03	169.0	79.0
-163.50	-0.2184E 03	-0.9095E 03	-0.2615E 03	-0.1945E 03	-0.9334E 03	169.6	79.6
-17.70	0.2911E 03	-0.1960E 03	0.2875E 02	0.3000E 03	0.1940E 03	7.9	97.9

CHANNEL NUMBERS 65 66 67

TEMP.	E(X)	E(Y)	GAMMA(XY)	E(MAX)	E(MIN)	PHI(MAX)	PHI(MIN)
14.10	0.1016E 03	-0.9102E 02	-0.3598E 03	0.2093E 03	-0.1988E 03	149.1	59.1
-6.50	-0.9132E 02	-0.4617E 02	-0.2021E 03	0.3883E 02	-0.1663E 03	130.1	40.1
-23.50	-0.3631E 03	-0.1069E 02	-0.1087E 02	-0.1079E 02	-0.3032E 03	91.1	1.1
-51.50	-0.5293E 03	-0.4673E 01	0.2084E 03	-0.1527E 02	-0.5492E 03	79.2	169.2
-66.50	-0.7213E 03	0.1519E 03	0.5086E 03	0.2206E 03	-0.7699E 03	74.9	164.9
-93.00	-0.9240E 03	-0.2531E 03	0.7647E 03	-0.1717E 03	-0.1C93E 04	74.1	164.1
-115.00	-0.1231E 04	0.3106E 03	0.9766E 03	0.4528E 03	-0.1373E 04	73.8	163.8
-157.50	-0.1643E 04	-0.2988E 03	0.1284E 04	-0.4917E 03	-0.1846E 04	73.3	163.3
-163.50	-0.1675E 04	-0.2691E 03	0.1262E 04	-0.4560E 03	-0.1862E 04	73.5	163.5
-17.70	0.7311E 03	-0.8734E 04	0.3314E 04	0.1013E 04	-0.9016E 04	9.6	99.6

CHANNEL NUMBERS 68 69 70

TEMP.	E(X)	E(Y)	GAMMA(XY)	E(MAX)	E(MIN)	PHI(MAX)	PHI(MIN)
14.10	-0.2757E 00	0.1492E 03	-0.7797E 02	0.1587E 03	-0.9833E 01	103.8	13.8
-6.50	-0.1569E 03	0.1698E 03	0.6367E 02	0.1722E 03	-0.1600E 03	84.5	174.5
-23.50	-0.2618E 03	0.1636E 03	0.2267E 03	0.1919E 03	-0.2901E 03	76.0	166.0
-51.50	-0.5556E 03	0.2177E 03	0.3498E 03	0.2554E 03	-0.5935E 03	77.8	167.8
-69.00	-0.6977E 03	0.3352E 03	0.5865E 03	0.4127E 03	-0.7752E 03	75.2	165.2
-93.00	-0.9260E 03	0.3839E 03	0.7892E 03	0.4936E 03	-0.1036E 04	74.5	164.5
-115.00	-0.1180E 04	-0.4521E 03	0.9763E 03	0.5875E 03	-0.1315E 04	74.5	164.5
-157.50	-0.1622E 04	0.4295E 03	0.1173E 04	0.5855E 03	-0.1778E 04	75.1	165.1
-163.50	-0.1575E 04	-0.2664E 03	0.1081E 04	0.4151E 03	-0.1722E 04	74.8	164.8
-17.70	0.1268E 04	-0.1183E 04	-0.1764E 03	0.1271E 04	-0.11Fct 04	177.9	87.9

CHANNEL NUMBERS 74 75 76

TEMP.	E(X)	E(Y)	GAMMA(XY)	E(MAX)	E(MIN)	PHI(MAX)	PHI(MIN)
-19.-10	-0.4206E 02	0.7746E 02	0.6006E 02	0.8459E C2	-0.4921E 02	76.7	166.7
-6.-30	0.1711E 03	0.3279E 02	0.5041E 02	0.4166E C2	-0.1209E 02	83.5	173.5
-23.-50	-0.3524E 03	0.3930E 01	0.3680E 02	0.4877E C1	-0.3533E 03	87.1	177.1
-51.-50	-0.5660E 03	-0.2765E 01	0.1333E 02	-0.8692E C1	-0.5801E 03	89.3	179.3
-65.-20	-0.6716E 03	0.7168E 02	-0.1111E 02	0.7172E C2	-0.6716E 03	90.4	164
-93.-00	-0.8165E 03	0.6962E 02	0.1042E 02	0.6965E C2	-0.8165E 03	89.7	179.7
-115.-00	-0.1024E 04	0.8475E 02	-0.8289E 00	0.8475E C2	-0.1024E 04	90.0	0.0
-157.-50	-0.1347E 04	0.1234E 03	0.3156E 02	0.1235E C3	-0.1347E 04	89.4	179.4
-163.-50	-0.1379E 04	0.1099E 03	0.3874E 02	-0.1101E C3	-0.1379E 04	89.3	179.3
-17.-70	-0.1575E 03	0.4124E 03	0.5590E 02	0.4136E C3	-0.1569E 03	87.2	177.2

CHANNEL NUMBERS 77 78 79

TEMP.	E(X)	E(Y)	GAMMA(XY)	E(MAX)	E(MIN)	PHI(MAX)	PHI(MIN)
-19.-20	0.1424E 03	0.1898E 03	0.3867E 02	0.1967E C3	0.1356E 03	70.4	160.4
-6.-40	-0.5955E 02	0.1222E 03	0.4761E C2	0.1253E C3	-0.6261E 02	82.7	172.7
-25.-50	-0.2504E 03	0.1717E 03	0.4263E 02	0.1728E C3	-0.2915E 03	87.3	177.3
-49.-50	-0.5332E 03	0.2763E 03	-0.8404E 01	0.2763E C3	-0.5332E 03	90.3	0.3
-75.-00	-0.7883E 03	0.2832E 03	0.3760E 01	0.2832E C3	-0.8825E 03	89.9	179.9
-102.-00	-0.1066E 04	0.3440E 03	0.2100E 02	0.3441E C2	-0.1060E 04	85.6	179.6
-125.-50	-0.1304E 04	0.3895E 03	0.5700E 02	0.3900E C3	-0.1305E 04	89.0	179.0
-184.-50	-0.1679E 04	0.1138E 04	0.4769E 02	0.1138E C4	-0.1679E 04	89.5	179.5
-196.00	-0.1726E 04	0.1240E 04	0.5145E 02	0.1240E C4	-0.1726E 04	89.5	174.5
-17.50	-0.1298E 03	0.1519E 04	0.3864E 02	0.1519E C4	0.1298E 03	89.1	179.1

CHANNEL NUMBER 80

TEMPERATURE	CORRECTED STRAIN
19.10	0.5547E 03
-0.30	0.5296E 03
-23.50	0.5045E 03
-51.50	0.4688E 03
-69.00	0.4600E 03
-93.00	0.5900E 03
-115.00	0.5333E 03
-157.50	0.3105E 03
-163.50	0.2471E 03
-17.70	0.4766E 04

CHANNEL NUMBER 81

TEMPERATURE	CORRECTED STRAIN
19.10	0.8943E 02
-0.30	-0.8638E 02
-23.50	-0.2794E 03
-51.50	-0.4553E 03
-69.00	-0.5682E 03
-93.00	-0.7746E 03
-115.00	-0.9525E 03
-157.50	-0.1457E 04
-163.50	-0.1484E 04
-17.70	0.2492E 03

CHANNEL NUMBER 82

TEMPERATURE	CORRECTED STRAIN
19.10	-0.3379E 02
-0.30	-0.2096E 03
-23.50	-0.4049E 03
-51.50	-0.5285E 03
-69.00	-0.1394E 03
-93.00	-0.5806E 03
-115.00	-0.9891E 03
-157.50	-0.1246E 04
-163.50	-0.1296E 04
-17.70	0.4725E 03

CHANNEL NUMBER 83

TEMPERATURE CORRECTED STRAIN

RUN 1	INFORMATION NOT AVAILABLE
RUN 2	INFORMATION NOT AVAILABLE
RUN 3	INFORMATION NOT AVAILABLE
RUN 4	INFORMATION NOT AVAILABLE
RUN 5	INFORMATION NOT AVAILABLE
RUN 6	INFORMATION NOT AVAILABLE
RUN 7	INFORMATION NOT AVAILABLE
RUN 8	INFORMATION NOT AVAILABLE
RUN 9	INFORMATION NOT AVAILABLE
RUN 10	INFORMATION NOT AVAILABLE

CHANNEL NUMBER 84

TEMPERATURE CORRECTED STRAIN

19.10	-0.7786E 03
-0.30	-0.6959E 03
-23.50	-0.6130E 03
-51.50	-0.5395E 03
-69.00	-0.7077E 03
-93.00	-0.5998E 03
-115.00	-0.4628E 03
-157.50	-0.4350E 02
-163.50	0.2064E 02
17.70	-0.6741E 03

CHANNEL NUMBER 85

TEMPERATURE CORRECTED STRAIN

19.10	0.3082E 03
-0.30	-0.2439E 02
-23.50	-0.1666E 03
-51.50	-0.4681E 03
-69.00	-0.5701E 03
-93.00	-0.7014E 03
-115.00	-0.7300E 03
-157.50	-0.3799E 03
-163.50	-0.3240E 03
17.70	0.3587E 03

CHANNEL NUMBER 86

***** TEMPERATURE CORRECTED STRAIN *****

19.10	0.2953E 02
-0.30	-0.3314E 02
-23.59	-0.5546E 01
-51.50	0.7535E 02
-65.00	-0.1365E 03
-95.00	-0.6923E 02
-115.00	0.1184E 03
-157.50	0.4572E 03
-163.50	0.5349E 03
17.70	-0.2993E 03

CHANNEL NUMBER 87

TEMPERATURE	CORRECTED STRAIN
RUN 1	INFORMATION NOT AVAILABLE
RUN 2	INFORMATION NOT AVAILABLE
RUN 3	INFORMATION NOT AVAILABLE
RUN 4	INFORMATION NOT AVAILABLE
RUN 5	INFORMATION NOT AVAILABLE
RUN 6	INFORMATION NOT AVAILABLE
RUN 7	INFORMATION NOT AVAILABLE
RUN 8	INFORMATION NOT AVAILABLE
RUN 9	INFORMATION NOT AVAILABLE
RUN 10	INFORMATION NOT AVAILABLE

CHANNEL NUMBER 88

TEMPERATURE	CORRECTED STRAIN
18.00	0.2360E 02
0.00	0.7494E 02
-25.00	0.1507E 03
-51.50	0.2086E 03
-66.50	0.2626E 03
-123.00	0.3338E 03
-156.00	0.3670E 03
RUN 8	INFORMATION NOT AVAILABLE
RUN 9	INFORMATION NOT AVAILABLE
15.00	0.1902E 02

CHANNEL NUMBER 89

TEMPERATURE CORRECTED STRAIN

16.70	-0.3346E 02
0.20	0.2174E 02
-24.00	0.8909E 02
-51.00	0.1413E 03
-67.00	0.-2024E 03
-124.00	0.-2722E 03
-161.00	0.3347E 03
RUN 8	INFORMATION NOT AVAILABLE
RUN 9	INFORMATION NOT AVAILABLE
14.90	0.4376E 04

CHANNEL NUMBER 90

TEMPERATURE CORRECTED STRAIN

15.80	-0.5495E 02
0.50	-0.-1085E 02
-23.00	0.3874E 02
-49.00	0.-7405E 02
-85.00	0.-1243E 03
-122.00	0.-2014E 03
-156.00	0.2555E 03
RUN 8	INFORMATION NOT AVAILABLE
RUN 9	INFORMATION NOT AVAILABLE
15.60	-0.4156E 02

CHANNEL NUMBER 91

TEMPERATURE CORRECTED STRAIN

RUN 1	INFORMATION NOT AVAILABLE
KUN 2	INFORMATION NOT AVAILABLE
KUN 3	INFORMATION NOT AVAILABLE
KUN 4	INFORMATION NOT AVAILABLE
KUN 5	INFORMATION NOT AVAILABLE
KUN 6	INFORMATION NOT AVAILABLE
KUN 7	INFORMATION NOT AVAILABLE
KUN 8	INFORMATION NOT AVAILABLE
KUN 9	INFORMATION NOT AVAILABLE
KUN 10	INFORMATION NOT AVAILABLE

CHANNEL NUMBER 92

TEMPERATURE CORRECTED STRAIN

RUN 1	INFORMATION NOT AVAILABLE
RUN 2	INFORMATION NOT AVAILABLE
RUN 3	INFORMATION NOT AVAILABLE
RUN 4	INFORMATION NOT AVAILABLE
RUN 5	INFORMATION NOT AVAILABLE
RUN 6	INFORMATION NOT AVAILABLE
RUN 7	INFORMATION NOT AVAILABLE
RUN 8	INFORMATION NOT AVAILABLE
RUN 9	INFORMATION NOT AVAILABLE
RUN 10	INFORMATION NOT AVAILABLE

CHANNEL NUMBER 93

TEMPERATURE CORRECTED STRAIN

16.90	-0.2937E 02
0.50	0.5368E 01
-24.00	0.5991E 02
-51.00	0.1044E 03
-87.50	0.1467E 03
-126.50	0.2133E 03
-163.50	0.2603E 03
RUN 5	INFORMATION NOT AVAILABLE
RUN 9	INFORMATION NOT AVAILABLE
15.10	-0.1220E 02

CHANNEL NUMBER 94

TEMPERATURE CORRECTED STRAIN

12.80	-0.1383E 02
0.70	0.3258E 02
-23.50	0.7648E 02
-50.00	0.1160E 03
-66.50	0.1872E 03
-124.00	0.2909E 03
-160.00	0.3701E 03
RUN 5	INFORMATION NOT AVAILABLE
RUN 9	INFORMATION NOT AVAILABLE
15.50	0.9529E 01

APPENDIX F

THE FINITE ELEMENT MODEL

APPENDIX F

THE FINITE ELEMENT MODEL

The test structure and panel were modelled with finite elements using the 'Stardyne' Programme*. As the structure is symmetrical about two axes through its centre only one quarter of the total was modelled and the appropriate boundary conditions applied in the stress analysis.

The aluminium framework of the test rig, a riveted assemblage of plates and channel sections, was modelled using 54 plate elements to represent the channel webs and the plates and 40 beam elements to represent the channel flanges.

The panel under test was modelled using 24 triangular sandwich elements (plate elements designed to model the particular properties peculiar to sandwich structures), and 7 beam elements which represent the edge stiffening of the panel. Framework and Panel were connected using rigid beam elements to represent the offset of the panel.

Material properties were taken as being isotropic and were as follows

For Carbon Fibre Sandwich	$E = 50000 \text{ N/mm}^2$ $\alpha = 1.9 \times 10^{-6}/^\circ\text{C}$ $\gamma = 0.33$	See para. 3.6
Core Shear Rigidity	$\alpha = 3.5 \times 10^{-6}/^\circ\text{C}$	
Core Shear Rigidity	252 N/mm ²	
For Aluminium Alloy	$E = 70,000 \text{ N/mm}^2$ $\gamma = 0.3$ $\alpha = 23.0 \times 10^{-6}/^\circ\text{C}$	

This model differs from the previous Finite Element Model in the following aspects.

1. Plate elements previously modelled with membrane stiffness only now have membrane and bending stiffness and are sandwich elements.
2. The panel was previously represented with quadrilateral plate elements.
3. The properties of carbon fibre were based on test results not as previously on theoretical calculations and manufacturers' data.

*Reference: MRI/STARDYNE 3 Users Manual
and MRI/STARDYNE Theoretical Manual

APPENDIX G

CALCULATION OF STRESS FROM THE MEASURED ORTHOGONAL STRAINS

APPENDIX G

CALCULATION OF STRESS FROM THE MEASURED ORTHOGONAL STRAINS

It is required to compare the actual stress levels in the lower surface of honeycomb panel (panel fixed) with the corresponding stress output from the theoretical model for a 50°C drop in temperature.

The model gave maximum stress at the edges of the panel. The location of these stresses being in close proximity to strain gauge positions used in practical test.

Method The figures 50 and 51 show the strain distribution in Y and X directions respectively. The measured strain recorded at strain gauge 1 was used at both temperatures $+19.1^{\circ}\text{C}$ and -23.5°C . for both X and Y directions.

Adding the strains at these two temperatures corresponds to a total strain at a drop of 42.6°C . This strain is therefore factored by $\frac{50}{42.6}$ to give an estimated strain at the required temperature of 50°C .

Using equations (1) and (2) the stresses in the X and Y directions may be calculated from the measured strains.

$$\epsilon_x = \frac{1}{E} \sigma_x - \nu \sigma_y \quad \dots \dots \dots (1)$$

$$\epsilon_y = \frac{1}{E} \sigma_y - \nu \sigma_x \quad \dots \dots \dots (2)$$

Notation

σ_x and σ_y - stresses in X and Y directions respectively.

ν - Poissons ratio

E - Youngs Modulus

ϵ_x and ϵ_y - strains measured in X and Y directions respectively.

Results

(a) From Figure 50

$\epsilon_y = 400 \times 10^{-6}$ for 42.6°C drop in temperature.

(b) From Figure 51

$$\epsilon_x = 600 \times 10^{-6} \text{ for } 42.6^\circ\text{C. drop in temperature.}$$

Constants

$$E = 50000 \text{ N/mm}^2$$

$$\nu = 0.3$$

Therefore for a 50°C drop in temperature

$$704 \times 10^{-6} = 2 \times 10^{-5} [\sigma_x - 0.3 \sigma_y] \quad \dots \dots \dots (1)$$

$$469 \times 10^{-6} = 2 \times 10^{-5} [\sigma_y - 0.3 \sigma_x] \quad \dots \dots \dots (2)$$

from which $\sigma_x = 46.4 \text{ N/mm}^2$

$$\cdot \sigma_y = 37.37 \text{ N/mm}^2$$

These stresses are now directly comparable with the predicted stresses.